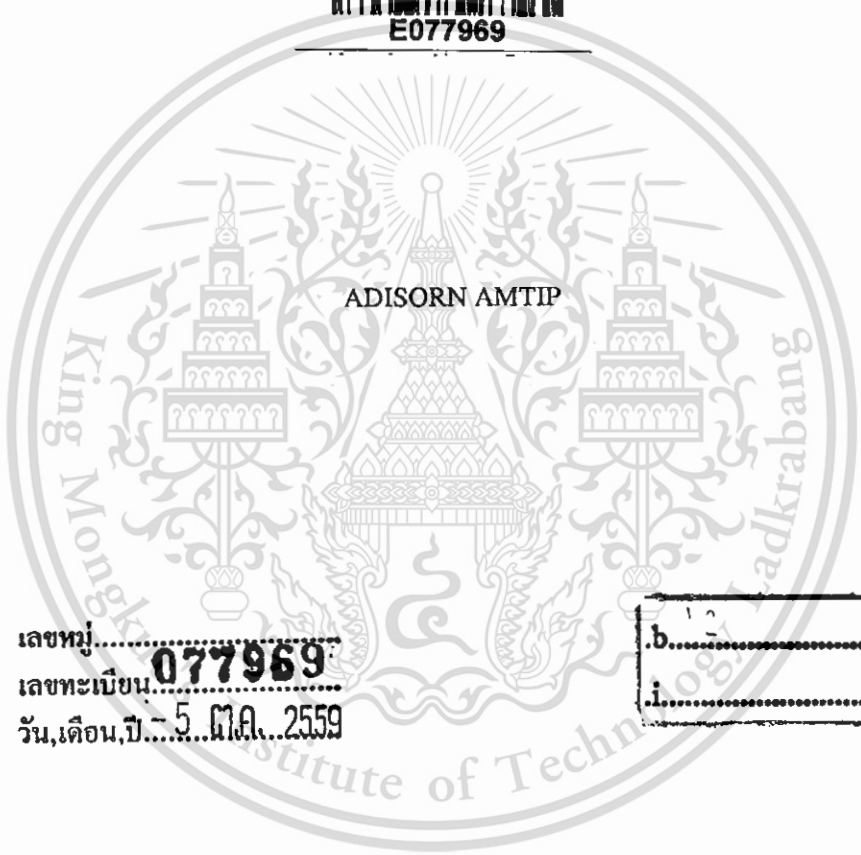
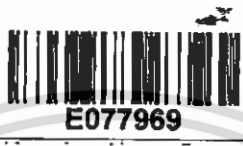


สำนักหอสมุดกลาง พระจอมเกล้าลาดกระบัง

AN ESTIMATION OF ENERGY LOSS IN  $\text{LiFePO}_4$  BATTERY  
CHARGING AND BALANCING SYSTEM FOR ELECTRIC  
VEHICLE APPLICATIONS



เลขหมู่.....**077969**.....  
เลขทะเบียน.....  
วัน,เดือน,ปี.....5 ต.ค. 2559



A THESIS SUBMITTED IN PARTIAL FULFILLMENT  
OF THE REQUIREMENT FOR THE DEGREE OF  
MASTER OF ENGINEERING IN AUTOMOTIVE ENGINEERING  
INTERNATIONAL COLLEGE  
KING MONGKUT'S INSTITUTE OF TECHNOLOGY LADKRABANG  
ACADEMIC YEAR 2015  
KMITL-2015-IC-M-004-09



**COPYRIGHT 2015**  
**INTERNATIONAL COLLEGE**  
**KING MONGKUT'S INSTITUTE OF TECHNOLOGY LADKRABANG**

This material is reserved for educational use only, not allowed for commercial use.

Forbidden to modify the content, and cite the document when use.

# ABSTRACT

Thesis Title      An estimation of energy loss in  
LiFePO<sub>4</sub> battery charging and balancing system  
for electric vehicle applications  
Candidate        Mr. Adisorn Amtip  
Degree            Master of Engineering  
Program          Automotive Engineering  
Thesis Advisors   Asst.Prof.Dr. Chaiwat Nuthong  
                      Dr. Teera Phatrapornnant  
                      Prof.Dr. Masaki Yamakita  
B.E.                2558

## Abstract

A study of an energy loss of 60 Ah LiFePO<sub>4</sub> battery plays an important role in the EV and HEV application. This thesis used battery-charging and balancing model for estimating their energy loss.

Battery charging model is designed in term of equivalent RC circuit and its unknown parameters is solved by using the Genetic Algorithm. The two battery samples on two condition of charging current is used in order to verify the model. The estimated energy loss show that the charging current had effect to the energy loss significantly. And then, simulation result presents the optimum charging current is 60 A (or 1C ).

To estimate energy loss in balancing schemes, this thesis focuses on exploring three kinds of passive-balancing schemes about energy loss and at various conditions e.g. considering at balancing current or state of charge among all cells ( $SOC_{max} - SOC_{min}$ ). The estimated results show that the different balancing schemes have effect on the energy loss slightly and state of charge among all cells affects to the energy loss significantly.

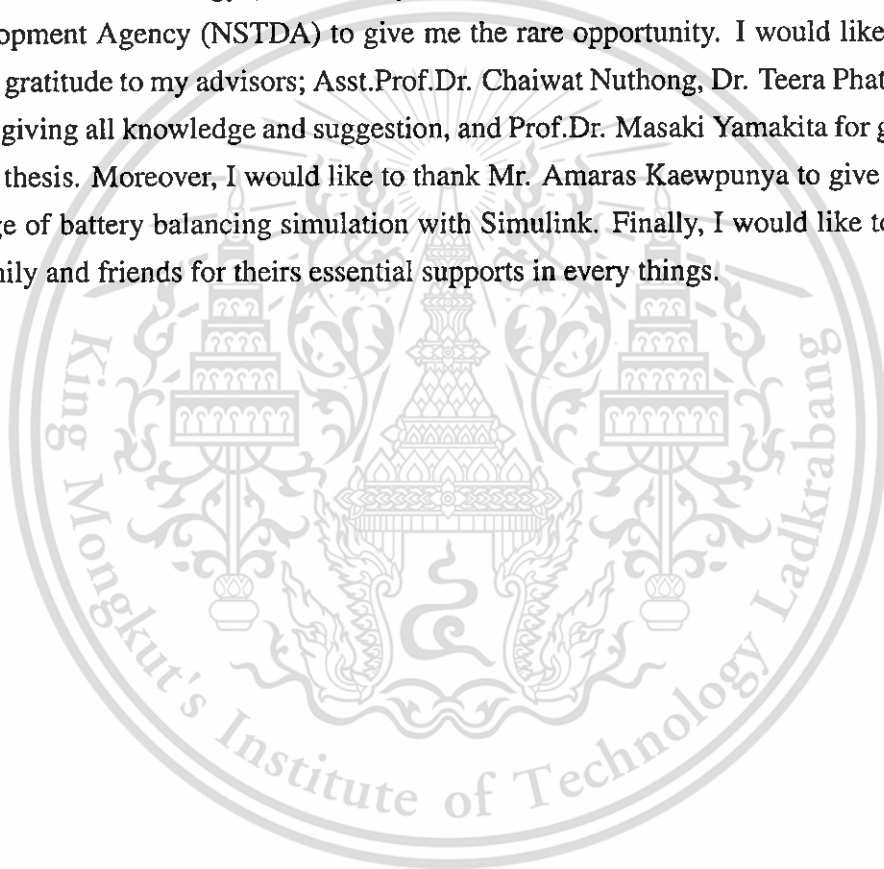
**Index Terms** —LiFePO<sub>4</sub>, EV application, passive balancing, energy loss, battery model

This material is reserved for educational use only, not allowed for commercial use.

Forbidden to modify the content, and cite the document when use.

# Acknowledgement

I really appreciate Thailand Advanced Institute of Science and Technology and Tokyo Institute of Technology (TAIST-Tokyo Tech) and National Science and Technology Development Agency (NSTDA) to give me the rare opportunity. I would like to express my gratitude to my advisors; Asst.Prof.Dr. Chaiwat Nuthong, Dr. Teera Phatrapornnant for giving all knowledge and suggestion, and Prof.Dr. Masaki Yamakita for guidance of the thesis. Moreover, I would like to thank Mr. Amaras Kaewpunya to give me knowledge of battery balancing simulation with Simulink. Finally, I would like to thank my family and friends for their essential supports in every things.



# Contents

<b>1</b>	<b>INTRODUCTION</b>	<b>1</b>
1.1	Background . . . . .	1
1.2	Objectives . . . . .	2
1.3	Scope of Research . . . . .	3
1.4	Hypothesis . . . . .	3
<b>2</b>	<b>LITERATURE REVIEW</b>	<b>4</b>
2.1	Battery Characteristics and Monitoring . . . . .	4
2.2	Battery Charging Techniques . . . . .	6
2.3	Battery Balancing Techniques . . . . .	7
2.4	Battery Model . . . . .	8
2.5	Battery Energy . . . . .	13
<b>3</b>	<b>EXPERIMENTAL PROCEDURE</b>	<b>14</b>
3.1	Charge Characteristics Tests of the Battery . . . . .	15
3.1.1	Charge and discharge instruments . . . . .	15
3.1.2	Open circuit voltage ( $V_{OC}$ ) test . . . . .	17
3.1.3	Battery-charging voltage ( $V_b$ ) test . . . . .	17
3.2	An Estimation of Battery-Charging Energy Loss . . . . .	19
3.2.1	Battery model and energy loss equation . . . . .	19
3.2.2	Parameters programing . . . . .	21
3.2.3	Optimization method and plan . . . . .	24
3.2.4	Model verification . . . . .	25
3.2.5	Energy loss estimation and simulation . . . . .	25
3.3	An Estimation of Energy Loss in the Battery-Balancing Schemes . . . . .	26
3.3.1	Battery model . . . . .	26
3.3.2	Three schemes of passive balancing . . . . .	28
3.3.3	Simulation model and condition . . . . .	31

<b>4</b>	<b>RESULTS AND DISCUSSION</b>	<b>33</b>
4.1	The Battery Characteristics . . . . .	33
4.1.1	The charging open-circuit voltage ( $V_{OC}$ ) . . . . .	33
4.1.2	The charging voltage ( $V_b$ ) and current ( $I$ ) . . . . .	33
4.2	The Energy Loss from Charging Battery . . . . .	36
4.2.1	The results of optimization using Genetic Algorithm . . . . .	36
4.2.2	Curve fitting of solved variables . . . . .	43
4.2.3	The model verification . . . . .	46
4.2.4	The energy loss estimation results . . . . .	56
4.2.5	The simulation and optimum charging current results . . . . .	58
4.3	The Energy Loss In The Battery Balancing Schemes . . . . .	60
4.3.1	Model verification . . . . .	60
4.3.2	The energy loss estimation results . . . . .	60
<b>5</b>	<b>CONCLUSION</b>	<b>64</b>
	<b>REFERENCES</b>	<b>66</b>
	<b>Appendices</b>	<b>69</b>
<b>A</b>	<b>MATLAB Short Code for Optimization</b>	<b>70</b>
<b>B</b>	<b>Simulink Diagram for Battery Balancing Energy Loss</b>	<b>73</b>
<b>C</b>	<b>Publication</b>	<b>75</b>
	<b>BIOGRAPHY</b>	<b>80</b>

# List of Figures

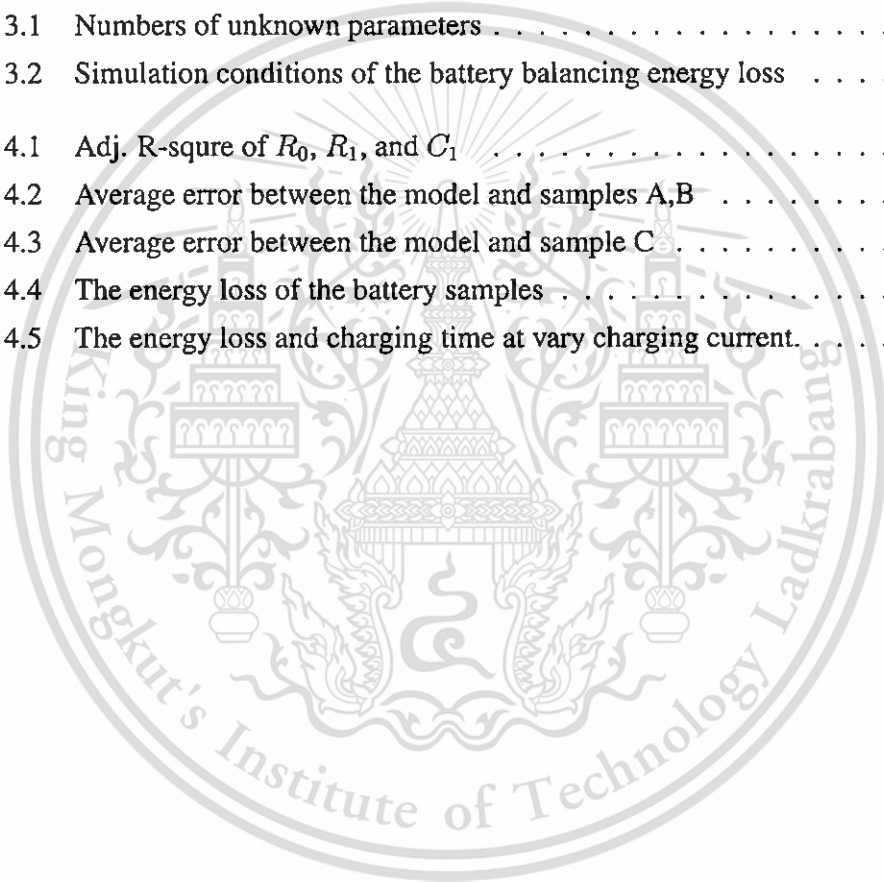
1.1	NECTEC's laboratory research . . . . .	2
2.1	OCV @ Different Temperature [3] . . . . .	5
2.2	Proposed charging process of LiFePO <sub>4</sub> (implementation of charger and battery management system for fast charging technique of the battery in electric bicycles) [11] . . . . .	6
2.3	Pulse charging (fast charging method for wireless and mobile devices using double-pulse charge technique) [11] . . . . .	7
2.4	SOC in (a) ideal system and (b) actual system. . . . .	7
2.5	Schematic diagrams for Mr. He's evaluating five models, (a) the Rint, (b) the RC, (c) the Theven, (d) the PNGV , and (e) the DP models [14].	9
2.6	The terminal voltage error curves between the simulation and experiment [14] . . . . .	10
2.7	The equivalent circuit used for Mr. Hu's battery model [15] . . . . .	10
2.8	The equivalent circuit used for Mr. Yao's battery model [17] . . . . .	11
2.9	Schematic diagram of the battery internal dynamic phenomena and the equivalent circuit [19] . . . . .	12
2.10	Zoom-in of last 5 min of energy supplied by battery when starting from different initial temperatures [21]. . . . .	13
3.1	Main Procedure Diagram . . . . .	14
3.2	The prismatic cell of LifePO <sub>4</sub> battery . . . . .	15
3.3	The programmable DC electronic loads (the battery-discharging instrument) . . . . .	16
3.4	The programmable DC power supply (the battery-charging instrument) .	16
3.5	the connection between the battery and the instruments . . . . .	17
3.6	The battery voltage and current in constant current-constant voltage (CC-CV) charging strategy . . . . .	18
3.7	The estimation of the battery-charging energy loss procedures . . . . .	19
3.8	Schematic diagram for the Thevenin model . . . . .	20

3.9	RC circuit . . . . .	20
3.10	Example of a liner spline function . . . . .	23
3.11	The energy loss estimation in the battery-balancing schemes diagram . . . . .	26
3.12	The equivalent circuit of Lithium-ion battery[13] . . . . .	27
3.13	The direction flow of current in passive balancing scheme (a) Battery 1 and 2 are charging, (b) Battery 1 is discharging and battery 2 is charging.	28
3.14	Two States balancing scheme of five batteries. . . . .	29
3.15	The Draining Then Changing (DTC) scheme of five batteries. . . . .	30
3.16	PWM (Pulse-width modulation) scheme of three batteries. . . . .	30
4.1	The open-circuit voltage ( $V_{OC}$ ) . . . . .	34
4.2	The charging voltage ( $V_b$ ) current ( $I$ ) at 120 A. . . . .	34
4.3	The charging voltage ( $V_b$ ) current ( $I$ ) at 60 A. . . . .	35
4.4	The SOC of two conditions . . . . .	35
4.5	The tested $V_b$ and optimized $V_b$ of battery A at 120 A charging current. . . . .	36
4.6	Histogram of error between the tested $V_b$ and optimized $V_b$ in battery A at 120 A charging current. . . . .	37
4.7	The tested $V_b$ and optimized $V_b$ of battery B at 120 A charging current. . . . .	38
4.8	Histogram of error between the tested $V_b$ and optimized $V_b$ in battery B at 120 A charging current. . . . .	38
4.9	The tested $V_b$ and optimized $V_b$ of battery A at 60 A charging current. . . . .	39
4.10	Histogram of error between the tested $V_b$ and optimized $V_b$ in battery A at 60 A charging current. . . . .	39
4.11	The tested $V_b$ and optimized $V_b$ of battery B at 60 A charging current. . . . .	40
4.12	Histogram of error between the tested $V_b$ and optimized $V_b$ in battery B at 60 A charging current. . . . .	40
4.13	$R_0$ with $SOC$ of each testing conditions . . . . .	41
4.14	$R_1$ with $SOC$ of each testing conditions . . . . .	42
4.15	$C_1$ with $SOC$ of each testing conditions . . . . .	42
4.16	$R_0$ fitting curve by using exponential equation . . . . .	43
4.17	$R_1$ fitting curve by using polynomial equation . . . . .	44
4.18	$C_1$ fitting curve by using polynomial equation . . . . .	44
4.19	The modeled $V_b$ and tested $V_b$ of battery A at 120 A charging current. . . . .	47
4.20	Histogram of error between modeled $V_b$ and tested $V_b$ in battery A at 120 A charging current. . . . .	47
4.21	The modeled $V_b$ and tested $V_b$ of battery B at 120 A current. . . . .	48

4.22	Histogram of error between modeled $V_b$ and tested $V_b$ in battery B at 120 A charging current. . . . .	48
4.23	The modeled $V_b$ and tested $V_b$ of battery A at 60 A charging current. . .	49
4.24	Histogram of error between modeled $V_b$ and tested $V_b$ in battery A at 60 A charging current. . . . .	50
4.25	The modeled $V_b$ and tested $V_b$ of battery B at 60 A charging current. . .	50
4.26	Histogram of error between modeled $V_b$ and tested $V_b$ in battery B at 60 A charging current. . . . .	51
4.27	Average error of $V_b$ at any SOC between the modle's estimation and the measurement results of battery A and B. . . . .	52
4.28	The modeled $V_b$ and tested $V_b$ of battery C at 120 A charging current. . .	52
4.29	Histogram of error between modeled $V_b$ and tested $V_b$ in battery C at 120 A charging current. . . . .	53
4.30	The modeled $V_b$ and tested $V_b$ of battery C at 60 A charging current. . .	53
4.31	Histogram of error between modeled $V_b$ and tested $V_b$ in battery C at 60 A charging current. . . . .	54
4.32	Average error of $V_b$ at any SOC between the modle's estimation and the measurement results of battery C. . . . .	55
4.33	Comparison of the $V_b$ estimating error in battery A, B, and C between charging current at 120 A and 60 A. . . . .	55
4.34	All of the samples's energy loss in percentage of total. . . . .	57
4.35	All of the samples's energy loss in percentage of energy comsumtion at that time. . . . .	57
4.36	All of the samples's energy loss in percentage of energy at that time. . .	58
4.37	Energy loss and charging time rescaling comparing with charging current.	59
4.38	Comparison of $V_{OC}$ between testing data and battery balancing model .	60
4.39	Comparison of total energy loss and $\Delta$ SOC in condition 1 for each scheme. . . . .	61
4.40	Comparison of total energy loss and $\Delta$ SOC in condition 2 for each scheme. . . . .	61
4.41	Comparison of total energy loss and $\Delta$ SOC in condition 3 for each scheme. . . . .	62
4.42	Comparison of total energy loss and $\Delta$ SOC in condition 4 for each scheme. . . . .	62
4.43	Comparison of balancing-time and $\Delta$ SOC. . . . .	63

# List of Tables

2.1	The terminal voltage errors of the model in term of statistics [14] . . . .	10
3.1	Numbers of unknown parameters . . . . .	23
3.2	Simulation conditions of the battery balancing energy loss . . . . .	32
4.1	Adj. R-squre of $R_0$ , $R_1$ , and $C_1$ . . . . .	45
4.2	Average error between the model and samples A,B . . . . .	51
4.3	Average error between the model and sample C . . . . .	54
4.4	The energy loss of the battery samples . . . . .	56
4.5	The energy loss and charging time at vary charging current. . . . .	58



# Chapter 1

## INTRODUCTION

### 1.1 Background

Presently, many researchers are interesting in alternative fuel for vehicles. Electric power in electric vehicle (EV) or hybrid electric vehicle (HEV) is a one of several choices which be popular. For example, researchers in NECTEC's laboratory have researched on changing commercial gasoline car to electric car shown in Fig. 1.1. The both kinds of electric vehicles need to use high efficient battery as electrical storage. Some scientists invested several types of rechargeable battery efficiently.  $\text{LiFePO}_4$  battery is a type of the battery that is highly recommended by them to use in the vehicle because it has high energy density (more than 120 Watt-hour per kg.), high power density (up to three time of capacity), high charging current, low self discharging, good safely, and high cycle life. However,  $\text{LiFePO}_4$  battery is sensitive for over charging voltage and discharging voltage. For this reason, it required the battery management system in order to protect the battery failure. Moreover, the battery management system (BMS) has many functions that help users to manage the battery. For example, the monitor function can help users to monitor the battery state detecting in options such as state of charge (SOC), state of health (SOH), voltage, current, and temperature. SOC of the battery is an indicator that presents the amount of electrical charge available at that point compared to the full capacity of a battery. It is expressed in term of percentage. 100% SOC means the battery is full charge, 0% SOC represents empty battery.

Normally, the vehicle's motor requests high voltage. Only one cell of the battery is not enough. For example, the motor used in NECTEC's laboratory (see Fig 1.1) needs more than 300 V to drive but a cell of the battery has about 3 V only, so the users recommend to use many batteries in a parallel pack in order to supply enough voltage. When using many batteries, a problem will occur in SOC of each them. In an ideal

system, if a pack of batteries have been charged or discharged for a long time, the SOC level of each battery is considered to be the same. However in reality, the SOC level of each battery will be different according to charging history [1]. Thus, the batteries in the pack will have unbalance SOC because their characteristics such as self-discharge current, internal resistance and capability are different. For this reason, in order to charge the pack of batteries, it is necessary to have some balancing process. It is one of BMS function called the battery-balancing function.

This thesis focused on a battery-charging and balancing energy loss which is one of big problems that users are concern about. The energy loss is results from two main causes. Firstly, the energy loss appears in the battery itself generally caused by heat, battery efficiency and cycle life. Secondly, the energy loss appears in a current that flows through resistors on balancing system during balancing the batteries. A purpose of this research is to estimate an energy loss in the battery charging and balancing system which will be useful to battery users.



Figure 1.1: NECTEC's laboratory research

## 1.2 Objectives

- To study battery-charging characteristics in order to use in a part of battery-managing determination.
- To estimate the values of energy loss in a battery-charging system.
- To estimate the values of energy loss in a battery-balancing system.

This material is reserved for educational use only, not allowed for commercial use.

Forbidden to modify the content, and cite the document when use.

### 1.3 Scope of Research

- To data LiFePO<sub>4</sub> battery open-circuit voltage ( $V_{OC}$ ), charging voltage ( $V_b$ ), and charging current ( $I$ ).
- To create the battery-charging model and verify it using MATLAB&Simulink.
- To estimate the battery-charging energy loss and simulate battery-charging module for optimizing its energy loss and charging time using MATLAB&Simulink.
- To create the battery-balancing model and verify it using MATLAB&Simulink.
- To estimate the battery-balancing energy loss of three schemes using MATLAB &Simulink

### 1.4 Hypothesis

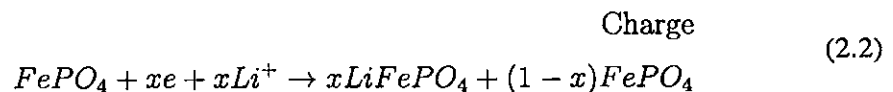
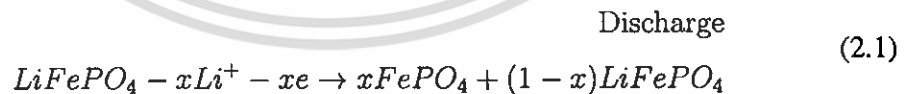
- In case of the battery-charging characteristic test, the testing environment is room temperature. The temperature which is controlled by air conditioner is about 25°C. There is also no cooling system for testing batteries.
- In case of the battery-charging and balancing model, there is assumption that an energy loss occurred by heat transfer is neglect. There is an energy loss in a battery internal resistance and resistance of balancing system only.
- The battery-charging model assumed that the battery characteristic can represent in term of equivalent circuit.
- The battery-balancing model represents ideal Lithium-iron battery which is in an linear formula assuming that the battery internal resistance is constant.

# Chapter 2

## LITERATURE REVIEW

### 2.1 Battery Characteristics and Monitoring

A  $\text{LiFePO}_4$  battery is a type of lithium-ion batteries which has been researched since 1997 founded by Goodenough [2]. Its cathode material made from  $\text{FePO}_4$  obtained by total chemical reaction of  $\text{LiFePO}_4$ . The overall electro-chemical reactions are as following equations. The equations explains when the battery is discharged, the expense of  $\text{LiFePO}_4$  provides electrode and lithium then becoming  $\text{FePO}_4$  as amount of the electrode. On the other way, when the battery is charged,  $\text{FePO}_4$  obtains electrode and lithium becoming  $\text{LiFePO}_4$ . The battery has a characteristic of self-voltage that is not under load of charge called "open circuit voltage ( $V_{oc}$ )". A battery  $V_{oc}$  depends on battery capacity or state of charge. On the research of Wang Jiayuan [3], the authors tested  $\text{LiFePO}_4$  battery by measuring its  $V_{oc}$  at different ambient temperature. This results informed that the open circuit voltage of the battery were related to ambient temperature (see Fig. 2.1).



The voltage, the current, and the temperature measurements are parts of monitoring function in battery management systems (BMS). In addition, there is state of charge (SOC) monitoring, normally SOC level is calculated by coulomb counting  $\int Q dt$  but

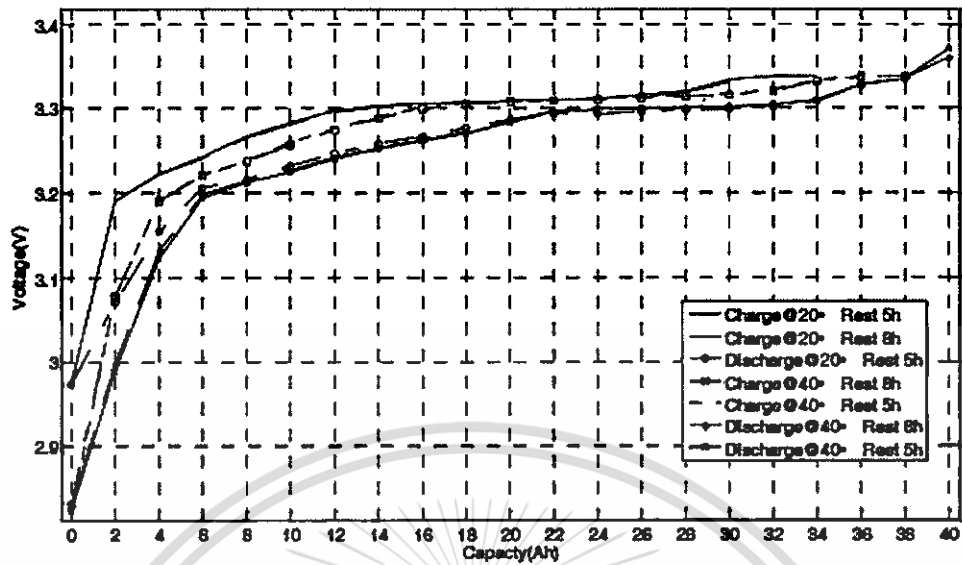


Figure 2.1: OCV @ Different Temperature [3]

a work of Chaoyoung Hou [4] calculated it by using derivative curve ( $\frac{dV}{dQ}$  vs  $Q$ ). This research designed accurate on-line estimation of the SOC. The authors informed that it was perfectly accurate to estimate SOC by using coulomb counting. His algorithm was effective.

Measurement error on state of charge is concerned by battery researcher. Many times had failure of SOC testing accurate results having effect from measurements. A work of Dong Tingting [5] estimated an algorithm based on Kalman filter in order to increase effective testing results. Finally, the authors informed that in order to reduce error from  $\text{LiFePO}_4$ 's battery measurement, it required stronger restriction to the voltage detection. When the algorithm was used, the error was less than the previous one significantly. There were also others algorithm used to estimate SOC level such as Adaptive Cubature Kalman filter [6], Nonlinear Predictive filter [7], and Extended Kalman filter [8]. Extend Kalman filter algorithm is the most popular to be improved by researchers. For example, Liye Wang [9] did research on improving EKF algorithm applied on estimate EV Battery SOC. The author improved EKF algorithm more suitable to the battery.

Moreover, a battery has a cycle life. Its energy capability decreases when a battery is used many times. A measurement that reflects the general of the capability compared its ideal or new one is "State of health (SOH)". Commonly, SOH is equal to 100 % if a battery still remains maximum energy capability. The end of working life in  $\text{LiFePO}_4$  battery is usually about 80 % SOH. A work of Jens Groot [10] tested SOH of  $\text{LiFePO}_4$

battery. Its results showed the SOH of 3 cells at 23 °C and 35 °C ambient temperature are obviously difference. 2 out of 3 reached 80 % after approximately 10000 cycles at 23 °C. In addition, the SOH of each cells will change at different ambient temperature. Furthermore, not only cycle times had effect to SOH, but also a battery impedance. The test showed the more battery is used, the more the impedance rises.

## 2.2 Battery Charging Techniques

On-topic of Lithium-ion battery-charging techniques, Jade Fattal [11] reviewed that there were two basic types of charging techniques. At first, there was proposed technique that using battery management systems (BMS) to detect voltage and control current input of the battery. This technique controlled charging current by constant current and constant voltage (CC-CV) (see Fig. 2.2). The second technique was called double pulse charging system which is popular to use for wireless and mobile devices (see Fig. 2.3). Moreover, there were several others technique such as Fuzzy controlled fast charging system, non-isolated boost charger, and Bi-directional power (presently used for Electric Vehicles (EV) and Plug-in Hybrid Electric Vehicles (PHEV)).

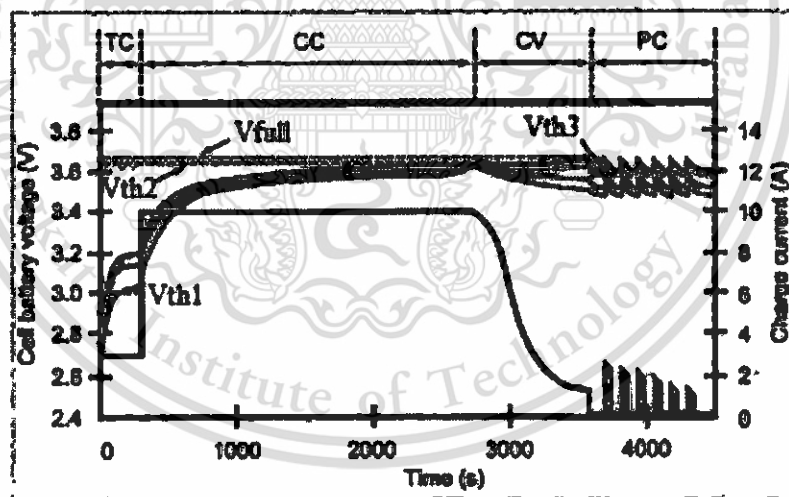


Figure 2.2: Proposed charging process of  $\text{LiFePO}_4$  (implementation of charger and battery management system for fast charging technique of the battery in electric bicycles) [11]

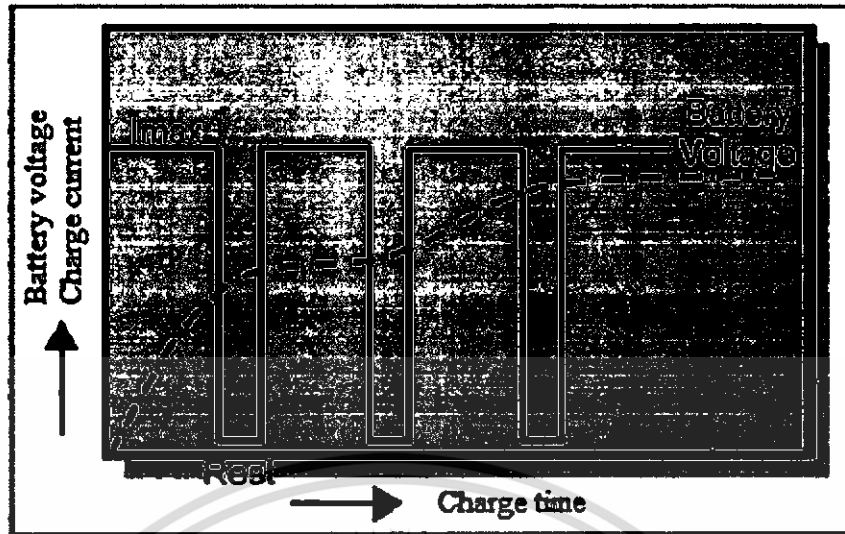


Figure 2.3: Pulse charging (fast charging method for wireless and mobile devices using double-pulse charge technique) [11]

### 2.3 Battery Balancing Techniques

Generally, there are two battery balancing techniques called passive balancing and active balancing. In an ideal system, when a pack of batteries have been charged or discharged for a long time, the SOC of each battery is considered to be the same. This is shown in Fig. 2.4(a). However in reality, the SOC level of each battery will be different according to charging history. This is illustrated in Fig. 2.4(b). Thus, the batteries in the pack will have unbalance SOC. Moreover, their other characteristics such as self-discharge current, internal resistance and capacity are also different. For this reason, in order to charge the pack of batteries, it is necessary to have some balancing process. One of the general battery balancing techniques studied in this project is passive balancing.

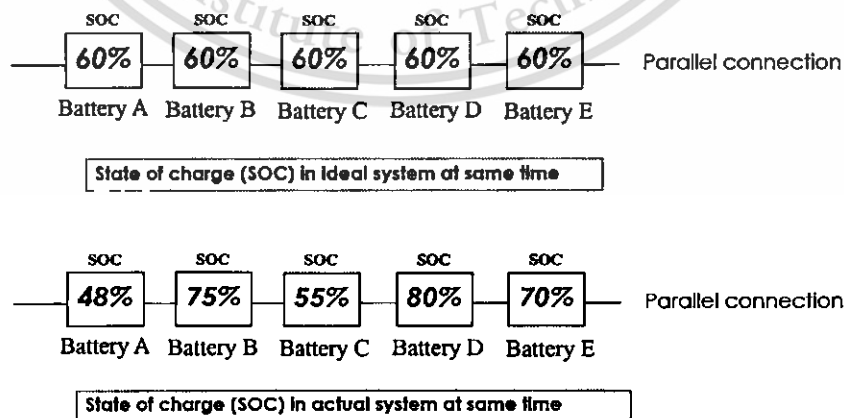


Figure 2.4: SOC in (a) ideal system and (b) actual system.

Moreover, each techniques also has sub-techniques. Mohamed Daowd [12] informed the balancing topologies that passive balancing was separated into two types, fixed shunting resistor and switching shunting resistor. In the other side, active balancing method has 3 different types, capacitor base, inductor/transformer base and converter base. The authors studied the several balancing techniques by simulation in MATLAB&simulink. They briefed details of these topologies then simulated them. After that, they discussed advantages and disadvantages of each topologies by comparison together based on several functions such as circuit design, application, balancing speed,...etc. Finally they got the results of eighteen different balancing techniques. The results informed that advantaged of passive balancing circuit that was used in this thesis had 3 differences compared with others, the first is not expensive, the second is simple to implement with small size, and the last is suitable for hybrid electric vehicle.

Moreover, Siqi Li [13] designed a new low cost direct battery balancing circuit using A multi-winding transformer with reduced switch count called 'MOSFETs'. When it are turned on, an energy at higher SOC battery will flow to lower one directly. According to theirs results, the energy transfer efficiency is above 90 % with the highest efficiency up to 90 %. It's very high efficient comparing with basic passive balancing technique.

## 2.4 Battery Model

Nowadays, in order to improve the charging and balancing batteries more efficiently, researches have tried to estimate the characteristics such as state of charge (SOC) and state of health (SOH) using a battery equivalent circuit. Generally, there are several equivalent circuit models used to represent Lithium-ion batteries. Hongwen He [14] evaluated five equivalent circuit models for state of charge estimation. The models consisted of the Rint, RC, Theven, PNGV, and dual polarization (DP) models, which are shown in Fig. 2.5(a)-(e) respectively. First, the Rint model was a basic battery model including Open circuit voltage ( $V_{oc}$ ), The internal resistance ( $R_0$ ), and the terminal voltage ( $V_b$ ). Secondly, the RC model, designed by SAFT battery company, has two capacitors, which are a surface capacitor ( $C_c$ ) having small capacitance, and a bulk capacitor ( $C_b$ ) represents energy capacity of a battery. The third model is the Thevenin model that has a parallel RC circuit which represents the dynamic characteristics of the battery. The forth one is the PNVG model. It is similar to the Thevenin modle but it has

additionally a capacitor ( $C_d$ ) that represents shifting value of open circuit voltage ( $V_{oc}$ ). The last one is DP model that was improved from the Thevenin model. It represents the polarization characteristics of the battery in term of two RC circuits, the one represents concentration polarization, and the other represents electrochemical polarization. The work showed results of verified model, that the DP model was the best following to the Thevenin, the PNGV, the RC, and the Rint respectively. Figure 2.6 shows the terminal voltage error ( $V_b$  error) between its simulation and experiment and Table 2.1 shows the comparison between the error results of each model in term of statistics. Even if the DP model was the best, the Thevenin model also had very low the error, value of which was almost close to the DP model significantly.

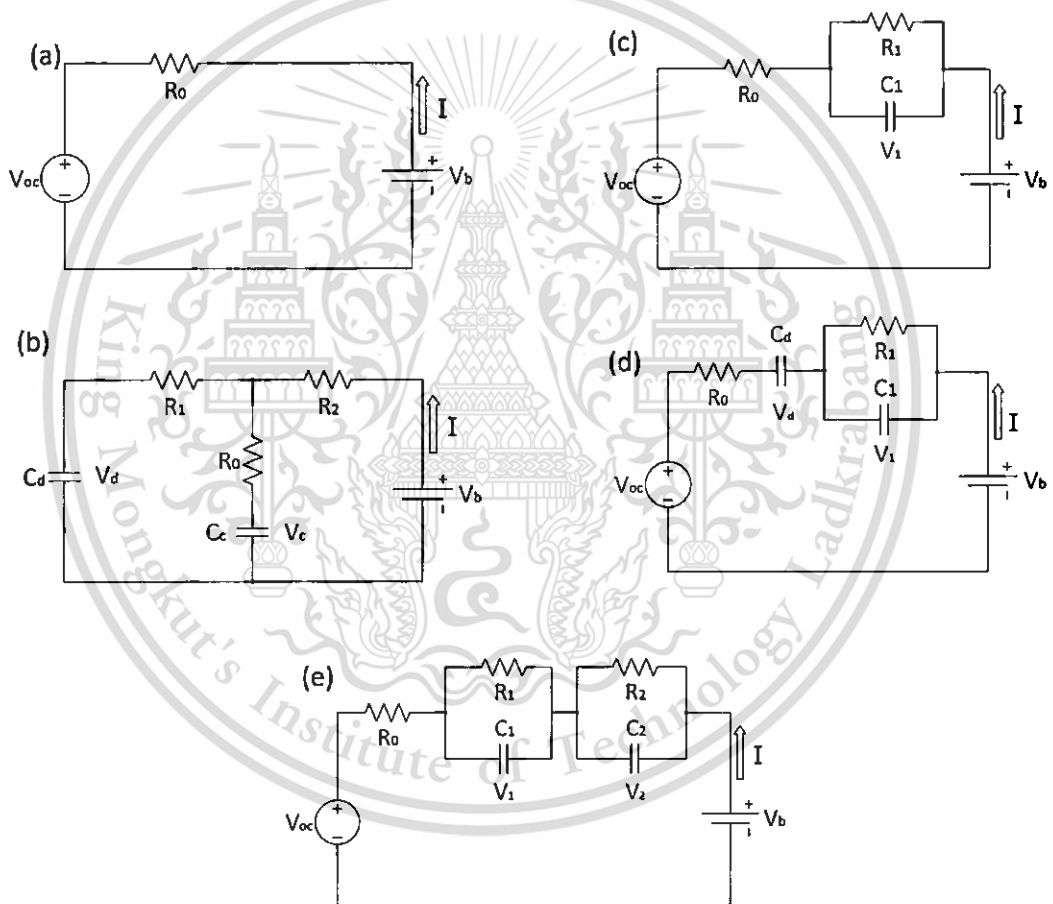


Figure 2.5: Schematic diagrams for Mr. He's evaluating five models, (a) the Rint, (b) the RC, (c) the Theven, (d) the PNGV, and (e) the DP models [14].

Moreover, one of important ideas that used to design battery-charging model in this thesis is works of Y. Hu [15]. The model was designed for identifying electrical and thermal characteristics of lithium ion battery based on equivalent circuit as well. Its parameters were programed on the state of charge, temperature, and current direction.

This material is reserved for educational use only, not allowed for commercial use.

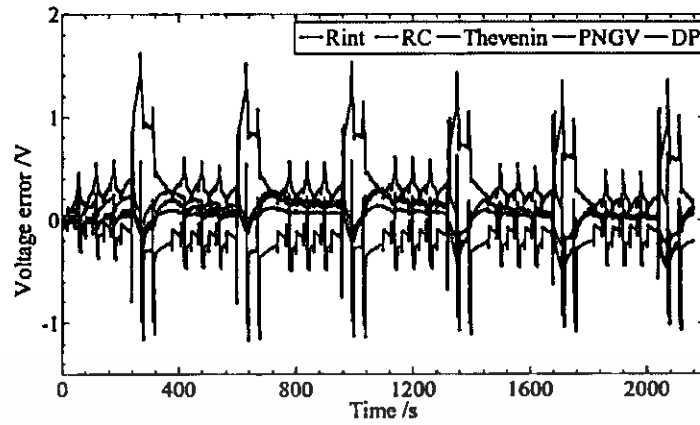


Figure 2.6: The terminal voltage error curves between the simulation and experiment [14]

Model	The Maximum (Volt)	The mean (Volt)	The Variance Volt <sup>2</sup>	Max.Error Rate %
The Rint	1.6229	0.3945	0.0762	2.8176
The RC	1.0785	0.2336	0.0463	2.0337
Thevenin model	0.2967	0.0455	0.0220	0.5151
PNGV model	0.5772	0.0875	0.0243	1.0020
DP model	0.2183	0.0429	0.0021	0.3790

Table 2.1: The terminal voltage errors of the model in term of statistics [14]

Figure 2.7 shows the equivalent circuit of the battery model (that is similar to DP model in work of Mr. He), which is consisted of open circuit voltage ( $V_{oc}$ ), internal resistance ( $R_0$ ), and  $n$  parallel RC circuits.

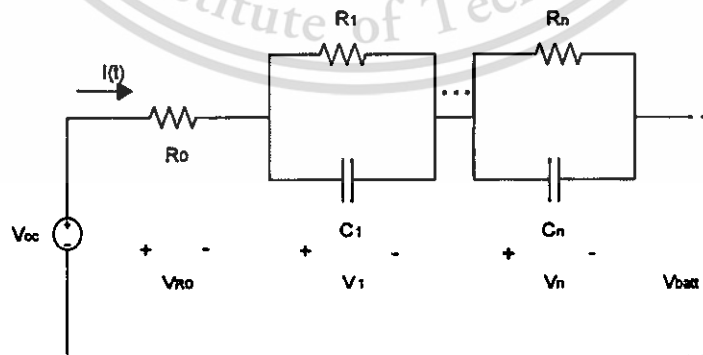


Figure 2.7: The equivalent circuit used for Mr. Hu's battery model [15]

Its equation was expressed as the summation of four voltage components, which

This material is reserved for educational use only, not allowed for commercial use.

are comprised of voltage across the parallel RC circuit ( $V_n$ , voltage across  $R_0$ , open circuit voltage ( $V_{oc}$ ), and the hysteresis voltage ( $V_h$ ). Specially,  $V_h$  represents thermal characteristic of a battery. The authors used a linear spline function in order to fit non-linear parameters. They used a sample of lithium-iron battery to collect data and used optimization method called Genetic Algorithm (GA). Their results verified that the RMS error in the model is less than 26mV efficiently. Moreover, Mr.Hu used the electro-thermal model to estimate real time state-of-charge (SOC) of a battery using linear parameter varying system techniques [16]. This work informed that parameters such as  $R_0$ ,  $R_n$ , and  $C_n$  were nonlinear functions of the SOC. Both the function curves fitting and the estimator used linear parameter varying technique (LPV) based on linear interpolation formula. The basic procedure of this estimator is collect voltage, temperature, and current then calculate SOC level. The advantages of this design are first using less computational load than other estimator. And then, its stability can be confirmed analytically based on inequalities formulas. Finally, user can require the performance of it in terms of convergence and tracking. The authors also concluded that it would the model will work well especially depending on designing the measurement experiment such as the tester temperature which has to control accurately as well as possible.

Another model, which is interesting, is model of Low Wen Yao [17]. This model shown in Fig. 2.8 is also similar to the previous models. Its difference is additional to series resistance ( $R_s$ ), which represented instantaneous voltage drop when the discharge started. In case of model variation, these optimized parameters that were in function of SOC were fit to curves by using exponential formula but this work did not inform their coefficient of determination such as R-squared. However, the result of its verification showed the model is efficient extremely.

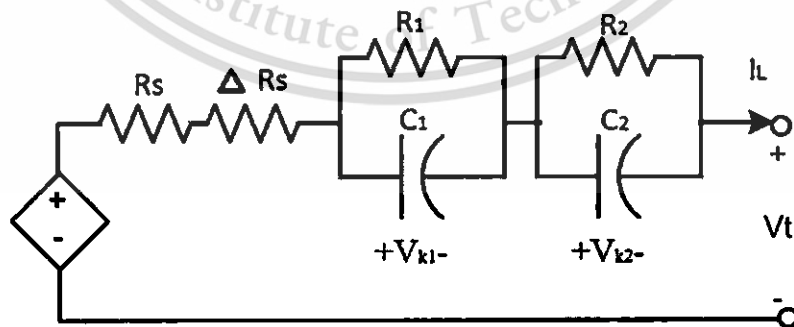


Figure 2.8: The equivalent circuit used for Mr. Yao's battery model [17]

Moreover, there was a advanced battery model that authors designed in a pack [18]. The pack model structure consisted of pack electrical model and pack thermal model. In the pack electrical model, a battery cell model which was basic on the PNGV model (see Fig. 2.5(d)) was defined as a class within the object orientated (OO) simulation environment Dymola, where the model can represent both battery modules and complete battery pack. The cells within a module may be defined to have either a series or parallel connection. The pack thermal model defined cooling circuit consisted of cooling plate passing coolant. The coolant is forced by an ideal pump with a mass flow rate. Its cell thermal model had relationships with SOC and input current. This result showed the pack model can represent voltage and temperature characteristics of real battery pack in Plug-in hybrid electric vehicle efficiently.

Another advanced battery model is a work of Daming Zhou [19]. The authors designed equivalent circuit based on electrochemical model including dynamic phenomena inside the battery. Figure 2.9 shows schematic diagram that can be divided into four regions and its equivalent circuit also represent all of them. The authors presented this model is more accurate than the DP model.

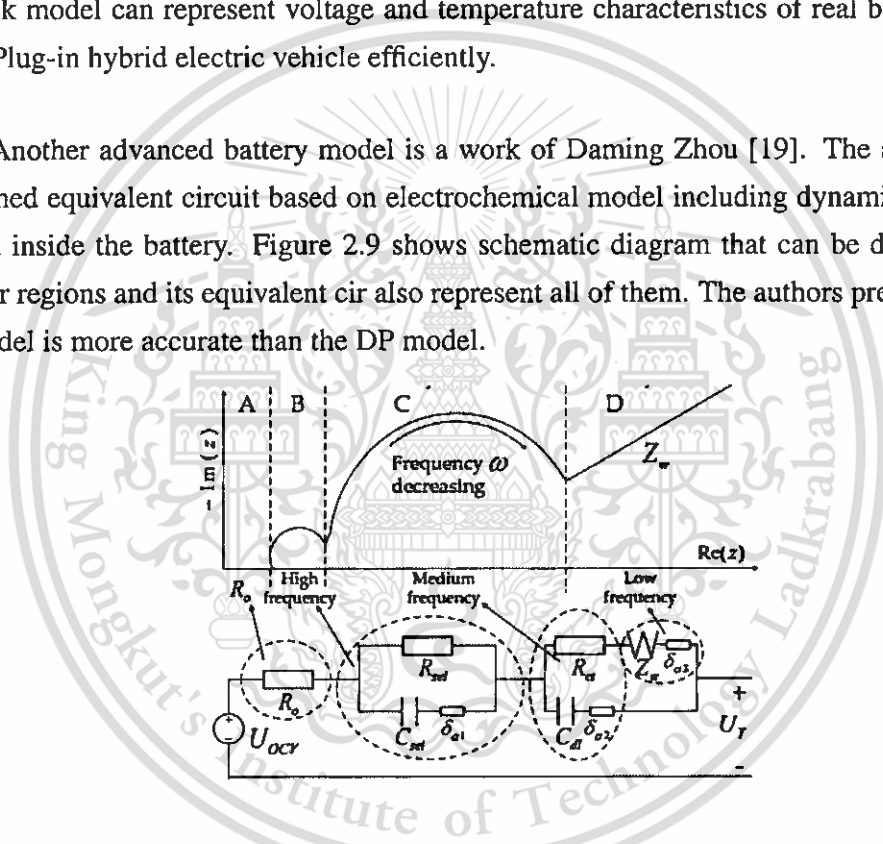


Figure 2.9: Schematic diagram of the battery internal dynamic phenomena and the equivalent circuit [19]

Moreover, there are researchers who improved former battery equivalent circuit to be more efficient. Rixin Xiao [20] applied Fractional Order (FO) method and Integral Order Calculus (IOC) method to the Thevenin and PNGV model as shown in Fig. 2.5(c) and (d). And then, they used the model to estimate SOC using extended Kalman filter (EKF). The result proved that the models that be modified by FOC method can simulate the output voltage and estimate the SOC more precisely.

## 2.5 Battery Energy

Researchers have studied battery energy consumption and loss in order to design a strategies for maximized energy saving. Ernesto Inoa [21] studied the battery energy loss depended on temperature by using the equivalent circuit. The authors used the circuit as the DP models, which is comprised of open circuit voltage, internal resistance, and two parallel RC elements (see Fig. 2.5(e)), including thermal model. The power and energy loss were calculated by using the parameters of the circuit and thermal model. The results showed that the energy loss will be higher if the battery's initial temperature is higher rather than lower as shown in Fig. 2.10. Moreover, they also proved that CC-CV charging method is near optimal in terms of energy loss.

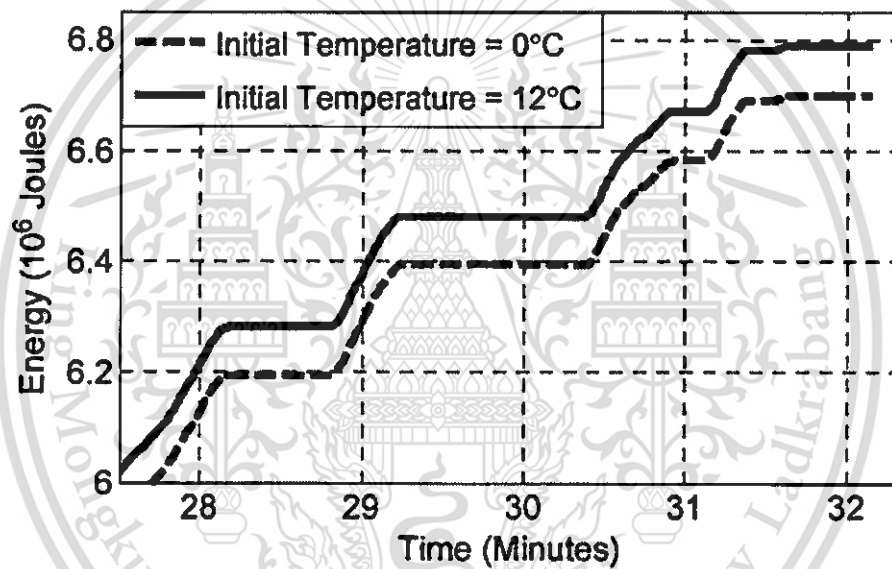


Figure 2.10: Zoom-in of last 5 min of energy supplied by battery when starting from different initial temperatures [21].

# Chapter 3

## EXPERIMENTAL PROCEDURE

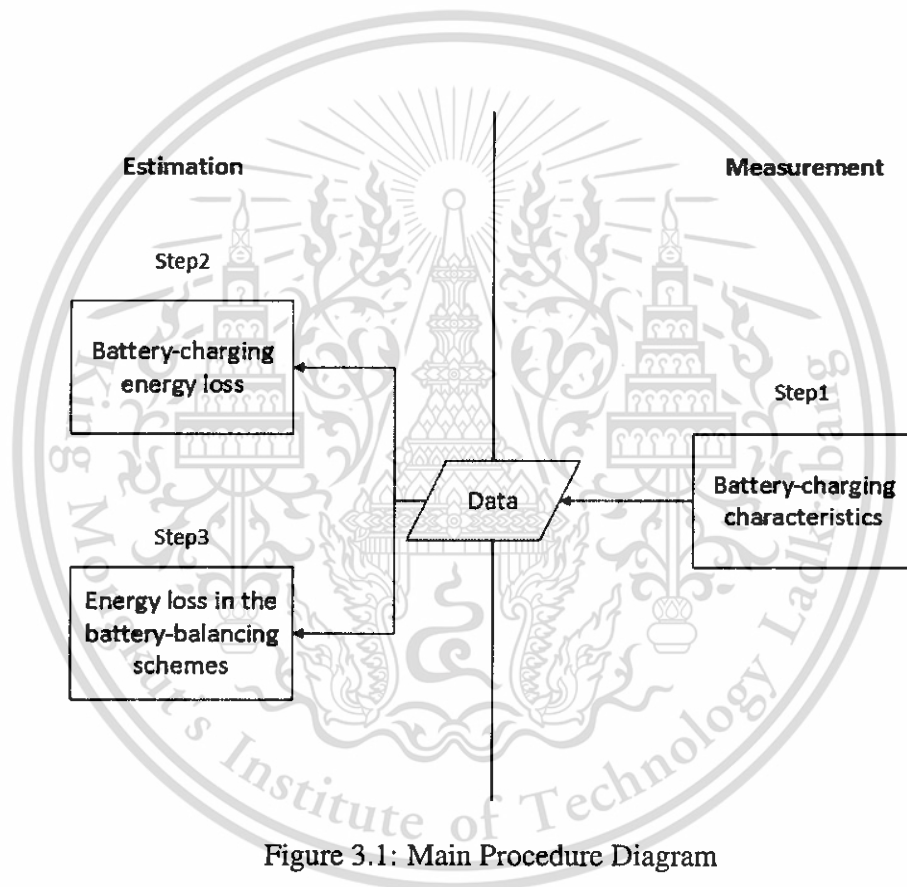


Figure 3.1: Main Procedure Diagram

Figure 3.1 shows main procedure of this thesis is separated into two sections which consist of an estimation of battery-charging energy loss and an energy loss in the battery-balancing schemes. Because the battery's charging characteristics technically need to be used in the both, this thesis is significantly begun by testing the battery charging in order to collect the characteristics before the estimation sections. Samples of battery measured in this thesis were manufactured by Thunder Sky Winston Energy Group Limited. They are  $\text{LiFePO}_4$  type which has formatted cell called prismatic cell as shown in Fig. 3.2. It is encased in semi-hard plastic case. This format is appropriate

This material is reserved for educational use only, not allowed for commercial use.

for large project and mass production due to its simple structure. The battery has 60 Ah capacity.



Figure 3.2: The prismatic cell of LiFePO<sub>4</sub> battery

In the first section, there is a focus of the internal energy loss while the battery is charging. Steps of this part start with creating battery model by using equivalent circuit. After that, the model will be verified by comparing battery's charging voltage from the measuring data. Finally, the energy loss will be estimated by using the model.

The other section focuses on an energy loss in the battery-balancing schemes. A battery model in this section is also created but it has not the same function as the first one. The model represents an ideal battery assuming that there is no energy loss from the battery itself because the second part needs to only focus on the study of the energy loss on balancing circuit. However, steps of this part are almost as same as the first one which consists of the model creating, the model verifying, and the energy loss estimating steps.

### 3.1 Charge Characteristics Tests of the Battery

The objective of the battery-charging characteristics test is to collect data of two important relationships used in steps of creating the battery balancing and charging model. The first relationship is between the open-circuit voltage ( $V_{OC}$ ) and state of charge (SOC). The other is between the charging voltage ( $V_b$ ) and time. Instruments of this test are consist of DC Electronic Loads and DC power supply.

#### 3.1.1 Charge and discharge instruments

Figure 3.3 shows the programmable DC electronic loads. It can be operate range of up to 60 V and 240 A. This instrument is used for discharging the battery to be empty

This material is reserved for educational use only, not allowed for commercial use.

in order to prepare it to charge characteristic test. After finishing discharging battery, the battery should be rest at least a day so as to protect effect of the battery voltage from discharging.

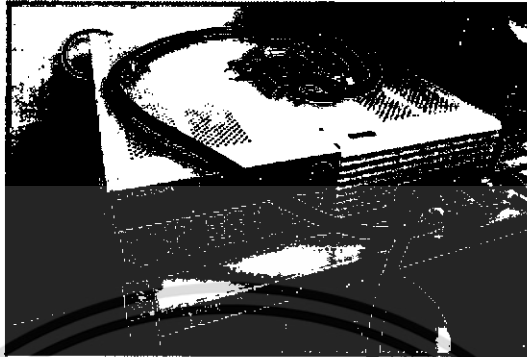


Figure 3.3: The programmable DC electronic loads (the battery-discharging instrument)

The programmable DC power supply (see Fig. 3.4) is used for charging the battery. It can be as multimeter to record charge data such voltage, current, and time. Moreover, it has the application to communicate between the instrument and computer. Its test system designed specifically for testing lithium-iron battery. This system also supports charge in constant current-constant voltage (CC-CV). For this reason, the instrument is suitable to use for this experiment. Figure 3.5 shows the connection of the supply (a) and the load (b) with the battery including its voltage and current measuring position.

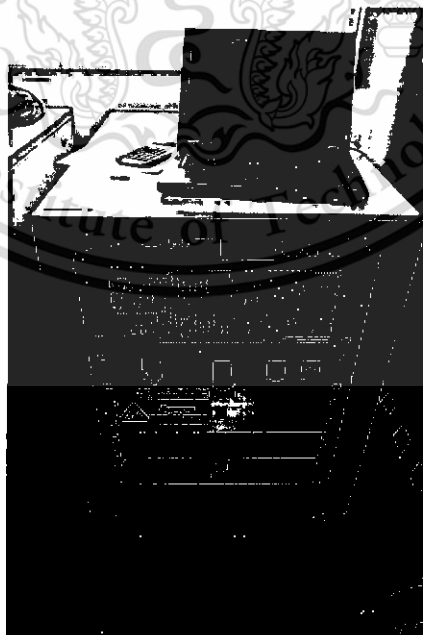


Figure 3.4: The programmable DC power supply (the battery-charging instrument)

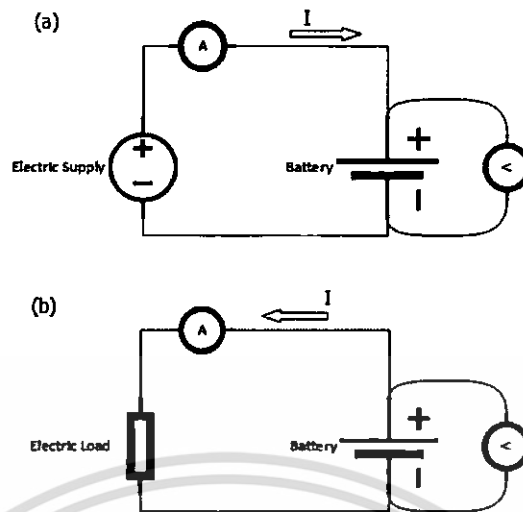


Figure 3.5: the connection between the battery and the instruments

### 3.1.2 Open circuit voltage ( $V_{OC}$ ) test

The open circuit voltage ( $V_{OC}$ ) test has two samples of the batteries in order to data  $V_{OC}$  which can be measured when the battery is not operated (charged or discharged) at least 1-4 hours according to the battery characteristic. This test had 2 conditions varied by charging current, 2C (120 A) and 1C (60 A) respectively. The data was recorded every 5 % of SOC. The steps are as follow:

1. Discharging the samples to empty.
2. Supplying current as the conditions to the samples until its SOC increases 5 % then resting it for 2-4 hours at the time that the battery voltage is nearly not change.
3. Recording theirs battery voltage.
4. Starting step 2-3 again until the samples are full state of charge.
5. Changing charging conditions.

### 3.1.3 Battery-charging voltage ( $V_b$ ) test

The battery-charging voltage ( $V_b$ ) test is record of the batteries voltage and current while the battery is charging continuously in constant current - constant voltage (CC-CV) charging strategy. At first state, the battery is charged by controlling charging current constantly until the battery voltage reaches to limited maximum voltage. This state

is called constant current (CC). After that, the current will be drop slightly but the battery is still in charge till the current can not flow to a battery. The second state is called constant voltage (CV). The CC-CV system is shown in Fig. 3.6. The battery-charging voltage test has three samples of the batteries in 2 conditions varied by charging current at 2C (120 A) and 1C (60 A) respectively. Their data which consists of  $V_b$  and  $I$  is recorded every 4 seconds of charging time.

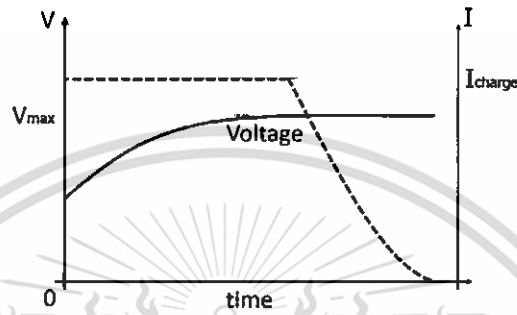


Figure 3.6: The battery voltage and current in constant current-constant voltage (CC-CV) charging strategy

## 3.2 An Estimation of Battery-Charging Energy Loss

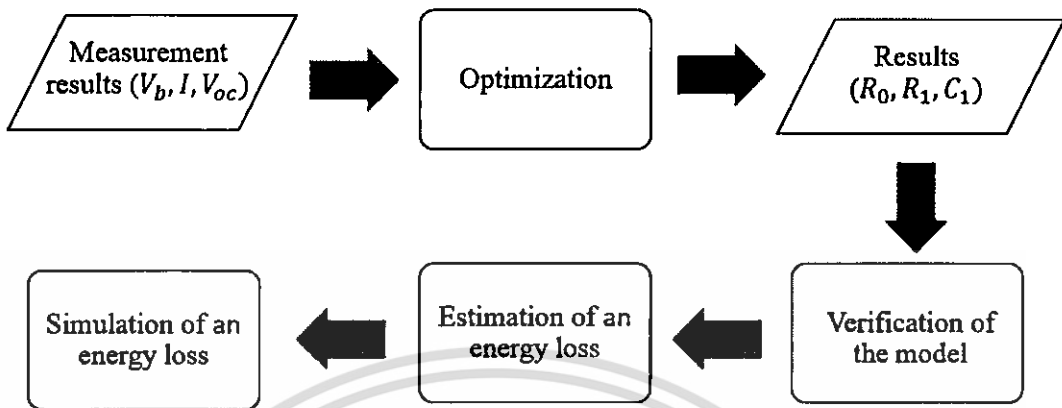


Figure 3.7: The estimation of the battery-charging energy loss procedures

Figure 3.7 shows the brief procedures of the estimation of the battery charging energy loss. First step is a design of the battery model and energy loss equation. Because a study of battery energy loss by using chemical equation is complex, an electric equivalent model is used to represent characteristic of battery. Second step is solve a battery model equation. It has many unknown parameters, so an optimization is a method that help to solve the parameters. After getting the unknown parameters, there is verification of the battery voltage by comparing ( $V_b$ ) from the model and the measurements. Finally, the model after verification is used to estimate and simulate the battery charging energy loss.

### 3.2.1 Battery model and energy loss equation

In case of modeling the battery, the  $RC$  Thevenin's equivalent circuit (see Fig. 3.8) is chosen as the battery model because of three reason; 1) It can represent the battery characteristic efficiently. 2) It is not much complicating to calculate the equivalent equation. 3) It has less unknown parameters than others efficient battery models. The model composes of three parts,  $R_0$ , parallel  $RC$  and  $V_{OC}$  ( open circuit voltage). Beneficially, the  $RC$  circuit represents the dynamic characteristic of the battery. Moreover, the circuit has  $V_{OC}$  which be measured in the test. According to Kirchoff's voltage Law, assuming that a current at counterclockwise direction is positive, the equivalent equation can be written as equation (3.1),

$$V_b = V_{oc} + IR_0 + V_1 \quad (3.1)$$

This material is reserved for educational use only, not allowed for commercial use.

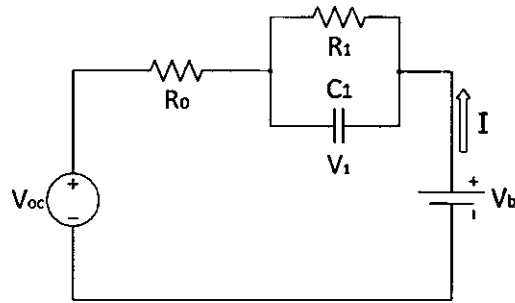


Figure 3.8: Schematic diagram for the Thevenin model

where  $V_b$  is the battery-charging voltage (V),  $V_{oc}$  is the open circuit voltage,  $V_1$  is the voltage drop at  $R_1 C_1$ ,  $R_0$  and  $R_1$  are resistors ( $\Omega$ ),  $C_1$  is capacitor (F),  $I$  is the charging current (A).

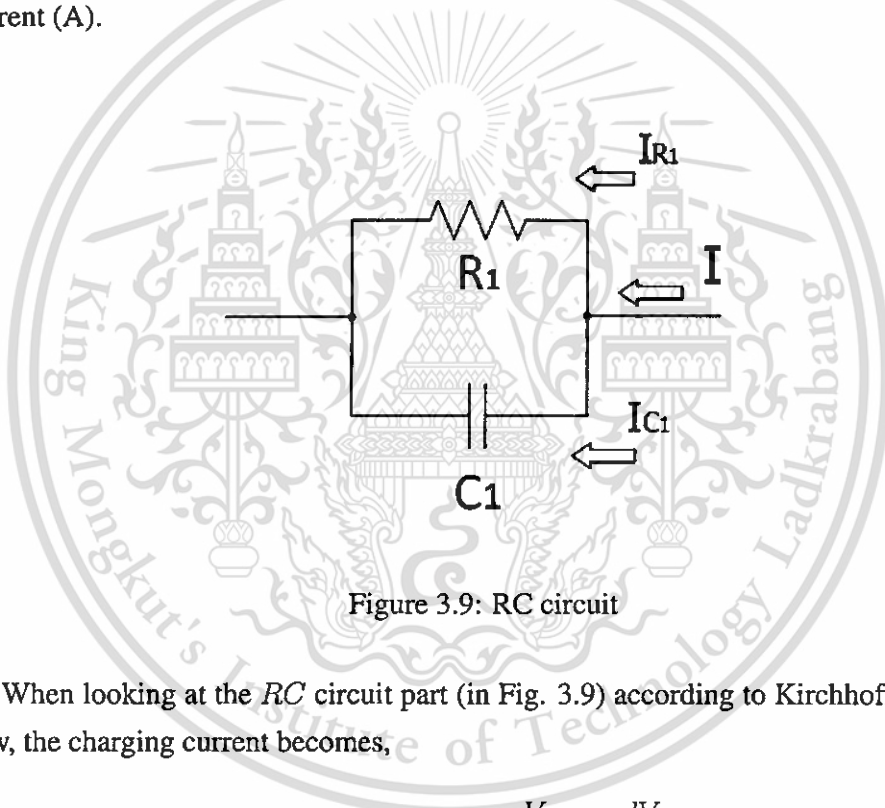


Figure 3.9: RC circuit

When looking at the  $RC$  circuit part (in Fig. 3.9) according to Kirchhoff's Current Law, the charging current becomes,

$$I = I_{R_1} + I_{C_1} = \frac{V_1}{R_1} + C \frac{dV_1}{dt} \quad (3.2)$$

,so equation (3.2) can be written as,

$$\frac{dV_1}{dt} = -\frac{V_1}{R_1 C_1} + \frac{I}{C_1} \quad (3.3)$$

The  $R_1 C_1$  and  $R_0$  represent the internal resistance of the battery so the power loss is shown in equation (3.4).

$$P_{loss} = I^2 R_0 + \frac{V_1^2}{R_1} \quad (3.4)$$

Thus, the energy loss in watt-hour (Wh) is as following equation.

$$E_{loss} = \frac{1}{3600} \int P_{loss}(t) dt \quad (3.5)$$

Moreover, the total power from charging battery can be calculated by using equation (3.6).

$$P_{total} = V_b I \quad (3.6)$$

Thus, the power loss in watt-hour (Wh) is as following equation,

$$E_{total} = \frac{1}{3600} \int P_{total}(t) dt \quad (3.7)$$

### 3.2.2 Parameters programming

Technically,  $V_{OC}$ ,  $R_0$ ,  $R_1$ , and  $C_1$  in this equivalent circuit model are functions of SOC according to equation (3.8). Moreover,  $V_b$  and  $I$  are functions of time ( $t$ ) according to equation (3.9).  $V_{OC}$ ,  $V_b$ , and  $I$  can be measured in the battery characteristics test.  $R_0$ ,  $R_1$ , and  $C_1$  are unknown variable that cannot be measured directly. Furthermore, all of the variables are non-linear functions.

$$\begin{aligned} R_0 &= f(SOC) \\ R_1 &= f(SOC) \\ C_1 &= f(SOC) \\ V_{oc} &= f(SOC) \end{aligned} \quad (3.8)$$

$$\begin{aligned} V_b &= f(t) \\ I &= f(t) \end{aligned} \quad (3.9)$$

According to the equation (3.2) that describes the  $V_1$ , because  $I$  is function of  $t$ , the solution of  $V_1$  is complicated to be solved. For this reason, there is assumption that  $I$  at short period of time is linear so the equation of  $I$  is equal to  $at + b$ . Therefore,  $I$  in equation (3.2) is substituted by  $at + b$ . The integration of  $dV_1$  is shown in equation (3.10) by substituting  $k = V(0)$ . After that, the solution is equal to equation (3.11).

$$\int dV_1 = \int \frac{-V_1}{R_1 C_1} + \frac{(at + b)}{C_1} dt, V(0) = k \quad (3.10)$$

$$V_1 = R_1 b + \exp(-t/(C_1 R_1))(C_1 a R_1^2 - b R_1 + k) + R_1 a t - C_1 R_1^2 a \quad (3.11)$$

by,

$$a = \begin{cases} 0 & t = 0 \\ (I_t - I_{t-1})/(t - t_{t-1}) & \text{else} \end{cases} \quad (3.12)$$

$$b = \begin{cases} I_t & t = 0 \\ I_{t-1} & \text{else} \end{cases} \quad (3.13)$$

$$k = \begin{cases} 0 & t = 0 \\ V_{t-1} & \text{else} \end{cases} \quad (3.14)$$

In order to estimate energy loss, the battery charging model has three unknown variables ( $R_0$ ,  $R_1$  and  $C_1$ ) being in a non-linear function of SOC as shown in equation (3.8). To fit the unknown parameters which are non-linear, a linear spline function is used. A linear spline function is the mathematical function that fit non-linear curve to linear equation by assumption that a non-linear curve is connection of each straight Line following Fig. 3.10. If would like to find  $F(x)$ , the equation is follow to (3.16) and (3.15). In this research,  $S$  is set by 0-100 % SOC at steps of 5 % following to matrix in equation (3.17). The overall unknown parameters are shown in Table 3.1.

$$F(x) = K_0 + \sum_{i=1}^n K_i U_x \quad (3.15)$$

by,

$$U(x) = \begin{cases} 1 & x > s_i \\ \frac{x - (s_{i-1})}{(s_i) - (s_{i-1})} & s_i > x > s_{i-1} \\ 0 & \text{else} \end{cases} \quad (3.16)$$

This material is reserved for educational use only, not allowed for commercial use.

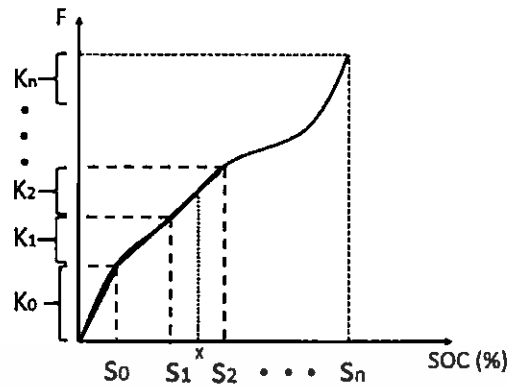


Figure 3.10: Example of a linear spline function

$$[S_0, S_1, S_2, \dots, S_{20}] = [0, 5, 10, \dots, 100] \quad (3.17)$$

SOC is the battery's stage of charge calculated by integrating the current with time (in a second unit). Using the tester capacity (60 Ah), the battery equation is according to (3.18).

$$SOC(t) = \frac{100}{Capacity \times 3600} \int I(t) dt \quad (3.18)$$

Table 3.1: Numbers of unknown parameters

Variables	Parameters	Numbers
$R_0$	$K_0, K_1, K_2, \dots, K_{20}$	21
$R_1$	$K_0, K_1, K_2, \dots, K_{20}$	21
$R_1$	$K_0 = C_1$	1

Table 3.1 shows summary numbers of unknown parameters.  $R_0, R_1$  indicated by linear spline function have both 21 parameters.  $C_1$  indicated by linear function has only one parameter, so there are 43 parameters totally. The reasons that indicating the unknown variables into 43 parameters are computational performance and effect on the unknown variables in error of optimization results. If parameters is set more, a computer will take longer time to process. Moreover, due to trial optimization,  $R_0, R_1$  have more effect on its error than  $C_1$ . For these reasons, the weight of  $R_0, R_1$  is more than the

other.

### 3.2.3 Optimization method and plan

In order to solve the unknown parameters, optimizations is the best choice. It solves the values by systematical computation in order to maximize or minimize a real function (in this case, a real function is  $V_b$  from test). To optimize the unknown parameters accurately,  $R_0$ ,  $R_1$ , and  $C_1$ , an optimization method called "Genetic Algorithm (GA) [22-25]" is chosen. GA method for solving complicated optimization problems that based on natural revolution. GA is efficient procedures for solving large unknown parameters. It is base on evolutionary computation that is a method for moving from one population of "Chromosomes" (in this case, the chromosomes are the 43 unknown parameters) to a new generation. The simple form of GA involves three types of operators: mutation, crossover, and selection. Mutation is the operator which changes some chromosomes in populations. Crossover is the operator randomly exchange a group of chromosomes between two population. Selection is the operator which filters some populations to be a new generation. A basic GA works as follows:

1. Start with a generated population of  $n$  randomly. In this optimization,  $n$  was equal to 200.
2. Calculate the fitness of each population by using the fitness function in equation. (3.19), where  $V_{b,test}$  is the battery voltage from the measurement and  $V_{b,i}$  is the battery voltage from the optimization at time  $i$ .
3. Select population to be individuals by using the stochastic uniform or stochastic universal sampling.
4. Cross over the pair at a randomly chosen group chromosomes from two individuals.
5. Mutate the chosen a chromosome. After individuals pass crossover and mutation steps, they become children.
6. Go to step 2

$$F(i) = \sum_{i=0}^t (V_{b,test} + V_{b,i})^2 \quad (3.19)$$

The measured samples that used in optimization are battery A and B at 120 A and 60 A CC-CV charging current. The optimization will input charging current from the measurements at any time then calculating the battery voltage  $V_b$ . The GA will try to fit  $V_b$  from calculation to the measurement results. The fitness function in equation (3.19) is closer to zero if the GA result is more accurate.

### 3.2.4 Model verification

The  $\text{LiFePO}_4$  battery model will be created after getting the unknown variables from the optimization. In order to verify the battery charging model, all samples of the measurement is used. At first, the battery model is verified by four samples of the battery A and B which were used in GA process in order to check the model is accurate. After that, the model is verified by the others samples of the battery C that does not depend on the GA process in order to check the model can use with others 60 Ah  $\text{LiFePO}_4$  battery cells.

### 3.2.5 Energy loss estimation and simulation

The model will estimate an energy loss of all samples by using equation (3.5). According to the power loss equation (3.4), the power loss is depended on charging current ( $I$ ),  $R_0$ ,  $R_1$ , and  $C_1$ . The variable  $R_0$ ,  $R_1$ , and  $C_1$  are solved by the optimization and  $I$  is from the measurements.

Moreover, the model will be used to simulate the energy loss and charging time at varying charging current. There is assuming that  $I$  during charging time is constant. Its condition is varying  $I$  since 20 A until 180 A at step of 20. Furthermore,  $\text{LiFePO}_4$  battery users have considered about what a value of charging current is suitable for getting low energy loss and fast charging time. Assuming that the users give an equal importance of the charging time and the energy loss, the simulation results will be rescaled by using equation (3.20),

$$x' = \frac{x - \min(x)}{\max(x) - \min(x)} \quad (3.20)$$

where  $x'$  is new scale,  $\min(x)$  is minimum actual scales,  $\max(x)$  is maximum actual scales,  $x$  is an actual scale that needs to rescaling. After rescaling, it can be identified that what charging current is optimal.

### 3.3 An Estimation of Energy Loss in the Battery-Balancing Schemes

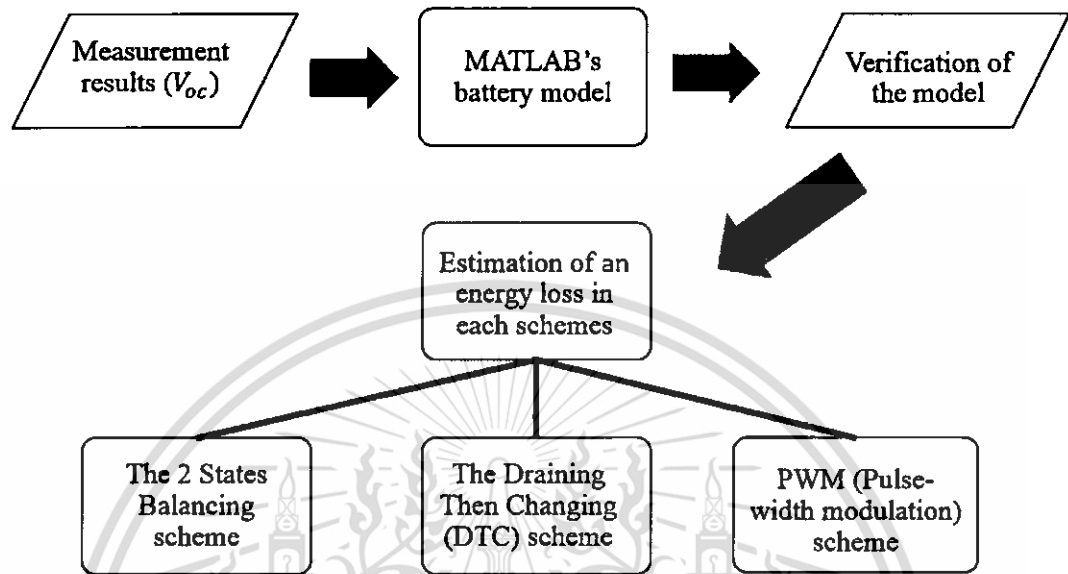


Figure 3.11: The energy loss estimation in the battery-balancing schemes diagram

The energy loss of the battery in the battery-balancing is estimated by using the model in MATLAB&Simulink which is assumed that the battery is ideal. It represents that the energy loss's position occurred on the resistors of balancing circuit only. The energy loss from heat transfer and the battery's internal resistance are neglect. The battery's model will be verified by comparison of  $V_{OC}$  between test and the model's computation. After that, the battery's model is used in the balancing circuits simulation's model. The simulation's model can estimate the energy loss in watt-hour (Wh) unit at the end of battery balancing circuit. Three balancing schemes are used in this research. Each schemes represents five-batteries balancing. Finally, there is discussion between the result of the energy loss of each schemes. The procedure of this section shows in Fig. 3.11

#### 3.3.1 Battery model

The equivalent circuit of Lithium-ion battery which is used in this research is shown below,

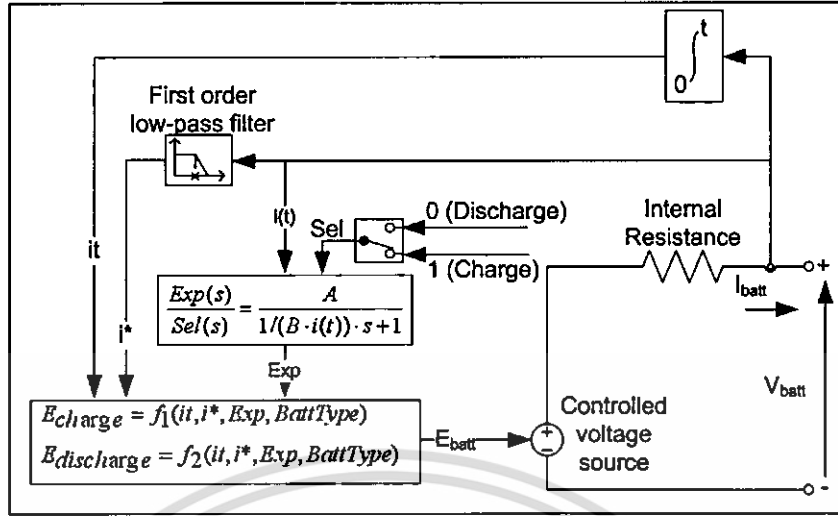


Figure 3.12: The equivalent circuit of Lithium-ion battery[13]

A battery – discharging model ( $i \leq 0$ )

$$f_1(it, i^*, i) = E_0 - K \frac{Q}{Q - it} (i^*) - K \frac{Q}{Q - it} it + A \exp(-B(it)) \quad (3.21)$$

A battery – charging model

$$f_2(it, i^*, i) = E_0 - K \frac{Q}{it + 0.1Q} (i^*) - K \frac{Q}{Q - it} it + A \exp(-B(it)) \quad (3.22)$$

where

$V_{Batt}$  = Nonlinear voltage (V),

$E_0$  = Constant voltage (V),

$Exp(s)$  = Exponential zone dynamics (V),

$Sel(s)$  = Represents the battery mode

( $Sel(s) = 0$  during battery discharge  $Sel(s) = 1$  during battery charging.),

$K$  = Polarization constant ( $Ah^{-1}$ )

or Polarization resistance ( $\Omega$ ),

$i^*$  = Low frequency current dynamics (A),

$i$  = Battery current (A),

$it$  = Extracted capacity (Ah),

$Q$  = Maximum battery capacity (Ah),

$A$  = Exponential voltage (V),

$B$  = Exponential capacity ( $Ah^{-1}$ ).

The details of the equivalent circuit of Lithium-ion battery can be seen in the work of O., Dessaint [25]. The circuit equation is shown in equation (3.21) and (3.22). However, the parameters are modified to represent the battery characteristics which were received from the charge characteristic test.

### 3.3.2 Three schemes of passive balancing

Figure 3.13(a) shows a passive balancing circuit which consists of resistors, a controller, a power source, switches and batteries. The circuit functions as follows. While batteries are charging, the switches are off and the current flows into the batteries only. In case the batteries do not require charging, the switches are on and the current flows passing through a resistor instead of the battery. However, there will be an amount of current drains from batteries and flows through the switch as well. This is shown in Fig. 3.13(b). Thus, the current flows through resistor 1 can be described as in the following equation,

$$I_{R1} = I_s + I_{Batt1} \quad (3.23)$$

where  $I_{R1}$  is the current flows through resistor 1,  $I_s$  is the current supplied from power supply,  $I_{Batt1}$  is the discharged current from battery 1.

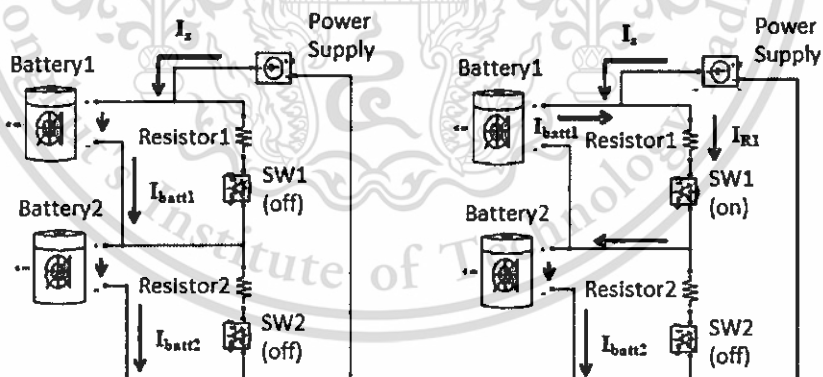


Figure 3.13: The direction flow of current in passive balancing scheme (a) Battery 1 and 2 are charging, (b) Battery 1 is discharging and battery 2 is charging.

The three balancing schemes have been studied in this project are; Two States (normally balancing), Draining Then Charging (DTC) and Pulse-Width Modulation (PWM) scheme.

The Two States scheme (see Fig. 3.14) is a balancing scheme which has two states for balancing the batteries. The first state is performed by fast charging all the batteries with 15 A current until one of the battery's SOC reaches a predefined target point (In this research, 80 % SOC of battery is used as the target point). For example, Fig. 3.14 shows that SOC level of batt1 and batt3 are higher than the others. Thus, the system stops fast charging when one of these batteries reaches the target point. Then, the second state is active. At this stage, the batteries are balancing with 1.4 A current until all of the batteries' SOC level reach the target point. Note that the balancing current in the second state depends on the resistance. In using a 2.5  $\Omega$  resistor, the balancing current is found to be 1.4 A.

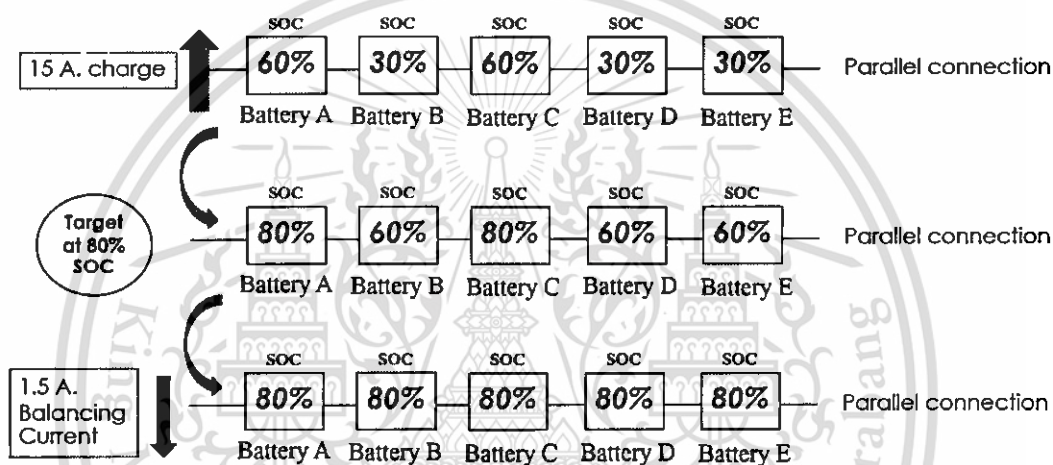


Figure 3.14: Two States balancing scheme of five batteries.

The DTC scheme (see Fig. 3.15), also has two states balancing. However, in the first state, the current is drained from the batteries that have higher SOC level. This process stops when all the batteries obtain the same SOC level at the initial lowest value of all of batteries. For example, batt1 and batt3 drain the current until they have the same SOC level at 1.4 A. This looks similar to balancing batteries but there is no current supplied from power supply. Thus, the current from the battery will flow through the resistor instead of the current from the power supply.

The last scheme is called Pulse-width modulation (PWM) scheme. Duty cycle of each battery charging current is different depending on the amount of the SOC level. In Fig. 3.16, it is obvious that battery 1 has the lowest SOC level of all three batteries. Therefore, it needs to be charged at 100% duty cycle. On the other hand, battery 2 has the highest SOC level so it uses a lower percentage of duty cycle to charge in the same period. The duty cycle equation is used to calculate a suitable time. PWM is used to

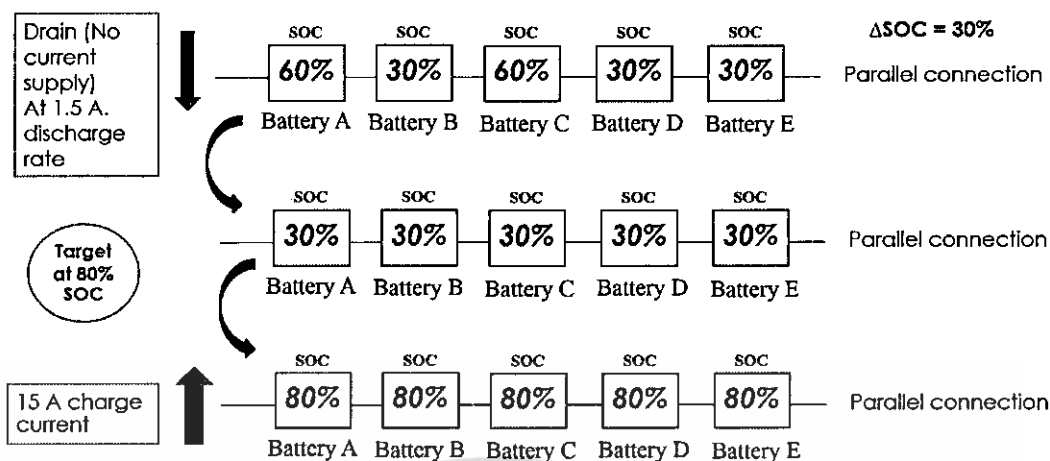


Figure 3.15: The Draining Then Charging (DTC) scheme of five batteries.

assist obtaining the target SOC level of all batteries at the same time. The equation (3.24) is calculated by simulation of charging time of battery model (with 1.4 A of charging current),

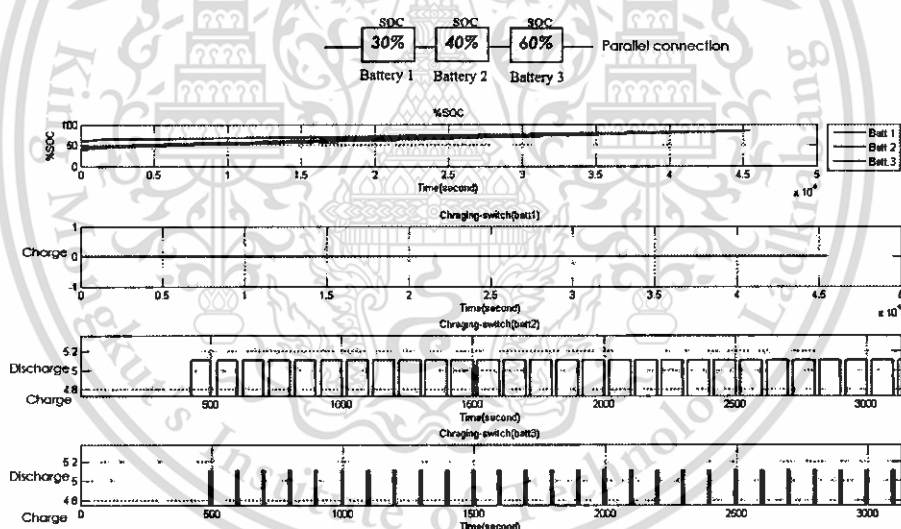


Figure 3.16: PWM (Pulse-width modulation) scheme of three batteries.

$$duty\ cycle = \alpha \left( \beta \frac{SOC_{now}^2}{SOC_{max}} + \gamma \frac{SOC_{now}}{SOC_{max}} + \delta \right) \quad (3.24)$$

where  $\alpha=0.64787$ ,  $\beta=0.01$ ,  $\gamma=1.5041$ , and  $\delta=0.0187$ .

$SOC_{now}$  is an SOC level of the battery at that time instant,  $SOC_{max}$  is maximum SOC level of all batteries at that time instant, and duty cycle is a time of the battery in that period. For example, duty cycle=60 means that the battery is charged for 60 second and then is not charged for 40 second with 100 second period. The parameters  $\alpha$ ,  $\beta$ ,  $\gamma$ , and  $\delta$

This material is reserved for educational use only, not allowed for commercial use.

are obtained from simulated curve fitting of increasing SOC per second and duty cycle.

### 3.3.3 Simulation model and condition

The balancing energy loss is caused by the current that flows through the resistor while the batteries are balancing. In this research, the study of energy loss will be focused only in this case. The corresponding energy loss will be studied using the calculation obtained from the external resistors. Thus, the energy loss depends on the current and the voltage at that particular external resistor. Energy loss is represented in term of watt-hour and can be written as,

$$E_{loss} = \frac{1}{3600} \int I_R V_R dt \quad (3.25)$$

$$Total E_{loss} = \sum_{i=1}^n E_{loss,i} \quad (3.26)$$

where  $E_{loss}$  is the energy loss in watt-hour (Wh),  $I_R$  is the current flows through the resistor  $R$ ,  $V_R$  is the voltage across the resistor  $R$  and  $t$  refers to time in second unit.

MATLAB&simulink is chosen to simulate energy loss of each scheme in Table 3.2. As previous discussion, the simulation of battery's internal energy loss is neglected because the battery model is assumed to be ideal and no internal energy loss. The only energy loss focused here comes from the current flows through each external resistor. This simulation assumed further that temperature has no effects on the batteries and resistors.

Simulation conditions are divided into four conditions (see Table 3.2). The first condition varies  $\Delta$ SOC from 5 % to 40 % with step of 5 % and set the highest SOC level to 60 %. The amount of batteries which have lower SOC level is 1 in order to compare the energy loss from each scheme. In the other conditions, the amounts of batteries which have lower SOC level is changed from 1 to 2, 3, and 4, and are called conditions 2 to 4 respectively. This setup is used for all three balancing schemes.

Conditions	1	2	3	4
<b>Amount of batteries</b>	5	5	5	5
<b><math>\Delta</math>SOC</b>	Varied from 5% to 40% with step of 5%			
<b>Initial lowest %SOC (ILS)</b>	Varied from 20% to 55% with step of 5%			
<b>Amount of batteries having ILS</b>	1	2	3	4
<b>Initial highest %SOC (IHS)</b>	60%			
<b>Amount of batteries having IHS</b>	4	3	2	1

Table 3.2: Simulation conditions of the battery balancing energy loss

# Chapter 4

## RESULTS AND DISCUSSION

### 4.1 The Battery Characteristics

This section shows two results that received from charging characteristics measurement. The first one shows charging open circuit voltage ( $V_{OC}$ ) measuring of two samples of the batteries at two different charging current (60 A and 120 A). The other shows the battery charging voltage ( $V_b$ ) and current ( $I$ ) of three samples of the batteries in two charging conditions using constant current-constant voltage strategy (CC-CV). All measurements had a problem which controlling battery temperature. From observation, the battery voltage and energy storage capability were depended on battery temperature directly. The problem was solved by controlling steady ambient temperature.

#### 4.1.1 The charging open-circuit voltage ( $V_{OC}$ )

Open circuit voltage ( $V_{OC}$ ) measuring results (see Fig. 4.1) inform that every samples of the batteries are nearly same  $V_{OC}$ . Moreover the  $V_{OC}$  is almost steady in the middle range of SOC. At the high range,  $V_{OC}$  value increases rapidly. Furthermore, this measurement shows that  $V_{OC}$  is not relative to charging current if the battery rests for enough time. Each sample of the batteries took different time to get steady voltage. For example, at 90 %SOC and 30 A charging current, battery A and B took about 2 hours and 2.5 hours respectively in order to get steady voltage.

#### 4.1.2 The charging voltage ( $V_b$ ) and current ( $I$ )

Figure 4.2 shows battery charging characteristics of three samples at 120 A charging current. Each current decreased when their voltage raised to limit. Each samples got different current significantly. It can suggest that a internal resistance of each sample was not same according to equivalent circuit equation (3.1),  $V_b$  is summations of  $V_{OC}$ ,

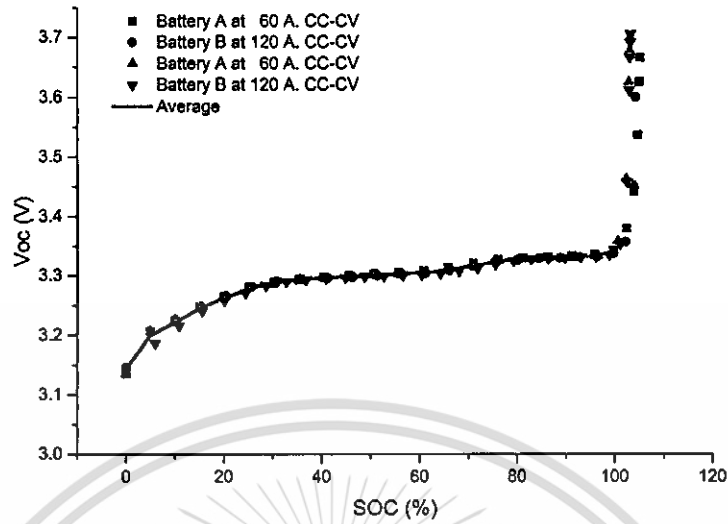


Figure 4.1: The open-circuit voltage ( $V_{OC}$ )

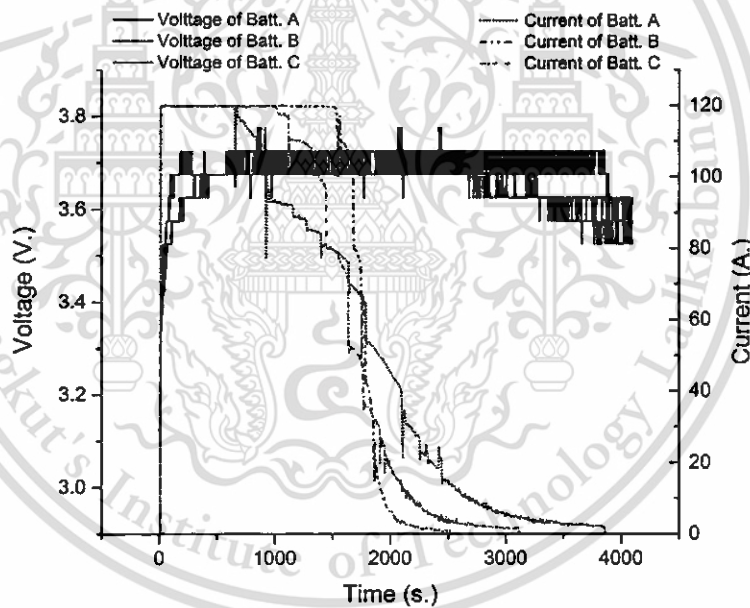


Figure 4.2: The charging voltage ( $V_b$ ) current ( $I$ ) at 120 A.

$V_{R_0}$ , and  $V_{R_1}$ . Because the  $V_{OC}$  of all samples from the result were nearly same,  $V_{R_0}$  or  $V_{R_1}$  values that represent the internal resistance are not same. The current attribute in 60 A current supply is different as well but their voltage rised to limit more slowly than the previous condition.

The SOC of battery charging tests (see Fig. 4.4) shows energy storage capability of each conditions. In ideal battery characteristic, a battery should be fully charge when

This material is reserved for educational use only, not allowed for commercial use.

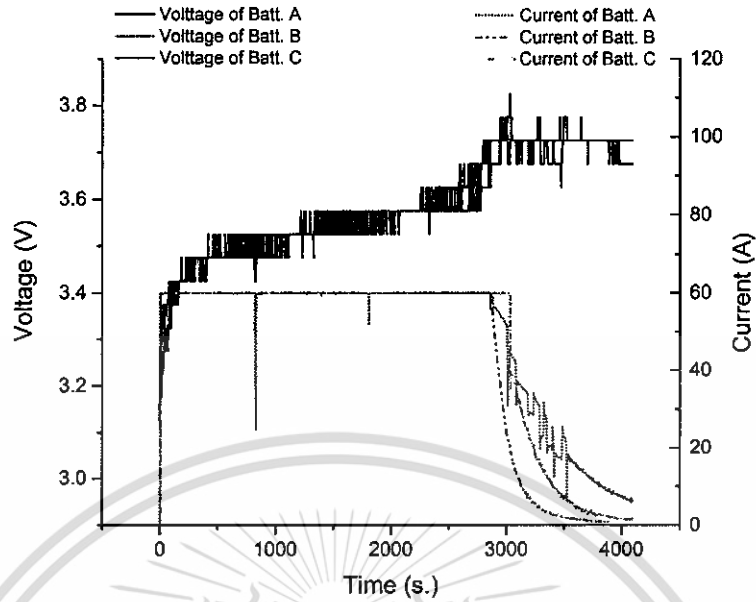


Figure 4.3: The charging voltage ( $V_b$ ) current ( $I$ ) at 60 A.

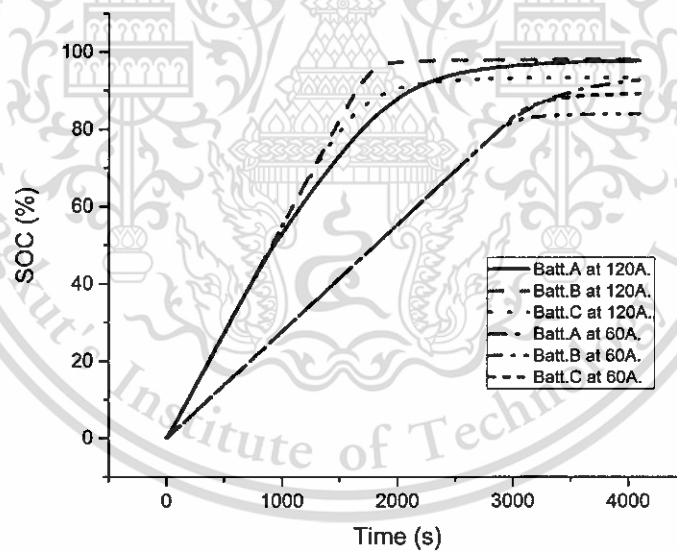


Figure 4.4: The SOC of two conditions

the current increase to zero but it is not true in this case. The samples SOC is not equal to 100 %. Moreover, each sample SOC is not same on different charging conditions. At 120 A charging current, samples SOC is more than at 60 A. It may be caused by uncontrollable variable such the battery temperature, the battery state of health (SOH) , or chemical reaction inside battery.

## 4.2 The Energy Loss from Charging Battery

This section informs the results of the optimization, the model verification, the energy loss estimation, and energy loss simulation respectively. At first,  $V_b$ ,  $I$ , and  $V_{OC}$  in four samples from the measurement were as inputs of the equation to solve  $R_0$ ,  $R_1$ , and  $C_1$  unknown variables by optimization using genetic algorithm (GA). The results will show the effectiveness of GA to solve large unknown variables. After that, the results of the samples were averaged by weight then fitted by curve in order to create LiFePO<sub>4</sub> battery model. And then, the model is verified to check the effectiveness. Checking the model had 2 steps, checking with the samples that used in GA process, and checking with the others samples not depending on GA process. After checking process, the model was used to estimate the battery energy loss by using its equation from equivalent circuit. Finally, the energy loss were simulated by varying charging current.

### 4.2.1 The results of optimization using Genetic Algorithm

The optimization results and theirs error are shown since Fig. 4.5 to Fig. 4.11. Figure 4.5 shows comparison of battery voltage ( $V_b$ ) between the measurement and optimization results of battery A at 120 A charging current. The blue triangle presents optimization error. Its mean error is 0.662 % and maximum error is 3.04 % at about 4000 seconds of charging time. As shown in histogram of this error (see Fig. 4.6), the error is mostly between 0-1 %. Its standard deviation is equal to 0.48.

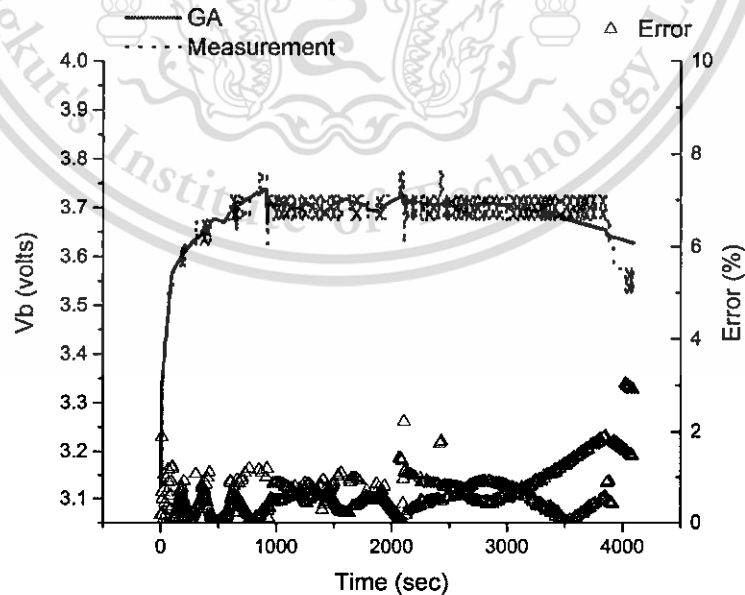


Figure 4.5: The tested  $V_b$  and optimized  $V_b$  of battery A at 120 A charging current.

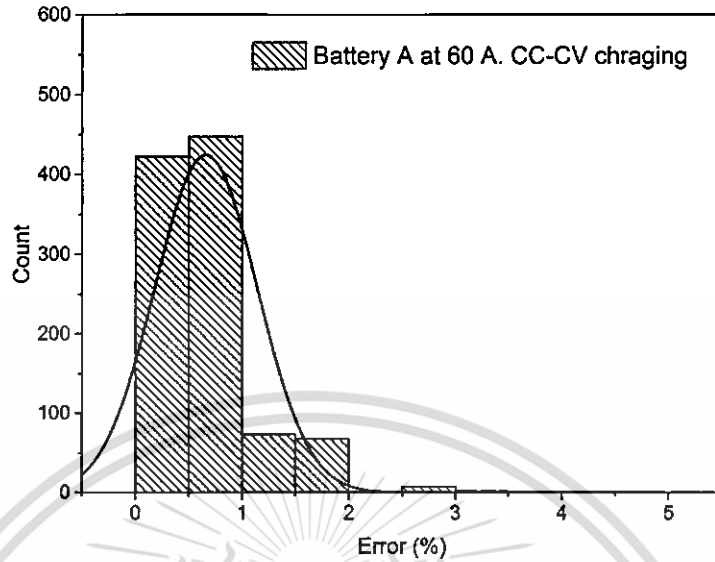


Figure 4.6: Histogram of error between the tested  $V_b$  and optimized  $V_b$  in battery A at 120 A charging current.

Figure 4.7 shows comparison of battery voltage ( $V_b$ ) between the measurement and optimization results of battery B at 120 A charging current. The blue triangle presents optimization error. Its mean error is 0.505 % and maximum error is 4.4270 % at the earliest state of charging time. As shown in histogram of this error (see Fig. 4.8), the error is mostly between 0-1 %. Its standard deviation is equal to 0.403.

Figure 4.9 shows comparison of battery voltage ( $V_b$ ) between the measurement and optimization results of battery A at 60 A charging current. The blue triangle presents optimization error. Its mean error is 0.729 % and maximum error is 3.96 % at 1000 seconds of charging time. As shown in histogram of this error (see Fig. 4.10), the error is mostly between 0-1.5 %. Its standard deviation is equal to 0.573.

Figure 4.11 shows comparison of battery voltage ( $V_b$ ) between the measurement and optimization results of battery B at 60 A charging current. The blue triangle presents optimization error. Its mean error is 0.395 % and maximum error is 5.41 % at the earliest state of charging time. As shown in histogram of this error (see Fig. 4.12), the error is mostly between 0-1 %. Its standard deviation is equal to 0.525.

From optimizing four samples of the batteries, the best converged  $V_b$  by GA is optimization of battery B at 60 A CC-CV charging current. The error shows that the earliest stage has more error than the other state. The maximum error being about 5.4 % and

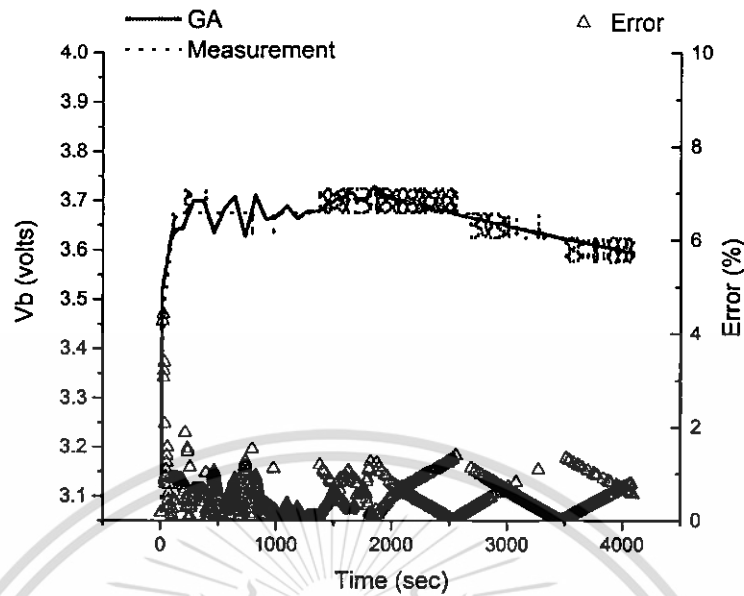


Figure 4.7: The tested  $V_b$  and optimized  $V_b$  of battery B at 120 A charging current.

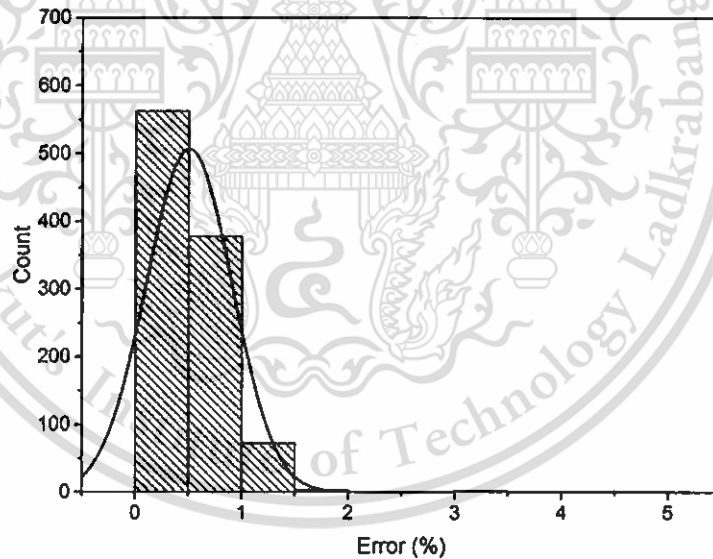


Figure 4.8: Histogram of error between the tested  $V_b$  and optimized  $V_b$  in battery B at 120 A charging current.

its average error being about 0.395 % represents high accurate. Moreover, the worst converged ( $V_b$ ) by GA is in battery A at 60 A CC-CV charging. This maximum error being 3.96 % and this average being 0.729 % also represents high accurate.

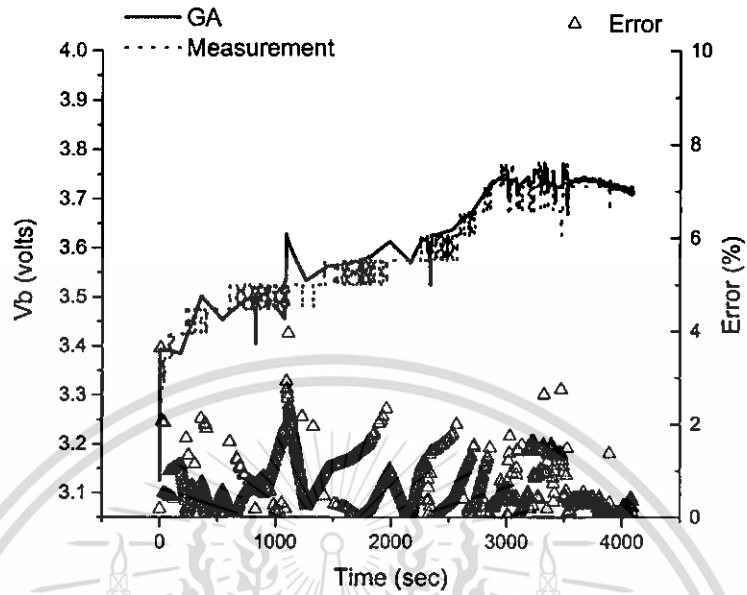


Figure 4.9: The tested  $V_b$  and optimized  $V_b$  of battery A at 60 A charging current.

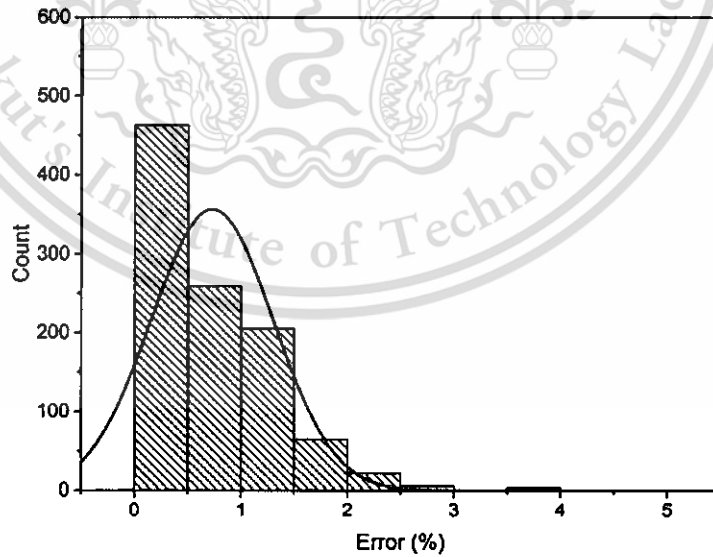


Figure 4.10: Histogram of error between the tested  $V_b$  and optimized  $V_b$  in battery A at 60 A charging current.

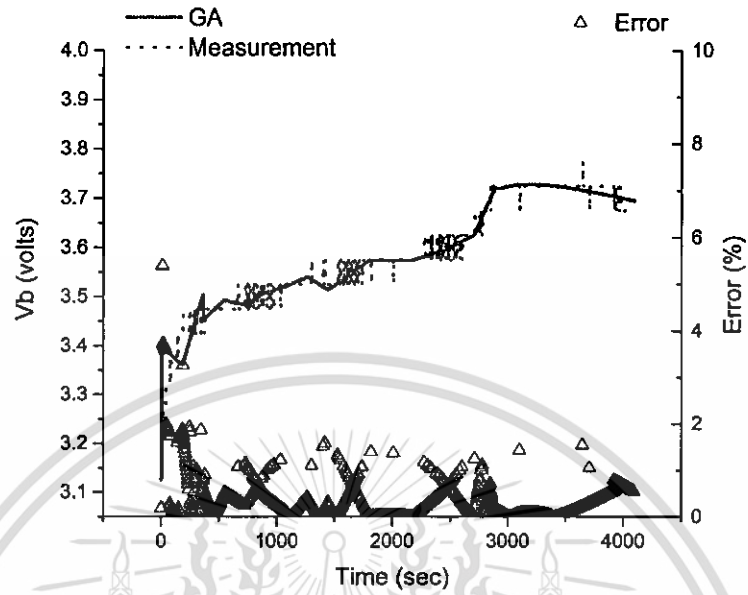


Figure 4.11: The tested  $V_b$  and optimized  $V_b$  of battery B at 60 A charging current.

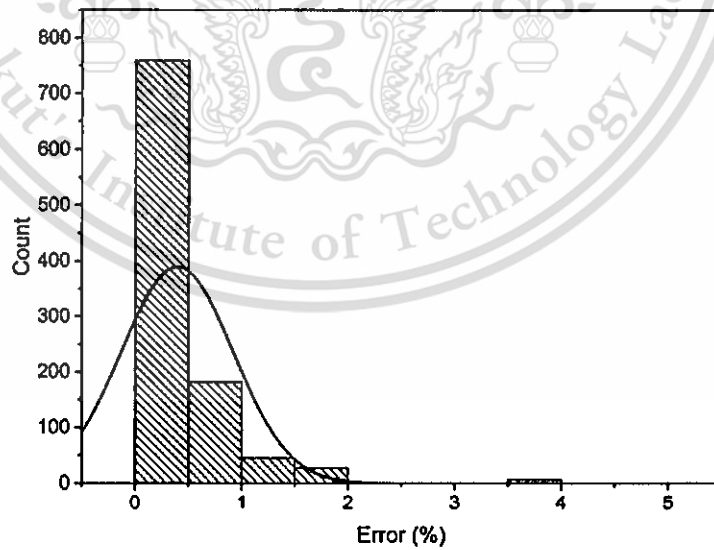


Figure 4.12: Histogram of error between the tested  $V_b$  and optimized  $V_b$  in battery B at 60 A charging current.

The optimization solutions outputted the  $R_0$ ,  $R_1$ ,  $C_1$  in a function of SOC as shown in Fig. 4.13 - 4.15. Test 1 is charging condition at 120 A and 60 A in test 2. As the results showing different parameter values of each battery and each conditions, even though the battery sample is same, the parameters of each SOC are not same at different charging current. For example,  $R_0$  of the battery A at 80 %SOC. charging current in test 1 is more than test 2. It can be conclude while the samples are charging, their characteristics are not same.

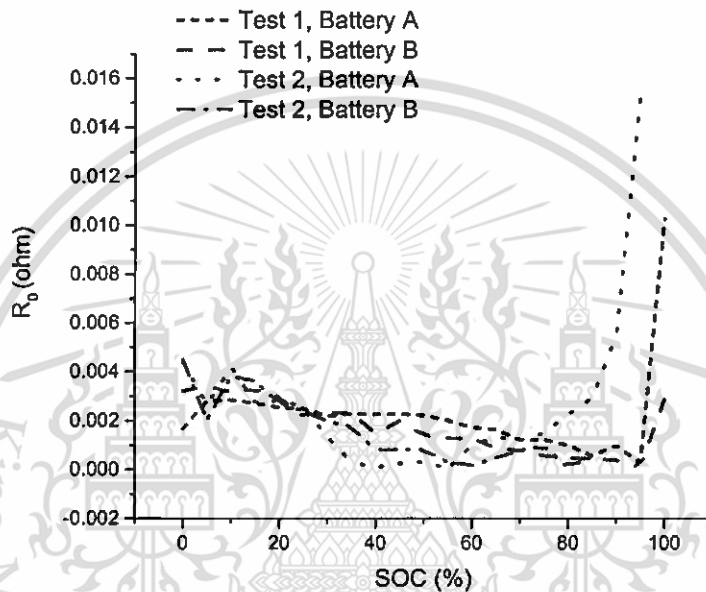


Figure 4.13:  $R_0$  with SOC of each testing conditions

As observation in the results,  $C_1$  values are very high (more than 100 kF) comparing with normal capacitor. It was rechecked that the values of  $C_1$  are reasonable by an energy storage value. An energy storage of a capacitor  $C_1$  is equal to  $\frac{1}{2}C_1 V_1^2$ . It's about 25,000 J. And then, an energy storage of the battery is equal to  $V_b \times Capacity \times 3600$  that is about 760,000 J. Because the energy storage of the battery is quite more than  $C_1$ , it can be conclude that  $C_1$  values are reasonable.

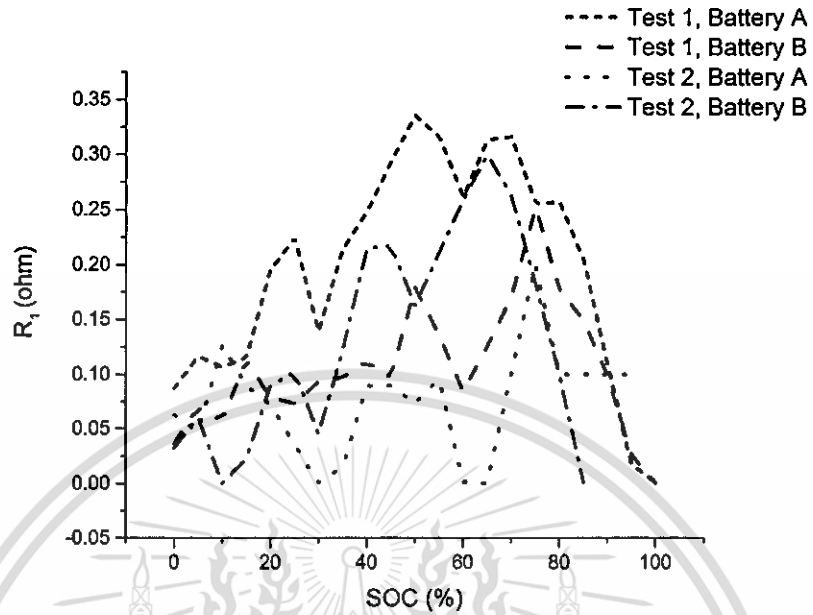


Figure 4.14:  $R_1$  with SOC of each testing conditions

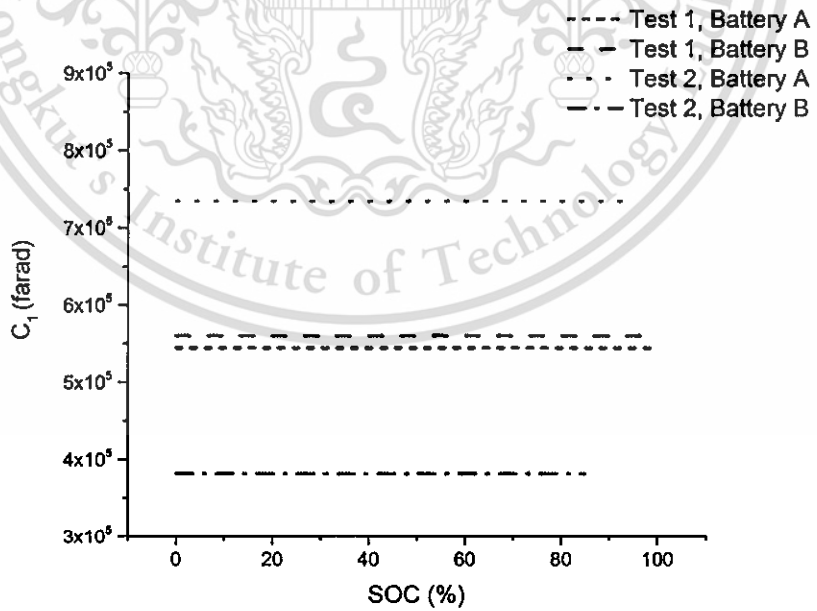


Figure 4.15:  $C_1$  with SOC of each testing conditions

## 4.2.2 Curve fitting of solved variables

In order to identify the variables  $R_0$ ,  $R_1$ , and  $C_1$ , the curve fitting process was used. Curve fitting is the process of constructing a mathematical function that has the best fit to a series of data points. This case used the equations in form of polynomial and exponential curve which present in equation (4.1) and equation (4.2) respectively,

$$F(x) = B_1x^2 + B_2x^2 + \dots + B_Nx^N + c \quad (4.1)$$

$$F(x) = c + A_1e^{(-\frac{x}{K_1})} + A_2e^{(-\frac{x}{K_2})} + \dots + A_Ne^{(-\frac{x}{K_N})} \quad (4.2)$$

where  $N$ =numbers of order. Thus, the curve fitting solutions are shown in fig. 4.16-4.18. The best fitness curve is detect from adj. R-square that was calculated by using equation (4.3),

$$\bar{R}^2 = 1 - \frac{SS_{res}/df_e}{SS_{tot}/df_t} \quad (4.3)$$

where  $SS_{res} = \sum_i^n (y_i - \bar{y})^2$ ,  $SS_{tot} = \sum_i^n (y_i - f_i)^2$ ,  $df_e = n - p - 1$ ,  $df_t = n - 1$ ,  $y_i$  is the value from the measurement,  $\bar{y}$  is mean  $y_i$ ,  $p$  is the total number of explanatory variables in the model (not including the constant term), and  $n$  is the sample size.

According to the results of adj. R-square shown on Table 4.1,  $N$  numbers of  $R_0$ ,  $R_1$ , and  $C_1$  which give best fitness curve of are equal to 2, 5, and 2 respectively.

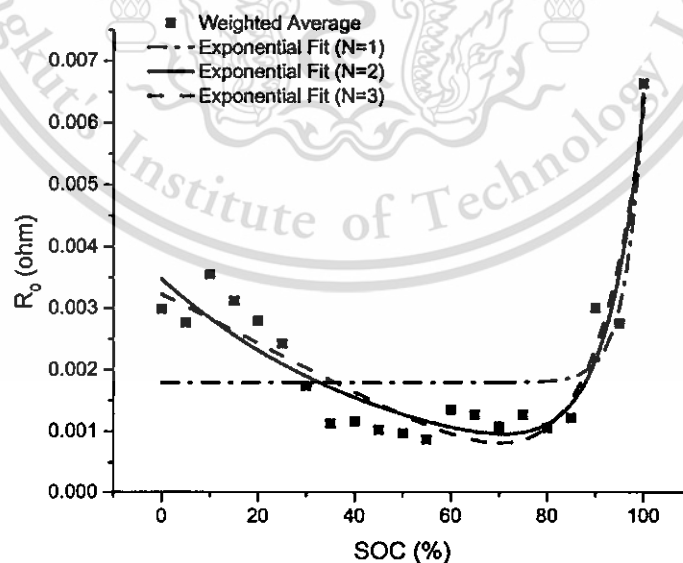


Figure 4.16:  $R_0$  fitting curve by using exponential equation

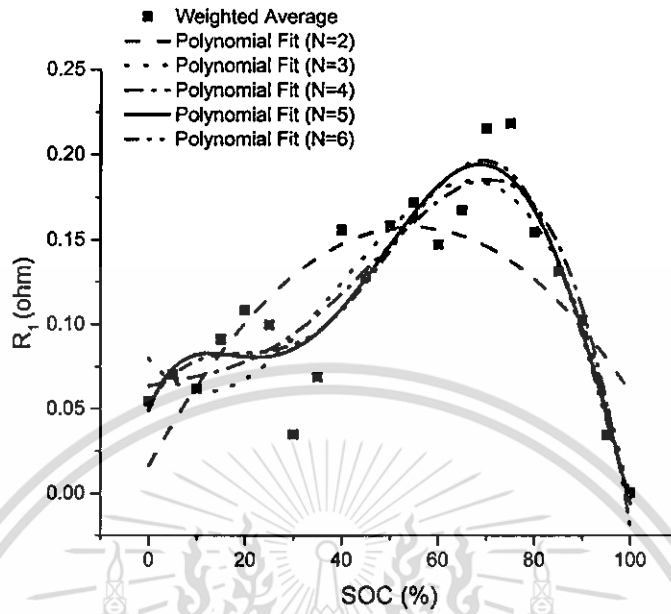


Figure 4.17:  $R_1$  fitting curve by using polynomial equation

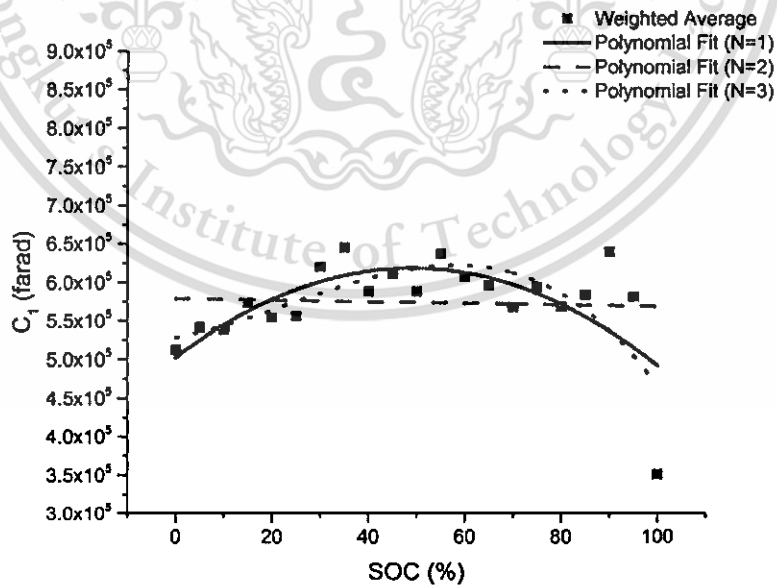


Figure 4.18:  $C_1$  fitting curve by using polynomial equation

N	p	df	SE <sub>est</sub>	SE <sub>est</sub>	Adj. R <sup>2</sup>
<b><i>R</i><sub>0</sub> with exponential fit</b>					
1	2	21	$1.473 \times 10^{-5}$	$3.751 \times 10^{-5}$	0.564
2	4	21	$4.1412 \times 10^{-5}$	$3.751 \times 10^{-5}$	0.862
3	6	21	$4.5366 \times 10^{-5}$	$3.751 \times 10^{-5}$	0.827
<b><i>R</i><sub>1</sub> with polynomial fit</b>					
2	2	21	$3.575 \times 10^{-2}$	$7.088 \times 10^{-2}$	0.044
3	3	21	$1.423 \times 10^{-2}$	$7.088 \times 10^{-2}$	0.764
4	4	21	$1.26 \times 10^{-2}$	$7.088 \times 10^{-2}$	0.778
5	5	21	$1.09 \times 10^{-2}$	$7.088 \times 10^{-2}$	0.794
6	6	21	$1.08 \times 10^{-2}$	$7.088 \times 10^{-2}$	0.782
<b><i>C</i><sub>1</sub> with polynomial fit</b>					
1	1	21	$7.6 \times 10^{10}$	$7.62 \times 10^{10}$	-0.05
2	2	21	$4.282 \times 10^{10}$	$7.62 \times 10^{10}$	0.3754
3	3	21	$4.04 \times 10^{10}$	$7.62 \times 10^{10}$	0.3747

Table 4.1: Adj. R-squre of  $R_0$ ,  $R_1$ , and  $C_1$

### 4.2.3 The model verification

After the curve fitting results, the battery charging model was created. The model can estimate  $V_b$ ,  $E_{loss}$ , and  $E_{total}$  by using equation (3.1) - (3.7). In the model, the variables  $R_0$ ,  $R_1$ , and  $C_1$  at any SOC, are equal to equation (4.4), (4.5), and (4.6) respectively. It was verified by six samples of the batteries. Four of them are the samples which used in the optimization procedure. Their results and errors are shown in Fig. 4.19 - 4.26.

$$R_{0,SOC} = c + A_1 e^{(-\frac{SOC}{K_1})} + A_2 e^{(-\frac{SOC}{K_2})} \quad (4.4)$$

where  $c = 3.19501 \times 10^{-6}$ ,  $A_1 = 1.01256 \times 10^{-6}$ ,  $k_1 = -7.528$ ,  $A_2 = 0.0035$ , and  $k_2 = 49.4921$ .

$$R_{1,SOC} = B_1 SOC^2 + B_2 SOC^2 + \dots + B_5 SOC^5 + c \quad (4.5)$$

where  $c = 0.0493$ ,  $B_1 = 0.00711$ ,  $B_2 = -5.1919 \times 10^{-4}$ ,  $B_3 = 1.5315 \times 10^{-5}$ ,  $B_4 = -1.7101 \times 10^{-7}$ , and  $B_5 = 6.211 \times 10^{-10}$ .

$$C_{1,SOC} = D_1 SOC^2 + D_2 SOC^2 \quad (4.6)$$

where  $c = 501842$ ,  $D_1 = 4766$ , and  $D_2 = -48.6385$ .

Figure 4.19 shows comparison of battery voltage ( $V_b$ ) between the measurement and the model's estimation of battery A at 120 A charging current. The blue triangle presents optimization error. Its mean error is 1.205 % and maximum error is 8.36 % at the earliest state of charging time. As shown in histogram of this error (see Fig. 4.20), the error is mostly between 0-1.5 %. Its standard deviation is equal to 0.98.

Figure 4.21 shows comparison of battery voltage ( $V_b$ ) between the measurement and the model's estimation of battery B at 120 A charging current. The blue triangle presents optimization error. Its mean error is 1.097 % and maximum error is 6.27 % at the middle state of charging time. As shown in histogram of this error (see Fig. 4.22), the error is mostly between 0-1.5 %. Its standard deviation is equal to 1.14.

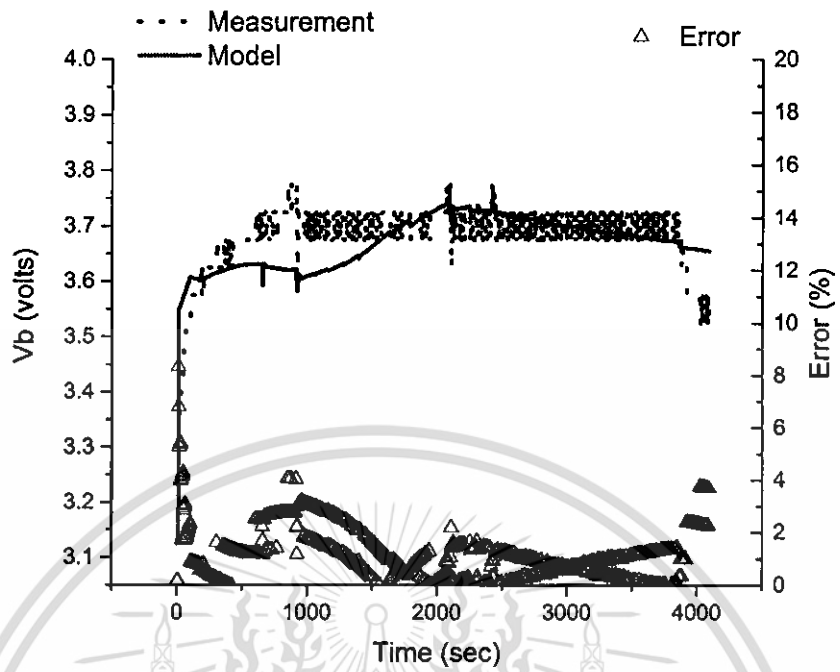


Figure 4.19: The modeled  $V_b$  and tested  $V_b$  of battery A at 120 A charging current.

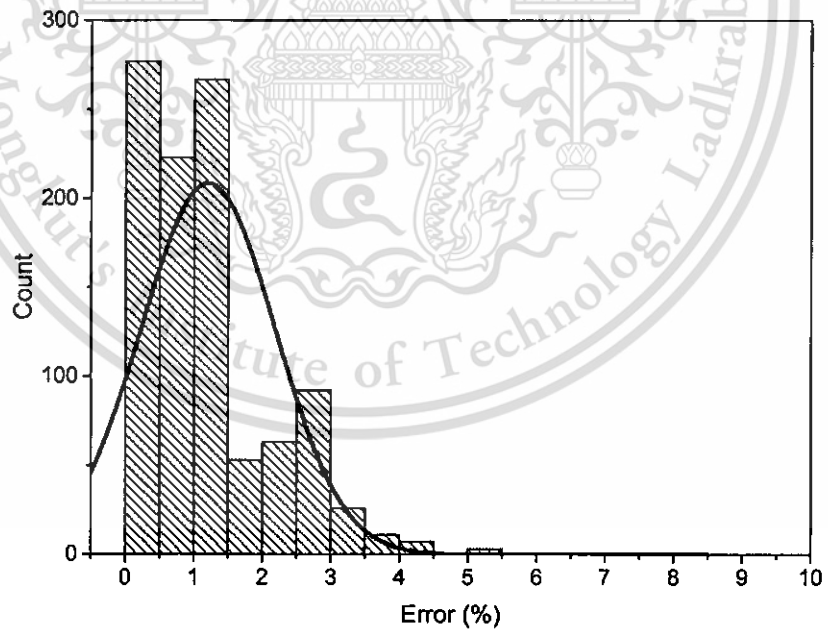


Figure 4.20: Histogram of error between modeled  $V_b$  and tested  $V_b$  in battery A at 120 A charging current.

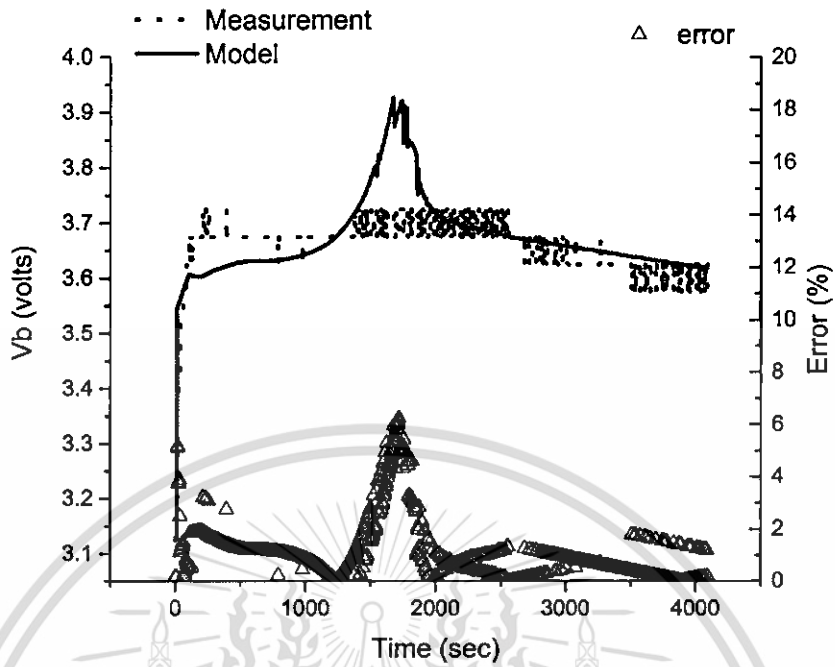


Figure 4.21: The modeled  $V_b$  and tested  $V_b$  of battery B at 120 A current.

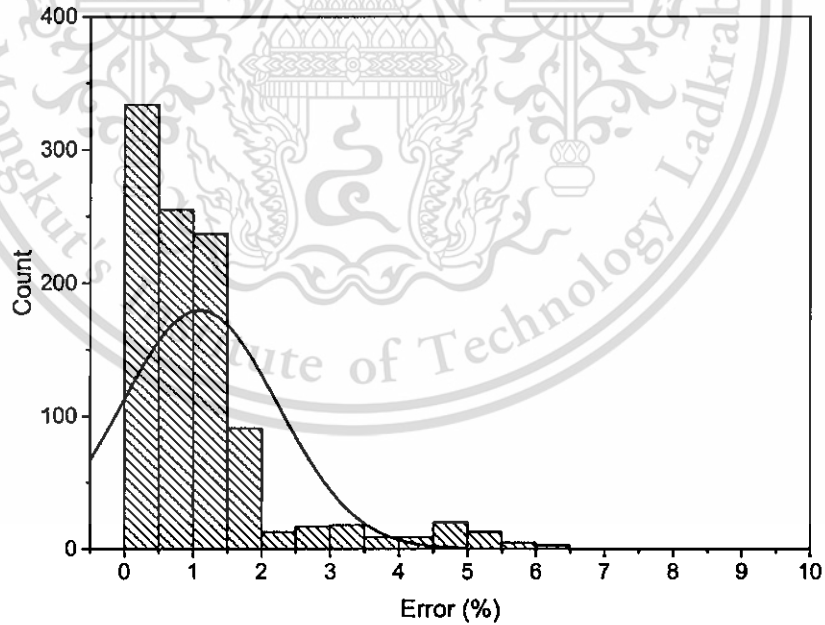


Figure 4.22: Histogram of error between modeled  $V_b$  and tested  $V_b$  in battery B at 120 A charging current.

Figure 4.23 shows comparison of battery voltage ( $V_b$ ) between the measurement and the model's estimation of battery A at 60 A charging current. The blue triangle presents optimization error. Its mean error is 0.634 % and maximum error is 2.34 % at the beginning and ending state of charging time. As shown in histogram of this error (see Fig. 4.24), the error is mostly between 0-1.5 %. Its standard deviation is equal to 0.44.

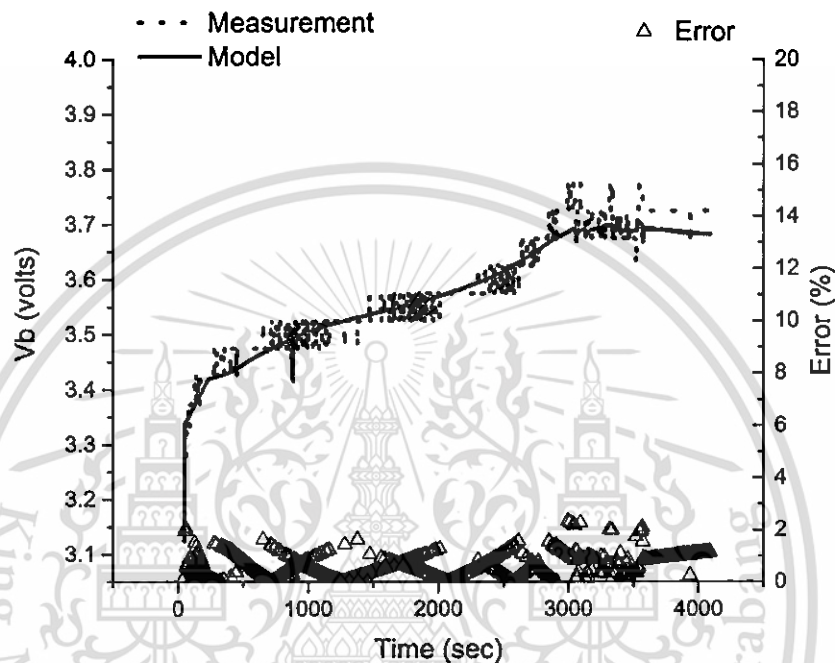


Figure 4.23: The modeled  $V_b$  and tested  $V_b$  of battery A at 60 A charging current.

Figure 4.25 shows comparison of battery voltage ( $V_b$ ) between the measurement and the model's estimation of battery B at 60 A charging current. The blue triangle presents optimization error. Its mean error is 1.1 % and maximum error is 3.78 % at about 3600 seconds of charging time. As shown in histogram of this error (see Fig. 4.26), the error is mostly between 0-2.3 % widely. Its standard deviation is equal to 0.878.

According to the overall errors shown in Table 4.2, the battery A estimation at 60 A charging current has the least error (0.634 % average and 2.34 maximum). The average of all estimations in battery A and B is equal to 1.009 % and their maximum average is 5.19 %. The estimation error is more than the optimization error because of different  $R_0$ ,  $R_1$ , and  $C_1$  variables of the battery in each sample tests. When using the identical variables as the model, the error occurs more. The variable also represents that the battery characteristic is depend on charging current and the battery itself. Moreover, It

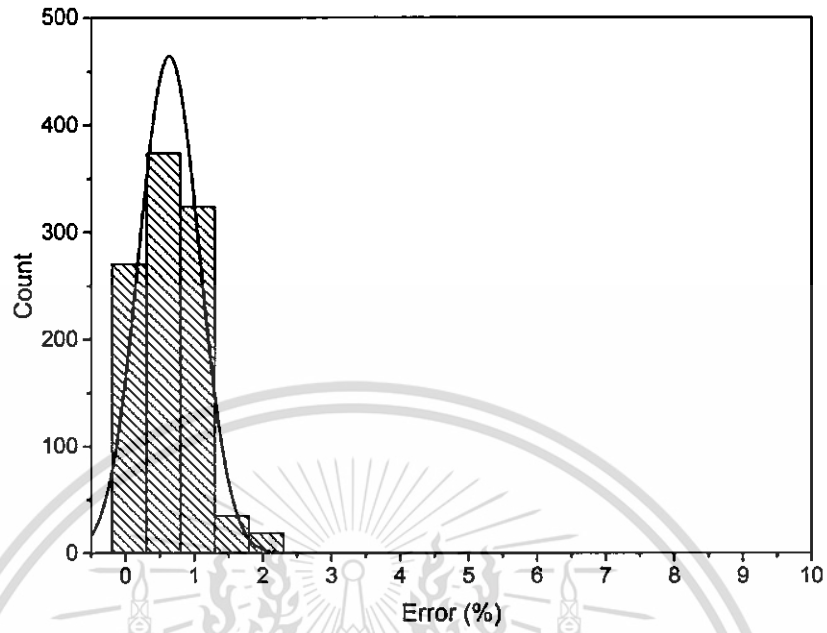


Figure 4.24: Histogram of error between modeled  $V_b$  and tested  $V_b$  in battery A at 60 A charging current.

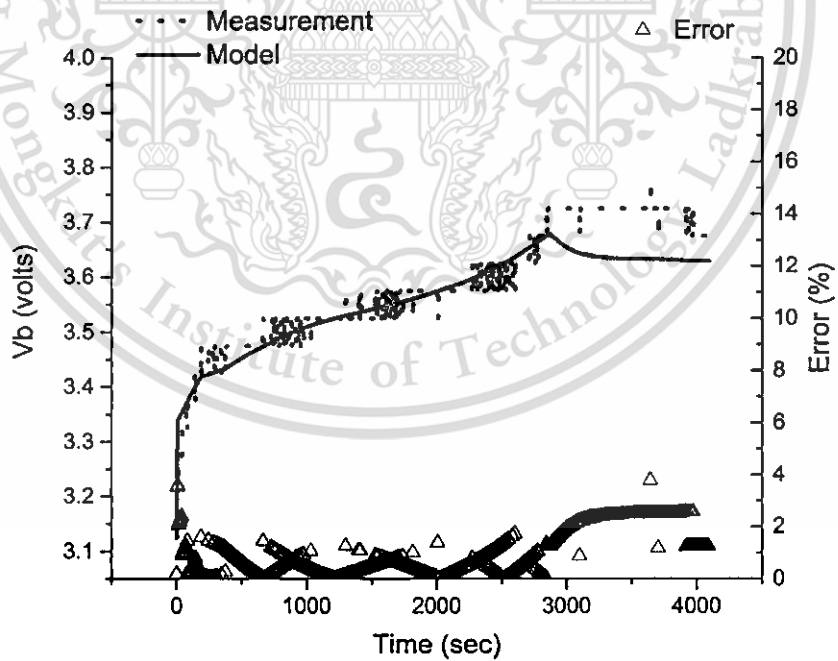


Figure 4.25: The modeled  $V_b$  and tested  $V_b$  of battery B at 60 A charging current.

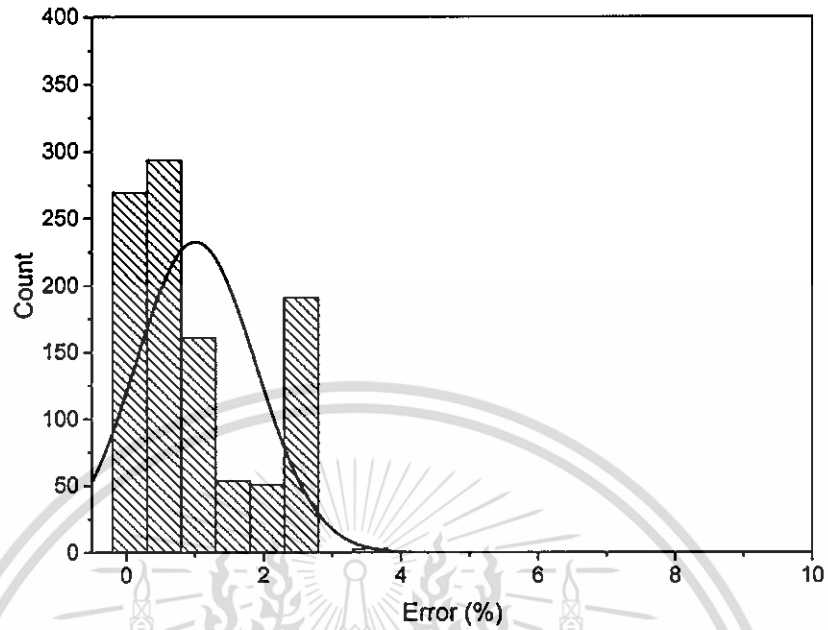


Figure 4.26: Histogram of error between modeled  $V_b$  and tested  $V_b$  in battery B at 60 A charging current.

can be concluded that each cells of  $\text{LiFePO}_4$  have a bit different the internal resistance.

Samples	Terminal	Charging Current	Mean (%)	Std (%)	SD
1	A	120	1.205	8.36	0.98
2	B	120	1.097	6.27	1.14
3	A	60	0.634	2.34	0.44
4	B	60	1.1	3.78	0.878
Average			1.009	5.19	

Table 4.2: Average error between the model and samples A,B

Figure 4.27 showing total average error of  $V_b$  at any SOC presents the most error occurs at 95 % SOC. As observation,  $V_b$  of each samples from the measurements at 95 % SOC are different (more than 1.5 %). That is the reason why the error occurs at 95 % SOC more than the others.

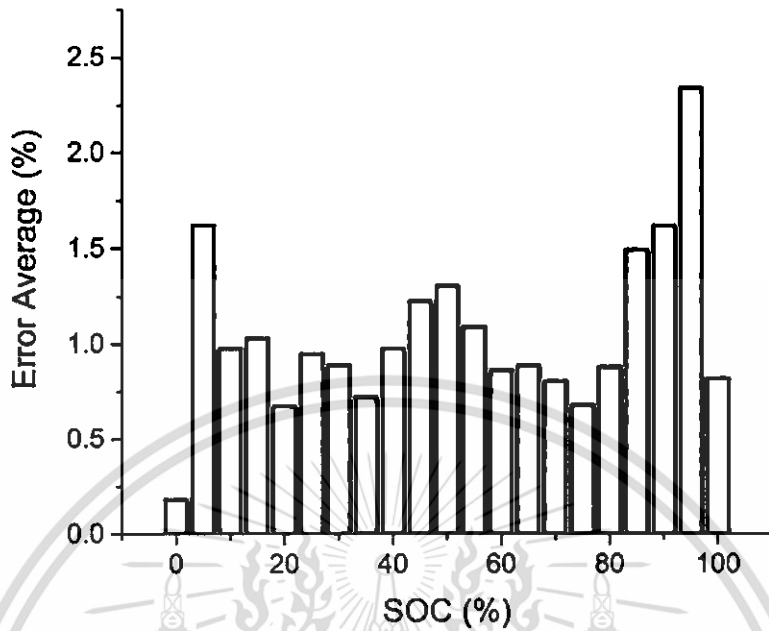


Figure 4.27: Average error of  $V_b$  at any SOC between the model's estimation and the measurement results of battery A and B.

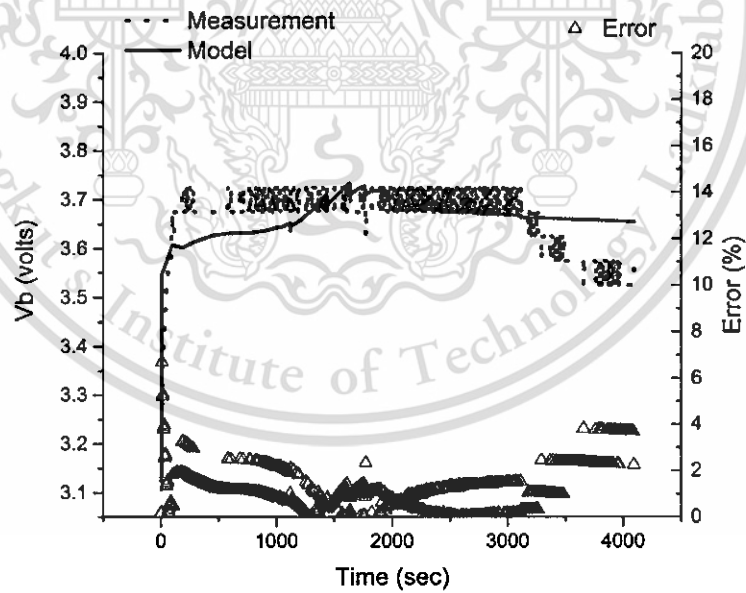


Figure 4.28: The modeled  $V_b$  and tested  $V_b$  of battery C at 120 A charging current.

Moreover, the model is verified by comparing  $V_b$  with the others two samples in battery C which are not used in the optimization procedure. Figure 4.28 shows comparison of battery voltage ( $V_b$ ) between the measurement and the model's estimation of battery

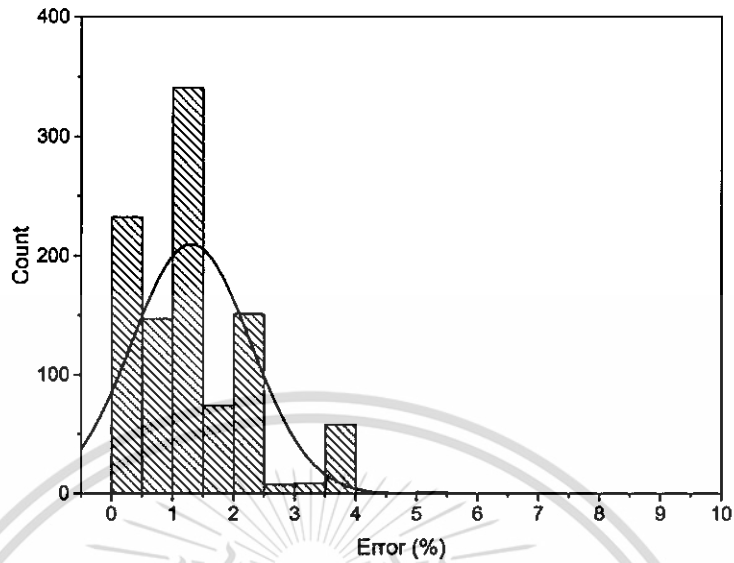


Figure 4.29: Histogram of error between modeled  $V_b$  and tested  $V_b$  in battery C at 120 A charging current.

C at 120 A charging current. The blue triangle presents optimization error. Its mean error is 1.303 % and maximum error is 6.70 % at the beginning of charging time. As shown in histogram of this error (see Fig. 4.29), the error is mostly between 0-1.5 % . Its standard deviation is equal to 0.97.

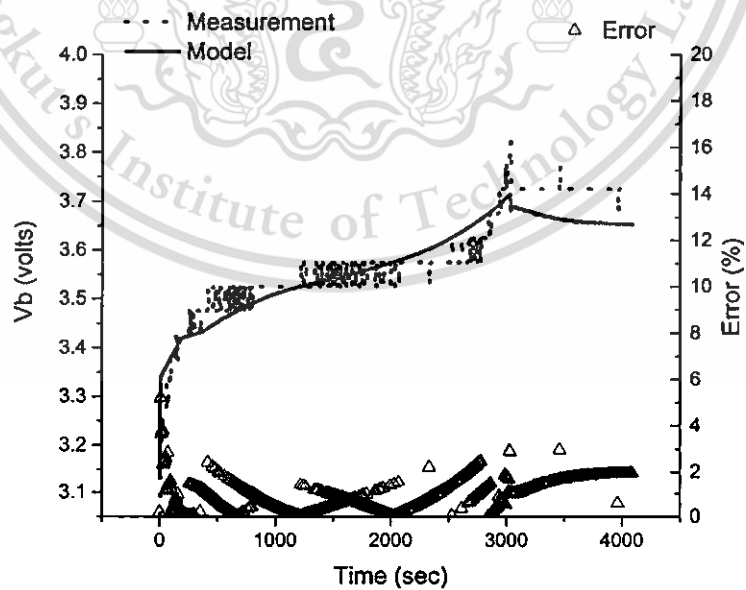


Figure 4.30: The modeled  $V_b$  and tested  $V_b$  of battery C at 60 A charging current.

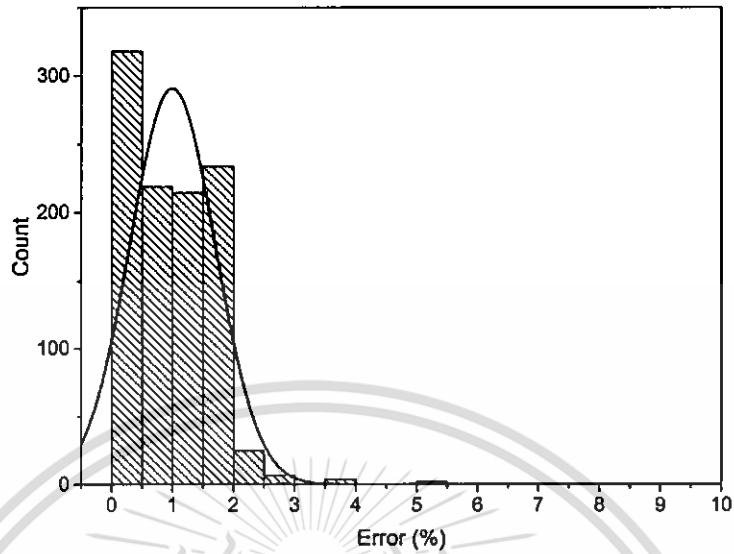


Figure 4.31: Histogram of error between modeled  $V_b$  and tested  $V_b$  in battery C at 60 A charging current.

Battery	Charging Current	Mean (%)	Max (%)	SD
A	120	1.303	6.70	0.97
C	60	0.997	5.23	0.86
<b>Average</b>		1.15	5.965	

Table 4.3: Average error between the model and sample C

Figure 4.30 shows comparison of battery voltage ( $V_b$ ) between the measurement and the model's estimation of battery C at 60 A charging current. The blue triangle presents optimization error. Its mean error is 0.997 % and maximum error is 5.23 % at the beginning of charging time. As shown in histogram of this error (see Fig. 4.31), the error is mostly between 0-2 %. Its standard deviation is equal to 0.86.

According to the overall errors shown in Table 4.3, the average of all estimations in the battery C is equal to 1.009 % and their maximum average is 5.965 %. It represents that the  $V_b$  estimating results of battery C is similar to battery A and B. In Figure 4.27 showing total average error of  $V_b$  at any SOC, the most error occurs at 5 % and more than 90 % SOC. It can be conclude that the model represents the  $\text{LiFePO}_4$  effectively.

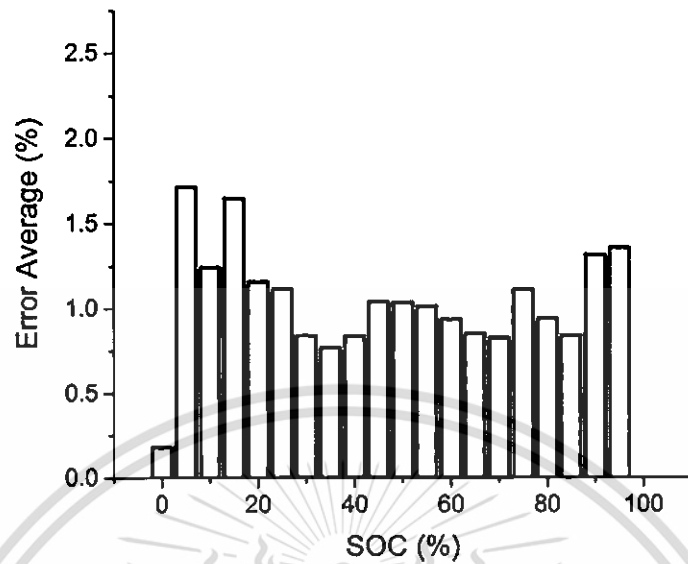


Figure 4.32: Average error of  $V_b$  at any SOC between the model's estimation and the measurement results of battery C.

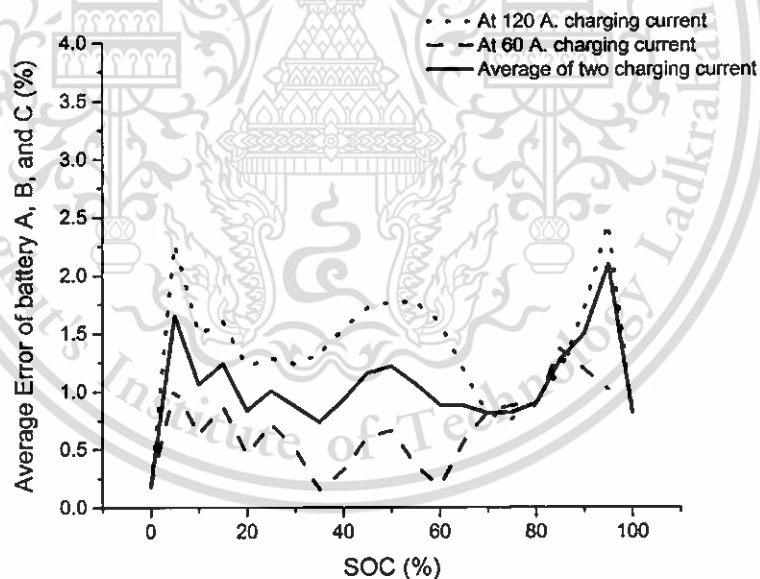


Figure 4.33: Comparison of the  $V_b$  estimating error in battery A, B, and C between charging current at 120 A and 60 A.

Furthermore, when comparing  $V_b$  estimating error in the battery A, B, and C between the charging current at 120 A and 60 A shown in Fig. 4.33, the 120 A charging current has more error than 60 A and the error more occurs at the low and high SOC.

#### 4.2.4 The energy loss estimation results

Table 4.4 and Figure 4.34 show the results of all the sample's energy loss. They represent that the battery at 120 A charging current happens higher energy loss than 60 A. The energy loss is about 6.5 % average at 120 A charging current and about 3 % average at 60 A charging current. It's about two times differently. Moreover, the battery B at 120 A charging current has highest energy loss because its constants current (CC) state takes the longest time according to the measurement results. However, the energy loss of the samples mostly are equal at the same charging conditions. Figure 4.35 shows all of the samples's energy loss in percentage of energy consumption at that time comparing with SOC. The result informs that an energy loss is high at low SOC in which an energy wastes about 12 % of total because the battery at low SOC has higher  $R_0$ ,  $R_1$  and charging current ( $I$ ) than the others. According to  $P = I^2 R$ , the higher  $R_0$ ,  $R_1$  and  $I$ , the more energy loss occurs.

No	Sam.	CC/CV Charge	$E_{\text{measured}}$ (Wh)	$E_{\text{total}}$ (Wh)
1	A	120	12.26	213.31
2	B	120	16.05	216.22
3	C	120	11.61	204.3
4	B	60	5.93	197.75
5	B	60	5.50	178.40
6	C	60	5.79	190.03

Table 4.4: The energy loss of the battery samples

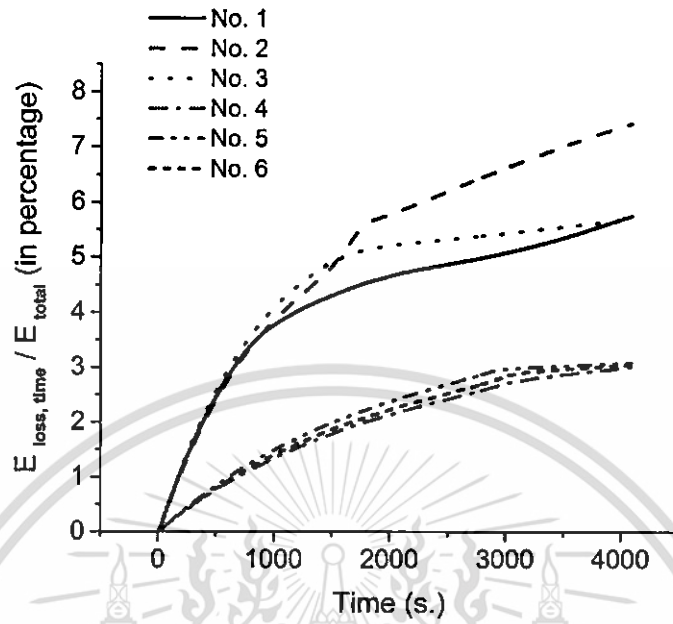


Figure 4.34: All of the samples's energy loss in percentage of total.

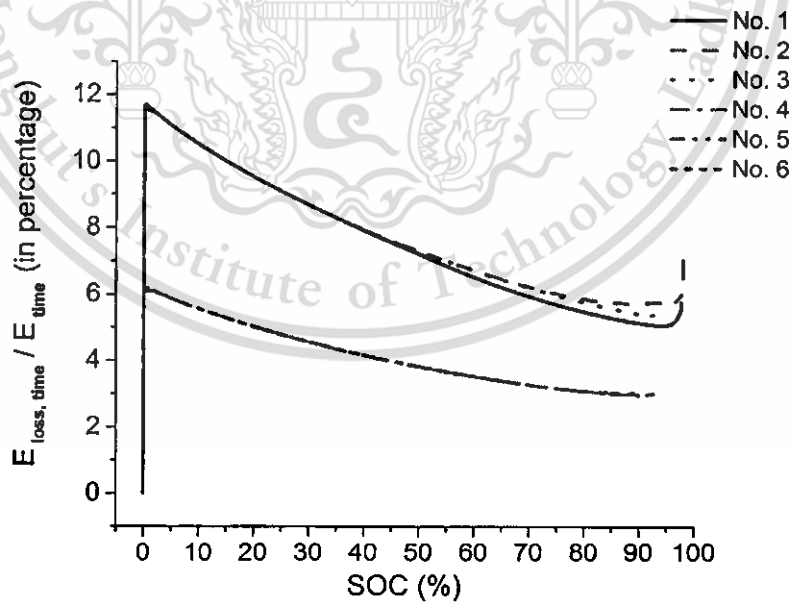


Figure 4.35: All of the samples's energy loss in percentage of energy consumption at that time.

#### 4.2.5 The simulation and optimum charging current results

According to Figure 4.36 and table 4.5 showing energy loss simulating result that varied constant charging current ( $I$ ), the energy loss at 180 A charging current is more than 80 times of the energy loss at 20 A, so the energy loss depends on charge current. The higher charging current, the more energy loss occurs. Additionally, the charging time at lower  $I$  takes longer than at higher  $I$  up to 9 times.

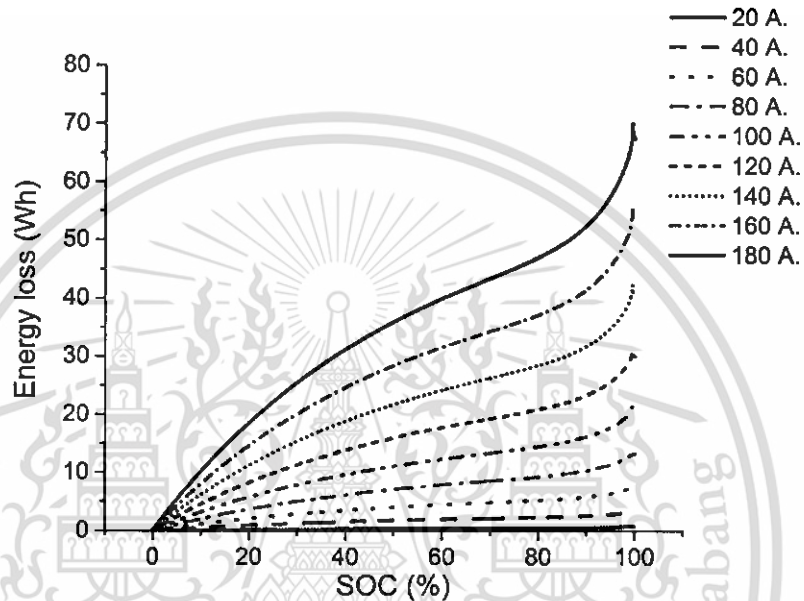


Figure 4.36: All of the samples's energy loss in percentage of energy at that time.

	30 A.	40 A.	60 A.	80 A.	100 A.
Time (minutes)	180	90	60	45	36
$E_{loss}/E_{total}, I=30$	1	4	9	16	25
	120 A.	140 A.	160 A.	180 A.	
Time (minutes)	30	25.71	22.5	20	
$E_{loss}/E_{total}, I=30$	36	49	64	81	

Table 4.5: The energy loss and charging time at vary charging current.

Moreover, after rescaling by using equation (3.20), assuming the weight of the energy loss and time is equal, as the result shown in Fig. 4.37, the energy loss and charging

This material is reserved for educational use only, not allowed for commercial use.

current are between 0-1. In the figure, the black line presents the battery charging energy loss after rescaling. The energy loss scale is more if the charging current is higher. On the other hand, the red line presents the battery charging time after rescaling. The charging time is lower if the charging current is higher. When summation of the both lines is equal to blue line, the minimum of blue line represents the optimum charging current which can obtain lowest charging time and energy loss. It's about 60 A.

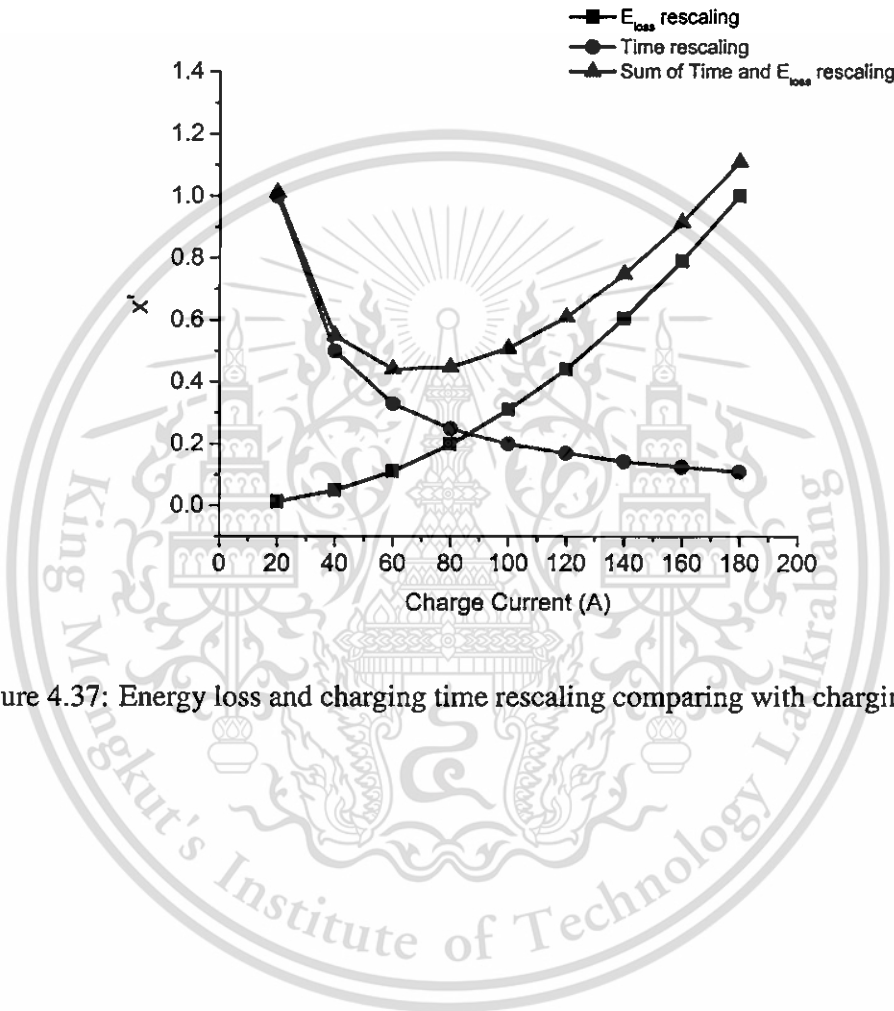


Figure 4.37: Energy loss and charging time rescaling comparing with charging current.

### 4.3 The Energy Loss In The Battery Balancing Schemes

This section shows results consisting of model verification and energy loss estimation. In simulation process, there was observation that the simulated results are linear. It might be not accurate comparing with non-linear simulation process. The following parts inform the details of this results.

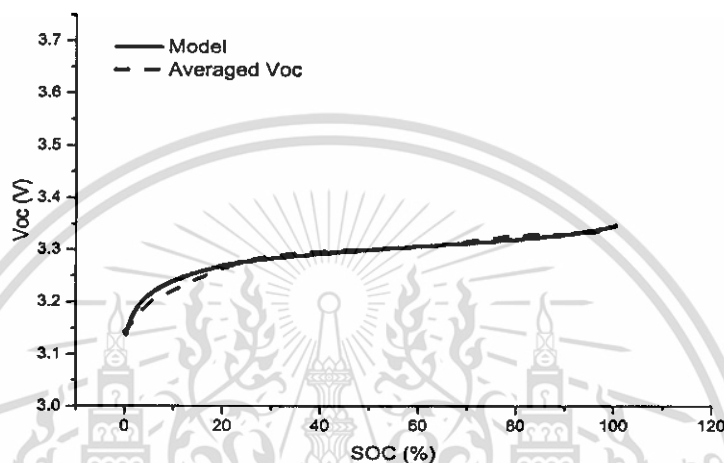


Figure 4.38: Comparison of  $V_{OC}$  between testing data and battery balancing model

#### 4.3.1 Model verification

According to the result on Fig 4.38, the battery-balancing model is accurate by comparing  $V_{OC}$ . However, this model assumed that the internal resistance is supposed constant during the charge and discharge, so the model is suitable for study balancing system only.

#### 4.3.2 The energy loss estimation results

Figure 4.39-4.39, from all of the results simulated MATLAB&simulink show the relationship between the energy loss in the battery-balancing schemes and  $\Delta SOC$  on each conditions. Comparing between each scheme, the estimation results of all conditions for varying  $\Delta SOC$  from 5 % to 40 % with step of 5 % present that the DTC scheme has the lowest energy loss (up to approximately 2.5 %). However, its charging time is found to be longer than the other schemes up to approximately 8 %.

Moreover, increasing  $\Delta SOC$  significantly increases energy loss. From the result, if  $\Delta SOC$  increase 35%, the energy loss will increase more than 8 times. It also informs

This material is reserved for educational use only, not allowed for commercial use.

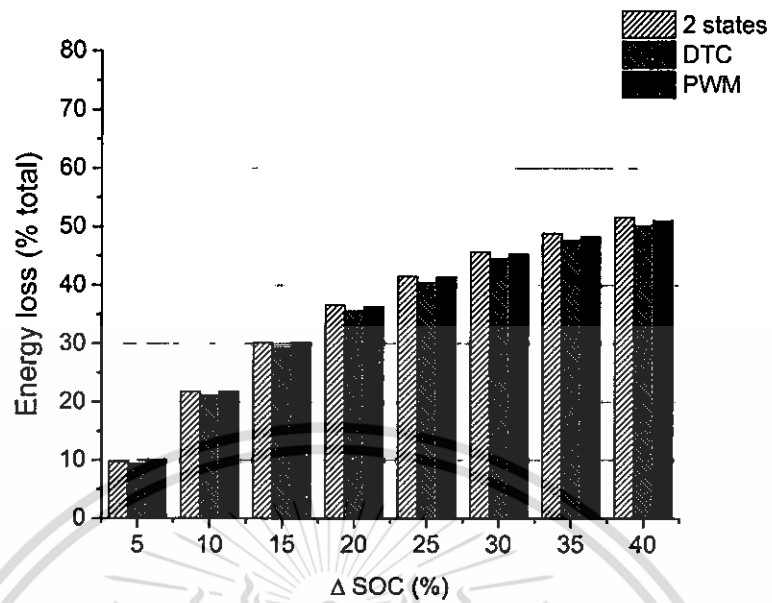


Figure 4.39: Comparison of total energy loss and  $\Delta$ SOC in condition 1 for each scheme.

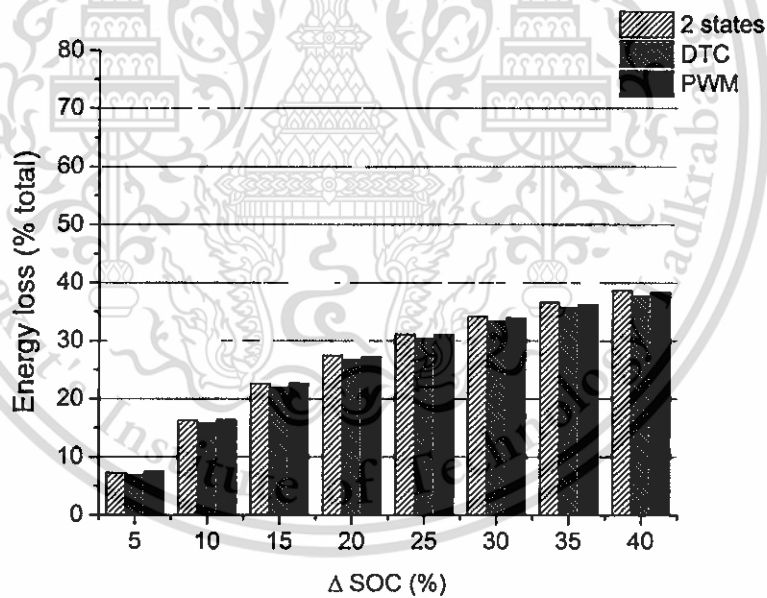


Figure 4.40: Comparison of total energy loss and  $\Delta$ SOC in condition 2 for each scheme.

that if the more balancing is used, the energy loss more occurs. This observation will be main idea to determine that it will be worth or not if the battery is balanced at high  $\Delta$ SOC. However, the high  $\Delta$ SOC appears because some battery cells are bad performance. The idea is that would be better if the bad ones are changed instead of doing balancing at high  $\Delta$ SOC. Finally, as the results, all of the trends are increase

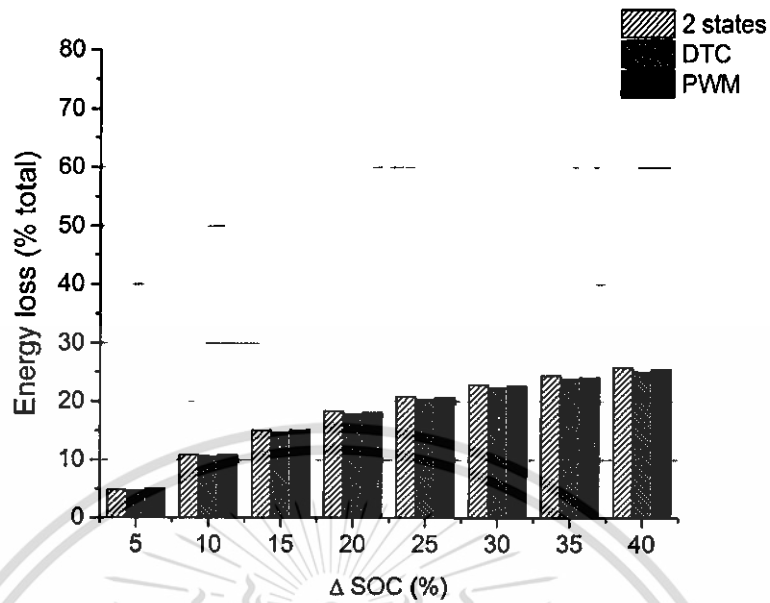


Figure 4.41: Comparison of total energy loss and ΔSOC in condition 3 for each scheme.

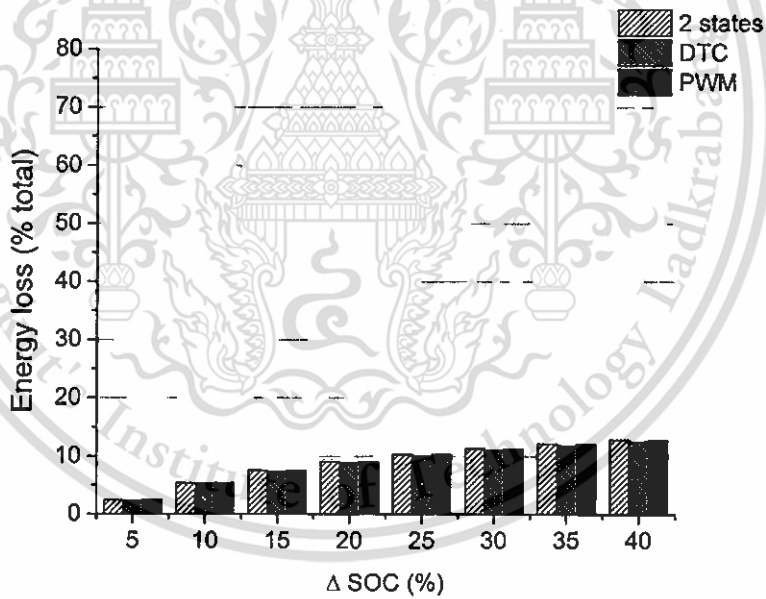


Figure 4.42: Comparison of total energy loss and ΔSOC in condition 4 for each scheme.

linearly.

From observation, the DTC scheme having the lowest energy loss and high charging time is caused by battery voltage at balancing time. Because  $P_{loss} = V_R I_R$ , the energy loss at lower  $V_R$  (or  $V_b$ ) is lower than others. The DTC scheme does the battery balancing state at lower battery voltage than the others. That is the reason why the DTC

This material is reserved for educational use only, not allowed for commercial use.

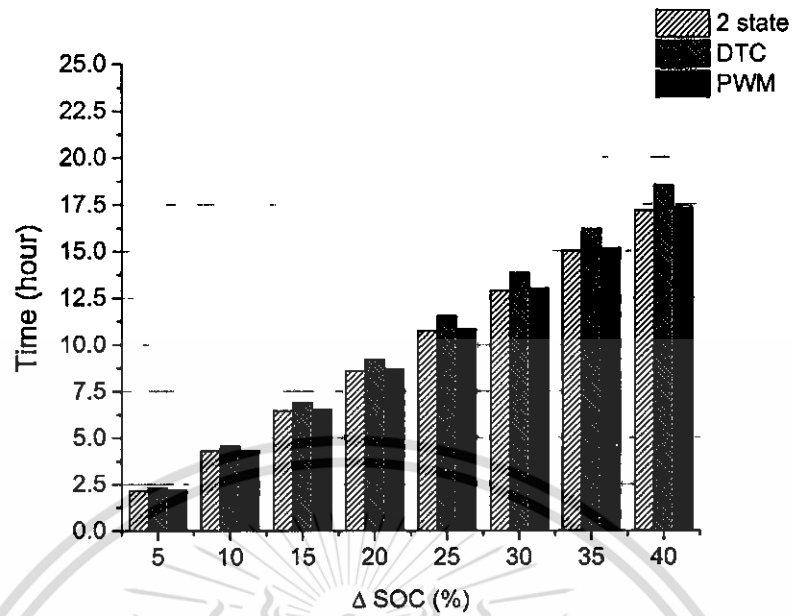


Figure 4.43: Comparison of balancing-time and  $\Delta$ SOC.

scheme has the lowest energy loss. On the other hand, because battery voltage is lower, the balancing current is also lower. If the balancing current is low, the battery will take more time to drain the energy out of the battery in case of balancing. That is the reason why the DTC scheme takes more balancing time.

# Chapter 5

## CONCLUSION

The battery model using the Thevenin equivalent circuit, which was solved by Genetic Algorithm (GA), represents the  $\text{LiFePO}_4$  battery characteristics efficiently (average error less than 1 %). Additionally, according to the estimation results of the battery-charging energy loss, the battery occurs higher energy loss at low state of charge (SOC) than at the middle and high SOC. And then, as simulated results, charge current affects to the energy loss. The more charge current is, the more energy loss occurs (up to 8000 % compared with the lowest charge current) and 60 A is the optimal charge current if assuming the battery-charging time is as important as the battery energy loss.

Moreover, the model identification process give more know-how to design new experiment and model significantly. In new design of battery model, There are three important things that should be considered in order to make the efficient battery model. Firstly, data should be corrected accurately using high efficient measuring instrument and controlling battery heat as soon as possible. Secondly, a model of the battery should be represent battery internal resistance, battery dynamic system, and battery heat transfers. Finally, it would be better if there are algorithms that filter an error from measurement before using mode.

From the estimation results of the battery-balancing energy loss, the scheme that provides the lowest energy loss is DTC scheme (less than 3%) and takes longer balancing time up to approximately 8 %. And then, the The relationship between the energy loss and  $\Delta\text{SOC}$  is significant, (the more  $\Delta\text{SOC}$  is, the more energy occurs). Moreover, balancing time depends on  $\Delta\text{SOC}$ . The system will waste more time if it has high  $\Delta\text{SOC}$ .

However, the simulation results show that the relationship between the energy loss and  $\Delta\text{SOC}$  is linear. This might not represent the actual values of them because the

battery model is ideal. The battery-balancing simulation results should be verified by the real experiment of battery balancing. Nevertheless, the simulation results are useful to approximately predict the values of energy loss for each balancing scheme. They also give a better understanding of each balancing scheme before performing real experiments.

Finally, when comparing the energy loss between charging and balancing battery, It represent that the important weight between charging and balancing battery is equal. The researcher who need to study in order to reduce an battery energy loss have to focus on the both. The energy loss in charging battery is highly about 20% depending on charging current and the energy loss in balancing is highly about 40 % depending on  $\Delta\text{SOC}$ .

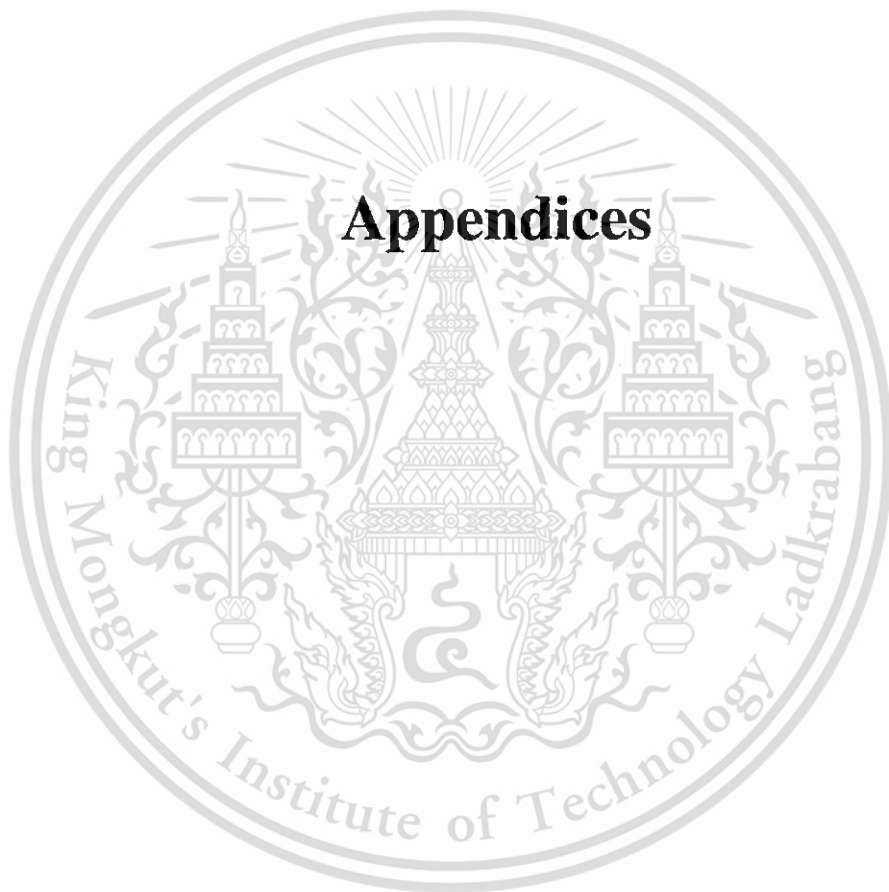
For future works, the battery model is needed to be more accurate. The first parameter that have to consider is  $V_b$  in term of the battery temperature. According to the experiment, there be found that the battery voltage is depended on the battery temperature directly. Other parameter that have to consider is state of health (SOH) of the battery. The battery voltage characteristic is not same when the battery is used in many times. However, the electric equivalent model is still not represents the battery's chemical reaction perfectly. Moreover, the battery model should represents the battery discharging characteristic in order to use it as non-linear model of battery balancing. Procedures of creating the model are the same as the battery-charging model, which consist of measuring discharging characteristics, optimizing the model, and verifying the model.

# REFERENCES

- [1] Davide Andrea, "Battery Management Systems for Large Lithium-ion Battery Packs", ISBN-13 © 2010 ARTECH HOUSE 685 Canton Street Norwood, MA 02062, 2010
- [2] K. padhi, K. S. Nanjundaswamy, and J. B. Goodenough, "Phospho-olivines as Positive-Electrode Materials for Rechargeable Lithium Batteries", *J. Electrochem. Soc.*, Vol. 144, No. 4, pp. 1188-1194.
- [3] Wang Jiayuan, Sun Zechang, Wei Xuezhe. "Performance and Characteristic Research in  $\text{LiFePO}_4$  Battery for Electric Vehicle Applications", IEEE, Tongji University, China 2009
- [4] Chaoyoung Hou, Jizhong Chen, Juan Hu, Huanling Wang, Shouping Xu. "An Online Calibration Algorithm of SOC for  $\text{LiFePO}_4$  Battery by using Characteristic Curve", *Electric Utility Deregulation and Restructuring and Power Technologies*, China Electric Power Research Institute. China, 2015.
- [5] Dong Tingting, Li Jun, Zhao Fuquan, You Yi, Jin QiQian. "Analysis on the Influence of Measurement Error on State of Charge Estimation of  $\text{LiFePO}_4$  Power Battery", IEEE, Jilin University, China, 2011
- [6] Bizhong Xia, Haiqing Wang, Yong Tian, Mingwang Wang, Wei Sun, Zhihui Xu. "State of Charge Estimation of Lithium-Ion Batteries Using an Adaptive Cubature Kalman Filter", *Energies journal*, Tsinghua University, China, 2015
- [7] Yin Hua, Min Xu, Mian Li, Chengbin Ma, Chen Zhao. "Estimation of State of Charge for Two Types of Lithium-Ion Batteries by Nonlinear Predictive Filter for Electric Vehicles", *Energies journal*
- [8] Hongwen He, Rui Xiong, Xiaowei Zhang, Fengchun Sun, JinXin Fan, "State-of-Charge Estimation of the Lithium-Ion Battery Using an Adaptive Extended Kalman Filter Based on an Improved Thevenin Model", IEEE, IEEE student members, 2011

- [9] Liye Wang, Lifang Wang, Chenglin Liao "Research on Improved EKF Algorithm Applied on Estimate EV Battery SOC", IEEE, Institute of Electrical Engineering, China, 2010
- [10] Jens Groot. "State-of-Health Estimation of Li-ion Batteries: Cycle Life Test Methods", Thesis for the degree of licentiate of engineering, Chalmers university of technology, Sweden, 2012
- [11] Jade Fattal, Paul Bou Dib, NAbil Karami."Review on Different Charging Techniques of a Lithium Polymer Battery", IEEE, University of Balamand, Lebanon, 2015
- [12] Modamed Daowd, Noshim Omar, Peter Van Den Bosssche, Joeri Van Mierlo. "Passive and Active Battery Ballancing comparison based on MATLAB simulation", IEEE, Universiteit Brussel, Belgium.
- [13] Siqi Li, Chris Mi, Mengyang Zhang."A High Efficiency Low Cost Direct Battery Balancing Circuit Using A Multi-Wind Transformer with Reduced Switch Count", IEEE, University of Michigan-Dearborn, USA.
- [14] Hounghwen He\*, Rui Xiong and Jinxin Fan. "Evaluation of Lithium-Ion Battery Equivalent Circuit Models for state of charge Estimation by an Experimental Approach", Energies 2011, Beijing Institute of Technology, China, 2011.
- [15] Y. Hu, S. Yurkovich."Battery Cell State-of-Charge Estimation using Linear Parameter Varying System Techniques", Journal of power sources, The Ohio State university, US, 2011.
- [16] Y. Hu, S. Yurkovich, Y. Guezennec, B.J. Yurkovich. "Electro-thermal battery model identification for automotive applications", Journal of power sources, The Ohio State university, US, 2010.
- [17] Low Wen Yao, Aziz, J. A., "'High Capacity LiFePO<sub>4</sub> Battery Model eith Consideration of Nonlinear Capacity Effects"' ,IEEE, Universiti Teknologi Malaysia, Malaysia, 2012.
- [18] Kotub Uddin, Alessandro Picarelli, Christopher Lyness, Nigel Taylor, James Marco. "An Acausal Li-Ion Battery Pack Model for Automotive Application", Energies 2014, the University of Warwick, UK, 2014.
- [19] Daming Zhou, Ke Zhang, Alexandre Ravey, Fei Gao and Abdellatif Miraoui. "Parameter Sensitivity Analysis for Fractional-Order Modeling of Lithium-Ion Batteries", Energies journal, Nothwestern Polytechnical University, China, 2016

- [20] Renxin Xiao, Jiangwei Shen, Xiaoyu Li, Wensheng Yan, Erdong Pan, Zheng Chen. "Comparisons of Modeling and State of Charge Estimation for Lithium-ion Battery Based on Fractional Order and Integral Order Methods", Energies journal, Kunming University of Science and Technology, China, 2016
- [21] Ernesto Inoa, Jin Wang. "PHEV Charging Strategies for Maximized Energy Saving", IEEE, IEEE members, 2011
- [22] Edward j. Beltrami. "An algorithmic Approach to Nonlinear Analysis and Optimization", Academic Press, Inc., State University of New York at Stony Brook, US, 1970
- [23] Mitsuo Gen, Runwei Cheng. "Genetic Algorithms & Engineering Optimization", John Wiley & Sons, Inc., Canada, 2000
- [24] Melanie Mitchell. "An introduction to Genetic algorithms", A Bradford Book The MIT Press, Massachusetts Institute of Technology, US, 1998
- [25] Tremblay, O., Dessaint, L. A. "Experimental Validation of a Battery Dynamic Model for EV Applications.", World Electric Vehicle Journal. Vol. 3 - ISSN 2032-6653 - © 2009 AVERE, EVS24 Stavanger, Norway, May 13 - 16, 2009



## Appendices

This material is reserved for educational use only, not allowed for commercial use.

Forbidden to modify the content, and cite the document when use.

# Appendix A

## MATLAB Short Code for Optimization



```

function [x,fval,exitflag,output,population,score] = GAcode(nvars,Aineq,bineq,lb,ub, ✓
PopulationSize_Data,CrossoverFraction_Data,Generations_Data,StallGenLimit_Data)
%% This is an auto generated MATLAB file from Optimization Tool.

%% Start with the default options
options = gaoptimset;
%% Modify options setting
options = gaoptimset(options, 'PopulationSize', PopulationSize_Data);
options = gaoptimset(options, 'CrossoverFraction', CrossoverFraction_Data);
options = gaoptimset(options, 'Generations', Generations_Data);
options = gaoptimset(options, 'StallGenLimit', StallGenLimit_Data);
options = gaoptimset(options, 'Display', 'off');
options = gaoptimset(options, 'PlotFcns', { @gaplotbestf @gaplotbestindiv });
[x,fval,exitflag,output,population,score] = ...
ga(@(x)objectiveF(Vdata,Time,x,SOC,I,cVoc),nvars,Aineq,bineq,[],[],lb,ub,[],[], ✓
options);
end
function F= objectiveF(Vdata,Time,x,SOC,I,cVoc)
%x is unknown variables
[Ploss,Vnew,V1]=voltageCurve(Time,x,SOC,I,cVoc);
fx=(Vnew-Vdata).^2;
F=sum(fx);
end
function [Ploss,Vdata,V1]= voltageCurve(Time,x,SOC,I,cVoc)

num=numel(SOC);
%% Separate unknown parameters
for i=1:1:21
L(i)=x(i);
J(i)=x(i+21);
end
R0(1)=L(1);
R1(1)=J(1);
for n=1:1:num

sR0=0;
sR1=0;
for i=1:1:20
if SOC(n)-SOC(1)>=(i*5)
Q(i)= 5;
else
if SOC(n)-SOC(1)<((i*5)-5)
Q(i)=0;
else
Q(i)= SOC(n)-SOC(1)-((i*5)-5);
end
end
sR0=sR0+(Q(i)*(L(i+1)/5));
sR1=sR1+(Q(i)*(J(i+1)/5));
end

R0(n)=R0(1)+sR0;
R1(n)=R1(1)+sR1;

```

This material is reserved for educational use only, not allowed for commercial use.

Forbidden to modify the content, and cite the document when use.

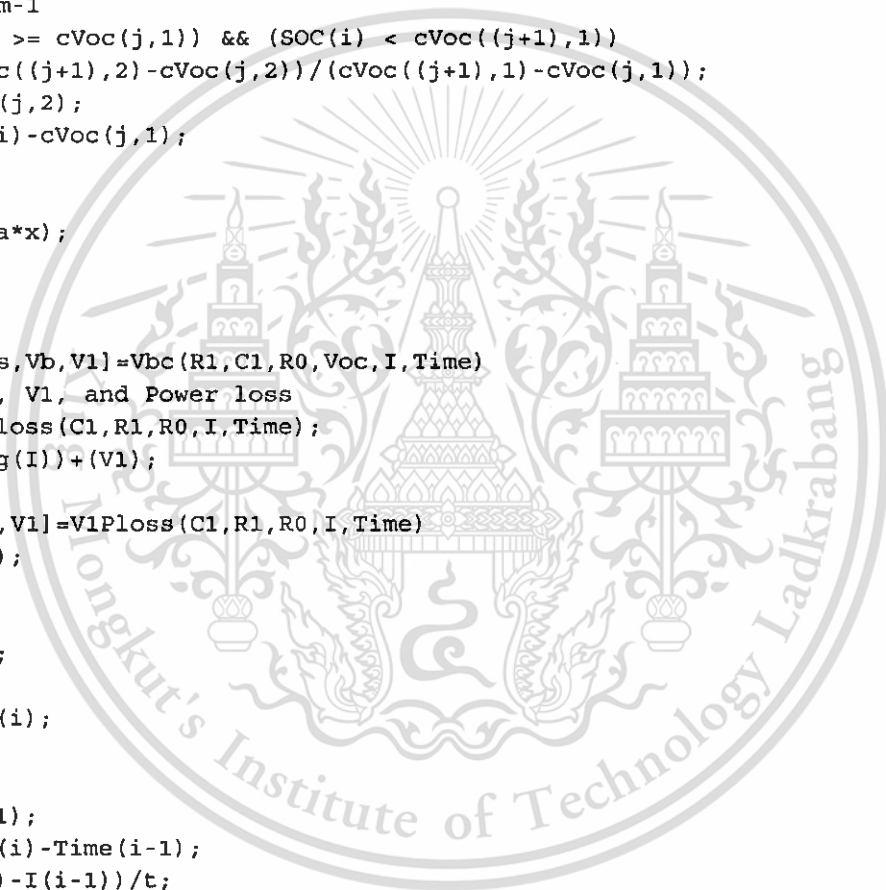
```

end
Voc=fVoc(cVoc,SOC);
C1=x(43)*100000;
[Ploss,Vdata,V1]=Vbc(R1,C1,R0,Voc,I,Time);

end
function Voc=fVoc(cVoc,SOC)
% Identify Voc in the function of time.
num=numel(SOC);
m=size(cVoc,1);
for i=1:1:num
    for j=1:1:m-1
        if (SOC(i) >= cVoc(j,1)) && (SOC(i) < cVoc((j+1),1))
            a=(cVoc((j+1),2)-cVoc(j,2))/(cVoc((j+1),1)-cVoc(j,1));
            b=cVoc(j,2);
            x=SOC(i)-cVoc(j,1);
        end
        end
        Voc(i)=b+(a*x);
    end
end
function [Ploss,Vb,V1]=Vbc(R1,C1,R0,Voc,I,Time)
%%Calculate Vb, V1, and Power loss
[Ploss,V1]=V1Ploss(C1,R1,R0,I,Time);
Vb=Voc+(R0*diag(I))+V1;
end
function[Ploss,V1]=V1Ploss(C1,R1,R0,I,Time)
num=numel(Time);
for i=1:1:num
    if i==1
        b=I(i);
        a=0;
        t=Time(i);
        c=0;
    else
        b=I(i-1);
        t=Time(i)-Time(i-1);
        a=(I(i)-I(i-1))/t;
        c=V1(i-1);
    end
end
V1(i)=R1(i)*b + exp(-t/(C1*R1(i)))*(C1*a*R1(i)^2 - b*R1(i) + c) + R1(i)*a*t - C1*R1(i)
^2*a;

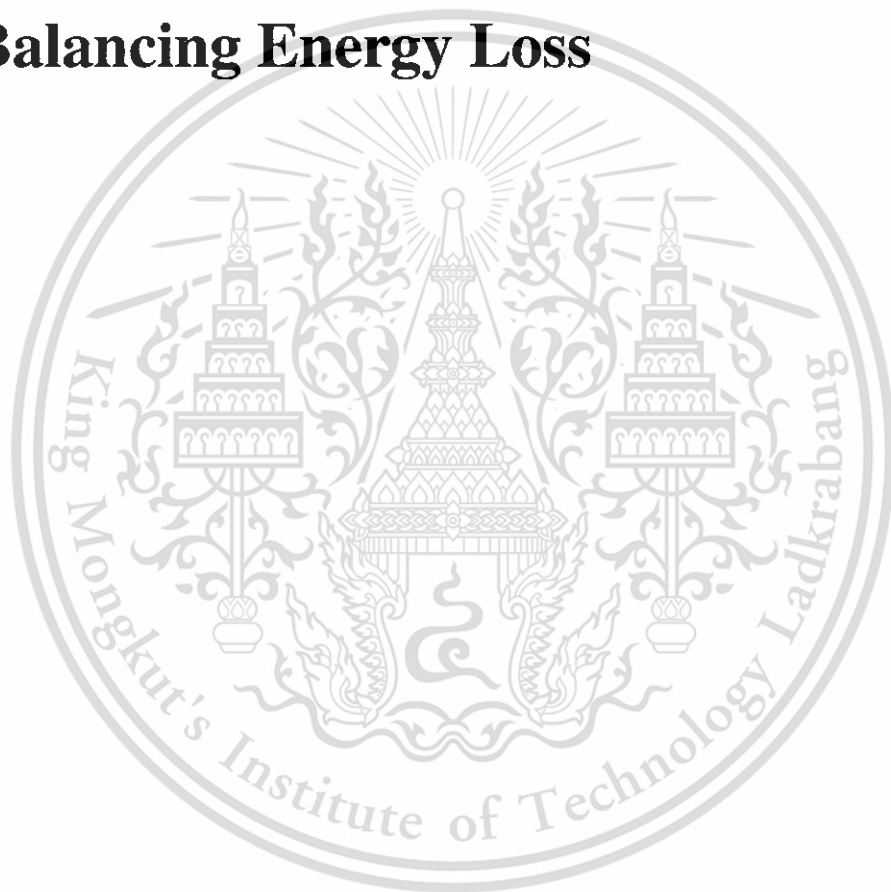
Ploss(i)=(V1(i)^2/R1(i))+R0(i)*(I(i)^2);
end
end

```

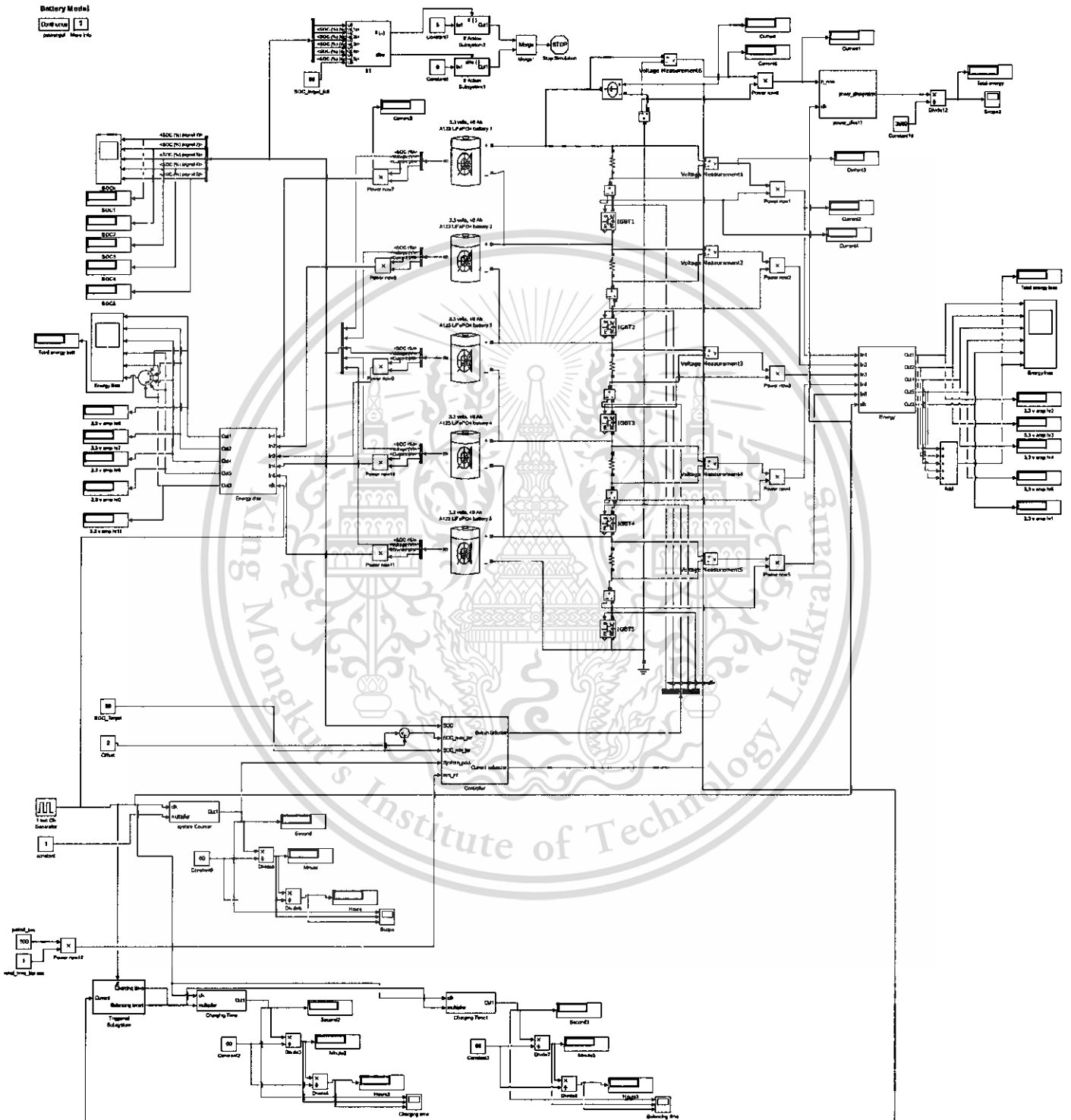


## **Appendix B**

### **Simulink Diagram for Battery Balancing Energy Loss**



# Main Battery Balancing Simulation Diagram



This material is reserved for educational use only, not allowed for commercial use.

Forbidden to modify the content, and cite the document when use.

# Appendix C

## Publication



This material is reserved for educational use only, not allowed for commercial use.

# A Study of Energy Loss in LiFePO<sub>4</sub> Battery-Balancing Schemes for Electric Vehicle Applications

Adisorn Amtip  
International College  
King Mongkut's Institute of Technology Ladkrabang  
Bangkok, Thailand  
adisornnut@gmail.com

Dr. Chaiwat Nuthong  
International College  
King Mongkut's Institute of Technology Ladkrabang  
Bangkok, Thailand  
chaiwat.kmitl@gmail.com

Dr. Teera Phatrapornnant  
Automotive Electronic Laboratory  
National Electronics and Computer Technology Center  
Pathumthani, Thailand  
teera.phatrapornnant@nectec.or.th

Amaras Kaewpunya  
Automotive Electronic Laboratory  
National Electronics and Computer Technology Center  
Pathumthani, Thailand  
amares.Kaewpunya@nectec.or.th

**Abstract**— High energy density LiFePO<sub>4</sub> battery plays an important role in the EV application. Due to strictly charging requirement, battery balancing is a necessary function in a battery management system (BMS) for charging this type of battery. Normally, there are two types of battery balancing circuit, i.e. active and passive balancing circuit. Because of simplicity, a passive circuit is chosen. Technically, passive balancing has energy loss while batteries are balancing. This research is focused on exploring three kinds of passive-balancing schemes about energy loss and at various conditions e.g. considering at balancing current or state of charge among all cells (SOC<sub>max</sub> - SOC<sub>min</sub>). The simulation results show that the different balancing schemes do not have significant effect on energy loss.

**Index Terms**—LiFePO<sub>4</sub>, EV application, passive balancing, State Of Charge(SOC), energy loss

## I. INTRODUCTION

Because of high fossil fuel cost, alternative fuel vehicles are of main interests among many researchers, especially, an electric vehicle (EV) and a hybrid electric vehicle (HEV). Both of them need to use electric power supply such as a battery. The battery itself is necessary to be a high efficiency one. A rechargeable battery is preferred to use in both EV and HEV because it can be charged and has high efficiency than the battery that cannot be recharged, especially lithium-ion battery. However, one of disadvantages of the rechargeable battery is that the battery management system (BMS) is required.

The battery management system (BMS) has many functions that help users to manage a battery and protect it from charging failures. Some functions consisted in BMS can be listed as battery protection, battery monitoring and optimization function. The battery balancing is a sub-function of optimization function. It helps to balance a state of charge (SOC) levels battery in order to get maximum efficiency.

## II. BMS WITH PASSIVE BALANCING SCHEME

In order to charge a pack of rechargeable batteries, BMS is required because of battery protection and SOC balancing reasons. There are commonly two balancing circuits in used, i.e. active balancing and passive balancing circuits. While active balancing circuit uses capacitors to store energy, the passive circuit does not consist of capacitors. This makes it less complicated compared to the active one.

However, though simpler, the passive balancing circuit suffers from energy loss. This project studies various balancing schemes in passive balancing circuit in order to minimize the energy loss. The following sections discuss about the specifications of battery which is used in the project and the effects of different kinds of passive balancing schemes to energy loss.

### A. The basic and advantages of LiFePO<sub>4</sub> battery

A LiFePO<sub>4</sub> battery is a type of rechargeable battery which has high energy density (>120 Wh/kg.) and high cycle life (>2000). It uses lithium-ion as the cathode material. The battery has been introduced since 1997.



Fig. 1. Prismatic cell of battery.<sup>[1]</sup>

Figure 1 shows a cell format called prismatic cell of such battery. It is encased in semi-hard plastic case. This format is appropriate for large project and mass production due to its simple structure. For these reasons, a prismatic cell has been chosen to use in this research.

## B. State of charge(SOC)

The state of charge (SOC) of a battery is the amount of electrical charge available at that point compared to the full capacity of a battery. It is expressed in term of percentage, e.g. 0% SOC refers to fully discharged battery and 100% SOC refers fully charged battery.

## C. Battery balancing and passive balancing

In an ideal system, when a pack of batteries have been charged or discharged for a long time, the SOC level of each battery is considered to be the same. This is shown in Fig. 2(a). However in reality, the SOC level of each battery will be different according to charging history [1]. This is illustrated in Fig. 2(b). Thus, the batteries in the pack will have unbalance SOC. Moreover, their other characteristics such as self-discharge current, internal resistance and capacity are also different. For this reason, in order to charge the pack of batteries, it is necessary to have some balancing process. One of the general battery balancing techniques studied in this project is passive balancing.

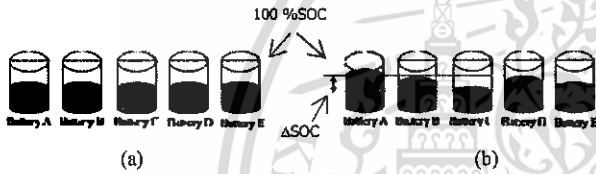


Fig. 2. SOC in (a) Ideal system and (b) Actual system.

Figure 3(a) shows a passive balancing circuit which consists of resistors, a controller, a power source, switches and batteries. The circuit functions as follows. While batteries are charging, the switches are off and the current flows into the batteries only.

In case the batteries do not require charging, the switches are on and the current flows passing through a resistor instead of the battery. However, there will be an amount of current drains from batteries and flows through the switch as well. This is shown in Fig. 3(b). Thus, the current flows through resistor1 can be described as in the following equation,

$$I_{R1} = I_s + I_{Batt1} \quad (1)$$

where  $I_{R1}$  is the current flows through resistor1,  $I_s$  is the current supplied from power supply and  $I_{Batt1}$  is the discharged current from battery1.

## D. Energy loss

In the passive-balancing battery system, an energy loss occurs according to two main causes. Firstly, the energy loss is caused by battery itself. In general, this energy loss comes from heat, battery efficiency and cycle life.

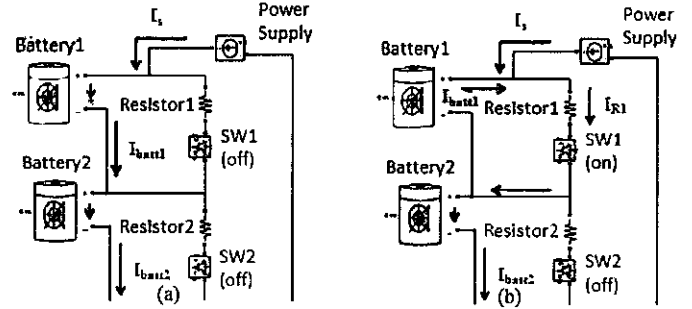


Fig. 3. The direction flow of current in passive balancing scheme (a) Battery 1 and 2 are charging, (b) Battery 1 is discharging and battery 2 is charging.

Secondly, the energy loss is caused by the current that flows through the resistor while the batteries are balancing. In this research, the study of energy loss will be focused only in this case. The corresponding energy loss will be studied using the calculation obtained from the external resistors. Thus, the energy loss depends on the current and the voltage at that particular external resistor. Energy loss is represented in term of Watt-hour and can be written as,

$$\text{Energy loss} = I_R V_R \times t \quad (2)$$

where  $I_R$  is the current flows through the resistor  $R$ ,  $V_R$  is the voltage across the resistor  $R$  and  $t$  refers to time in hour unit.

## E. Three schemes of passive balancing

The three balancing schemes have been studied in this project are; (i) Two States (normally balancing), (ii) Draining Then Charging (DTC) and (iii) Pulse-Width Modulation (PWM) scheme.

The Two States scheme (see Fig. 4) is a balancing scheme which has two states for balancing the batteries. The first state is performed by fast charging all the batteries with 15 A current until one of the battery's SOC reaches a predefined target point (In this research, 80% SOC of battery is used as the target point). For example, Fig. 4 shows that SOC level of batt1 and batt3 are higher than the others. Thus, the system stops fast charging when one of these batteries reaches the target point. Then, the second state is active. At this stage, the batteries are balancing with 1.4 A current until all of the batteries' SOC level reach the target point. Note that the balancing current in the second state depends on the resistance. In using a 2.5  $\Omega$  resistor, the balancing current is found to be 1.4 A.

The DTC scheme (see Fig. 5), also has two states balancing. However, in the first state, the current is drained from the batteries that have higher SOC level. This process stops when all the batteries obtain the same SOC level at the initial lowest value of all of batteries. For example, batt1 and batt3 drain the current until they have the same SOC level at 1.4 A. This looks similar to balancing batteries but there is no current supplied from power supply. Thus, the current from the

battery will flow through the resistor instead of the current from the power supply.

The last scheme is called Pulse-width modulation (PWM) scheme. Duty cycle of each battery charging current is different depending on the amount of the SOC level. In Fig. 6, it is obvious that batt1 has the lowest SOC level of all three batteries. Therefore, it needs to be charged at 100% duty cycle. On the other hand, batt2 has the highest SOC level so it uses a lower percentage of duty cycle to charge in the same period. The duty cycle equation is used to calculate a suitable time. PWM is used to assist obtaining the target SOC level of all batteries at the same time. The equation (3) is calculated by simulation of charging time of battery model (with 1.4A of charging current)

$$\text{duty cycle} = \alpha \left( \beta \frac{SOC_{now}^2}{SOC_{max}} + \gamma \frac{SOC_{now}}{SOC_{max}} + \delta \right) \quad (3)$$

where  $\alpha = 0.64787, \beta = 0.01, \gamma = 1.5041$ , and  $\delta = 0.0187$ .  $SOC_{now}$  is an SOC level of the battery at that time instant,  $SOC_{max}$  is maximum SOC level of all batteries at that time instant, and duty cycle is a time of the battery in that period. For example, duty cycle = 60 means that the battery is charged for 60 second and then is not charged for 40 second with 100 second period. The parameters  $\alpha, \beta, \gamma$ , and  $\delta$  are obtained from simulated curve fitting of increasing SOC per second and duty cycle.

### III. SIMULATION MODEL AND CONDITIONS

MATLAB&Simulink is chosen to simulate energy loss of each scheme. The simulation of battery's internal energy loss is neglected because the battery model is assumed to be ideal and no internal energy loss. The only energy loss focused here comes from the current flows through each external resistor. This simulation assumed further that temperature has no effects on the batteries and resistors.

#### A. The battery model and validation

The equivalent circuit of Lithium-ion battery which is used in this research is shown below.

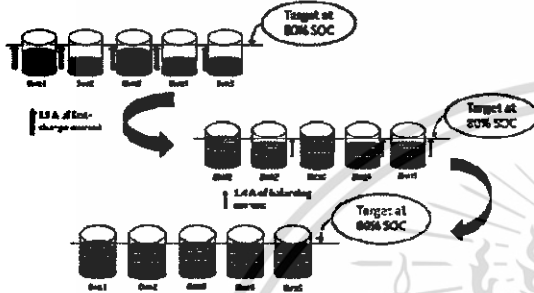


Fig. 4. Two States balancing scheme of five batteries.

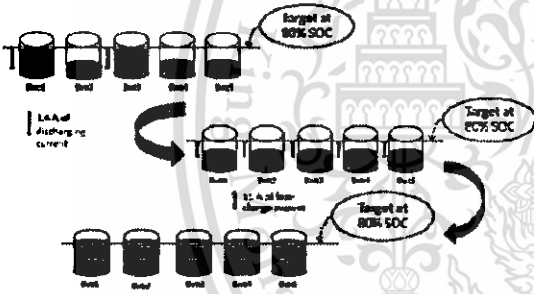


Fig. 5. The Draining Then Changing (DTC) scheme of five batteries.

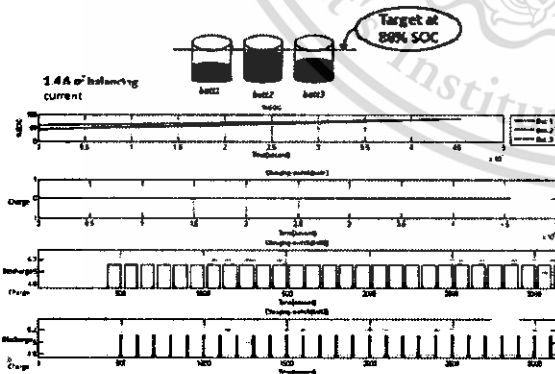


Fig. 6. PWM (Pulse-width modulation) scheme of three batteries.

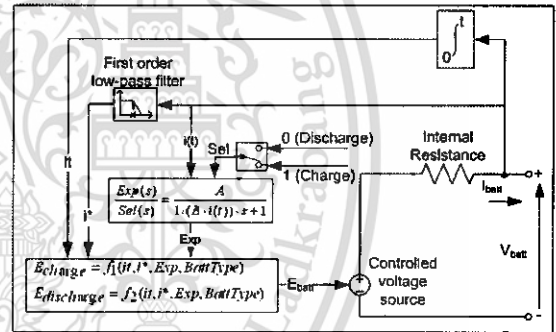


Fig. 7. The equivalent circuit of Lithium-ion battery.

The details of the equivalent circuit of Lithium-ion battery can be seen in the work of O., Dessaint[2]. However, the parameters are modified to represent LiFePO<sub>4</sub> battery characteristics of Winston Battery Limited, Model SP-LFP60AHA which is the battery used for this project.

#### B. Simulation conditions

Simulation conditions are divided into four conditions. The first condition varies  $\Delta SOC$  from 5% to 40% with step of 5% and set the highest SOC level to 60%. The amount of batteries which have lower SOC level is 1 in order to compare the energy loss from each scheme. In the other conditions, the amounts of batteries which have lower SOC level is changed from 1 to 2, 3, and 4, and are called conditions 2 to 4 respectively. This setup is used for all three balancing schemes.

#### IV. RESULTS AND DISCUSSION

The simulation results of all conditions for varying  $\Delta SOC$  from 5% to 40% with step of 5% show that the DTC scheme resulted in the lowest energy loss (up to approximately 2.5%). However, its charging time is found to be longer than the other schemes up to approximately 8%. Although, the DTC scheme shows the lowest energy loss but the difference from the other two schemes is insignificant.

Moreover, the results when comparing between each condition for varying  $\Delta SOC$  and the amount of lower SOC level batteries in the pack give insignificant improvement concerning energy loss between balancing schemes. All of these are shown in Fig. 8-11.

#### V. CONCLUSION AND FUTURE WORKS

From simulation results, the scheme that provides the lowest energy loss is DTC scheme. However, the difference of energy loss of each balancing schemes is insignificant (less than 3%). The simulation results show that the relationship between the energy loss and  $\Delta SOC$  is linear. This might not represent the actual relationship between these two values. The two main reasons lie in the battery model and temperature independent assumption. Because of these reasons, the simulation results are needed to be verified by the experiments. Nevertheless, the simulation results are useful to approximately predict the values of energy loss for each balancing scheme. They also give a better understanding of each balancing scheme before performing real experiments.

The future work for this project is to develop a new battery model which takes internal energy loss into account. In addition, the energy loss in resistor will be studied in the scope of temperature dependent. With these modifications, the obtained results should represent the real experiments more accurately.

#### ACKNOWLEDGMENT

I really appreciate Thailand Advanced Institute of Science and Technology and Tokyo Institute of Technology (TAIST-Tokyo Tech) and National Science and Technology Development Agency (NSTDA) to give me an opportunity. Thank you, Dr.Chaiwat Nuthong, Dr.Teera Phatrapornnant for excellent advice, and Mr.Amares Kaewpunya, Assistant Researcher, for giving simulation knowledge.

#### REFERENCES

- [1] Davide Andrea, "Battery Management Systems for Large Lithium-ion Battery Packs", ISBN-13 © 2010 ARTECH HOUSE 685 Canton Street Norwood, MA 02062, 2010
- [2] Dynamic Model for EV Applications." World Electric Vehicle Journal. Vol. 3 - ISSN 2032-6653 - © 2009 AVERE, EVS24 Stavanger, Norway, May 13 - 16, 2009.
- [3] T. Zupa and O. Liska, "Charging module for newest types of rechargeable batteries LiFePO<sub>4</sub>", Technical University of Kosice, Slovakia 2010
- [4] A. Chih-Chiang Hua, B. Zong-Wei Syue, "Charge and Discharge Characteristics of Lead-Acid Battery and LiFePO<sub>4</sub> Battery", 2010

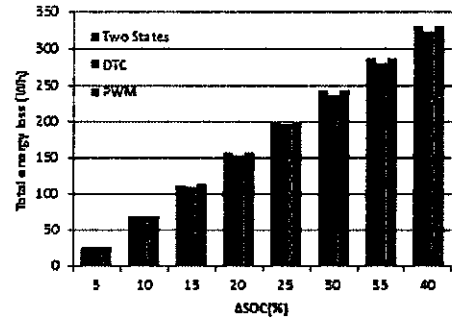


Fig. 8. Comparison of total energy loss in condition 1 for each scheme.

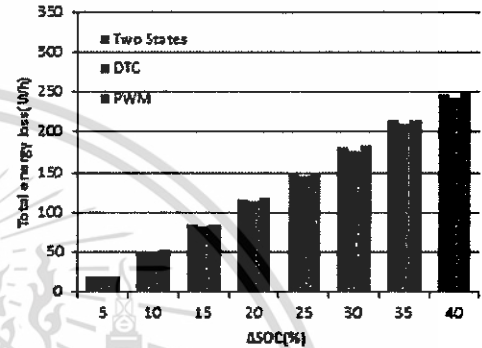


Fig. 9. Comparison of total energy loss in condition 2 for each scheme.

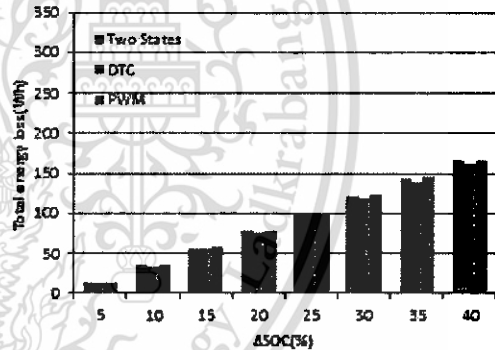


Fig. 10. Comparison of total energy loss in condition 3 for each scheme.

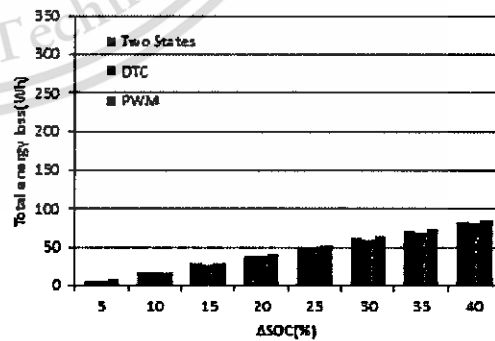


Fig. 11. Comparison of total energy loss in condition 4 for each scheme.

# BIOGRAPHY

**NAME** Mr. Adisorn Amtip

**DATE OF BIRTH** 15 June 1988

## EDUCATION RECORD

**HIGH SCHOOL** High School Graduation  
Watsuthiwararam school, 2006

**BACHELOR'S DEGREE** Bachelor of Engineering (Automotive Engineering)  
Thai-Nichi Institute of Technology, 2011

**MASTER'S DEGREE** Master of Engineering (Automotive Engineering)  
King Mongkut's Institute of Technology Ladkrabang, 2015

## HONOUR AND SCHOLARSHIP

**2010** 1st prize Rookie awards in 8th JSAE- Japan formula student competition at Ecopa stadium, shizuoka JAPAN

**2011 - 2013** Scholarship for Study Master Degree in Automotive Engineering at KMITL by TAIST-Tokyo Tech, 2011

## PUBLICATION

- A. Amtip, R. Sutthisong, P. Phanophat, D. Kaewdook, S. Tamna, W. Wongsuwan, J. Chaichanawong, N. Limjeerajarus (2011.) "Performance enhancement of FSAE racing cars by improving a throttle valve", 2010 JSAE KANTO International Conference of Automotive Technology for Young Engineers (ICATYE), Yokohama, Kanagawa, Japan, March 9, 2011.
- A. Amtip, R. Sutthisong, P. Phanophat, D. Kaewdook, S. Tamna, W. Wongsuwan, J. Chaichanawong, N. Limjeerajarus (2011)." Improvement of a throttle enhancing engine performance of FSAE racing cars", The 7th International Conference on Automotive Engineering (ICAE7), Bangkok, Thailand, March 29, 2011.
- A. Amtip, T. Phatrapornnant, C. Nuthong, A. Kaewpunya (2014). "A Study of Energy Loss in LiFePO<sub>4</sub> Battery Balancing Schemes for Electric Vehicle Applications", The International Electrical Engineering Congress 2014 (IEECON2014), Pattaya, Thailand, 2014.